E-230-902

FINAL TECHNICAL REPORT

PROJECT E220–903/E230–902

REMOTE DETECTION OF SEVERE STORMS AND TORNADOES IN GEORGIA

By

E. F. Greneker, C. S. Wilson, J. I. Metcalf

Prepared for

THE STATE OF GEORGIA
OFFICE OF THE GOVERNOR

THE GEORGIA GENERAL ASSEMBLY

THE BOARD OF REGENTS
UNIVERSITY SYSTEM OF GEORGIA

December 1975

ENGINEERING EXPERIMENT STATION
Georgia Institute of Technology
Atlanta, Georgia 30332

EXECUTIVE SUMMARY

I. Background

The number of tornadoes occurring each year in Georgia has increased during the past few years. This increase, illustrated by National Weather Service (NWS) storm data, includes such occurrences as the 65-mile Jonesboro-to-Athens tornado of 1973, the four tornadoes which were part of the "jumbo outbreak" of 4 April 1974, and the Atlanta tornado of 1975 that severely damaged the governor's mansion and the northwest side of Atlanta. Because of the increased interest by state officials in the possibilities for advance detection and warning of tornadoes, a project was begun in 1973 by the Applied Engineering and Electronics Technology Laboratories of the Engineering Experiment Station. The objective of this project, applying the most up-to-date technology and most promising past research by others, was to determine if any unique storm "signature" consistently observable by radar or detectable from the electromagnetic signals generated by the thunderstorm itself could be associated with the imminent occurrence of a tornado. A pilot tornado detection system, consisting of a weather radar and thunderstorm electromagnetic impulse (sferics) monitoring apparatus, was built at Georgia Tech and operated during the 1975 tornado season. The results obtained with the Georgia Tech system and additional related analysis of NWS radar data are described in this report.

II. Results

The data base was limited by (1) the continuing improvements that were made in the detection system throughout the tornado season and (2) the lack of tornadoes within the surveillance area of the system. However, the results

obtained with the Georgia Tech system tend to reinforce those from other sources.

The best results from the Georgia Tech system were obtained in the case of the Atlanta tornado of 24 March 1975, which passed within 3 miles of the Georgia Tech campus. The rate of electromagnetic impulses from the storm reached high values in three peaks about 20 - 30 minutes apart as the storm approached, dropped to near zero while the tornado was on the ground, and rose rapidly to very high values as soon as the tornado lifted. This near-cessation of electromagnetic signals, if repeatable, could be used for warning people who are in the path of the tornado, although by itself it does not provide the advance warning that would be most desirable. More investigation of the peak signal rates preceding a tornado could lead to advance warning capability.

Distinctive features of the storm radar echoes were observed in conjunction with several tornado occurrences during 1975. The echo of the storm that produced the Atlanta tornado exhibited a "hook" at one side about 15 minutes before the tornado touched down. In the case of the Fort Valley and Lyons tornadoes, storm cells were observed to merge prior to the occurrence of the tornadoes. Echo rotation was observed in the case of the Bainbridge tornado. These echo motions reveal significant variations in the wind field around the storms. Consistent detection of these wind variations would increase significantly the probability of detecting a developing tornado 15 - 20 minutes before it touches down. The full utilization of this warning potential depends on having the capability of measuring the wind flow within the storm (i.e., by Doppler radar).

Long-term and short-term trends of Georgia tornado activity were derived from NWS data for the periods 1953-1969 and 1970-1975. These data showed that

the annual rate of tornado occurrence in the most recent 5 years was about double that in the preceding 17 years. More important for purposes of public warning, the recent data revealed a shift in time of tornado occurrence. Peak tornado occurrence in the 1953-1969 period was around 5:00 p.m. (Eastern Standard Time), with a secondary peak about 9:00 a.m. In the recent period the peak is around 3:00 - 4:00 p.m., and the secondary peak at 6:00 a.m. This apparent short-term shift implies that new approaches to the problem of public warning should be developed, as people may be at work, or asleep at home, during these times. The requirement of rapid dissemination of warnings is imperative because of the short path lengths of many Georgia tornadoes; most are less than 5 miles. Tornadoes moving at ground speed of 35 knots would transverse this distance in less than 9 minutes, leaving little time for warning "downstream" residents if no advanced tornado detection system is utilized.

III. Recommendations

Observations at Georgia Tech during the 1975 tornado season and observations reported from other locations indicate that several specific improvements should be made to the Georgia Tech tornado detection system. The most effective utilization of the electromagnetic impulse monitors requires (1) more precise directional data for the received signals, and (2) a more widely deployed sferics network. These improvements will permit the recording and display of signals received from individual thunderstorms.

As additional funding becomes available, minor modifications should be made to the present radar system to improve its sensitivity, and complete data-recording capability added to permit reprocessing of storm data and careful study of radar echo features. Ultimately, a high-powered Doppler

radar should be installed, in addition to the present equipment, in order to measure the wind flow within storms. This improvement will provide an enhanced capability for early identification of tornado development in storms. Further development and successful utilization of these techniques could provide the basis for a more effective early detection capability that could be utilized by warning agencies.

Tornado statistics need to be evaluated in a continuing program to determine the persistence of the trends in time of occurrence that we deduced from the NWS storm data. On the basis of these trends, the public warning procedures need to be reviewed and modified.

Final Technical Report

Project E220-903/E230-902

REMOTE DETECTION OF SEVERE STORMS AND TORNADOES IN GEORGIA

By

E. F. Greneker, C. S. Wilson, J. I. Metcalf

December 1975

Prepared for

The State of Georgia

Office of the Governor

The Georgia General Assembly

The Board of Regents
University System of Georgia

Engineering Experiment Station
Georgia Institute of Technology
Atlanta, Georgia 30332

FOREWORD

This research project was conducted by personnel of the Radar Technology Division of the Applied Engineering Laboratory and the Communications Technology Group of the Electronics Technology Laboratory, Engineering Experiment Station, Georgia Institute of Technology, Atlanta, Georgia 30332. Mr. E. F. Greneker served as Project Director with Mr. C. S. Wilson serving as Assistant Project Director.

This project was sponsored under internal projects E220-903 and E230-902 and funded jointly by the Board of Regents of the University System of Georgia and the Engineering Experiment Station.

The authors acknowledge the support and guidance of Dr. H. A. Ecker, Director of the Applied Engineering Laboratory; Mr. D. W. Robertson, Director of the Electronics Technology Laboratory; Mr. J. L. Eaves, Chief of the Radar Technology Division; and Mr. R. W. Moss, Chief of the Communications Technology Group. We are grateful to Mr. H. H. Jenkins for his participation in the planning and early stage development of sferics equipment, State Senator James W. Tysinger for his untiring support of the project and Chancellor George W. Simpson for his financial support. We also appreciate the contributions by Dr. W. W. McDougald, Mr. W. T. Herrington, and Mr. J. R. Stephens of the University of Georgia School of Journalism in the operation of the Athens sferics station and by Mr. R. M. Boyd of Georgia Tech in supplying meteorological observations. We acknowledge the support of the National Weather Records Center and of the Atlanta forecast office of the National Weather Service, under the direction of Mr. R. W. Harms.

The authors are grateful to Research Engineer E. E. Martin, Co-op Trainees G. L. Hyatt and J. D. Kascak, Student Assistants M. D. Dvorscak and C. W. Conkle, and Technicians B. J. Wilson and P. A. Carlton for their contributions to building the sferics and radar systems and keeping them operational. The authors also wish to thank Mrs. F. B. Bechtold, Radar Technology Division Secretary, Mr. A. Bauman and Mr. M. J. Sinclair for their assistance in preparing materials for this report.

TABLE OF CONTENTS

TABLE OF CONTENTS (Contd.)

TABLE OF CONTENTS (Contd.)

LIST OF FIGURES

SECTION I

INTRODUCTION

The tornado has been Georgia's worst single type of recurring natural disaster during the past decade. Over this 10-year period, 275 tornadoes were recorded in the state, resulting in 32 deaths, hundreds of injuries, and over 200 million dollars in property damage. In 1972, Georgia had the distinction of being the state with the second highest number of tornado occurrences in the Nation.

Figure 1, furnished by the National Weather Service (NWS), shows the occurrences of tornadoes on a county-by-county basis for the years 1953 - 1969. A study of tornado occurrences in Georgia from 1970 through July 1975 was prepared by Georgia Tech and will be presented in Section VI, entitled "Short Term Trends in the Occurrence of Georgia Tornadoes."

The incidence rate of tornadoes occurring in Georgia increased and peaked during 1971 and 1972. The total number of tornado occurrences decreased in 1973, but during the spring of that year the Jonesboro-to-Athens tornado occurred, leaving destruction and death over a continuous path in excess of 65 miles.

A. Tornado Prediction and Formation

At present no reliable method exists for predicting with absolute accuracy tornado occurrence before the tornado forms. The National Weather Service issues tornado watches on the basis of observed meteorological conditions, radar and satellite reports. When these conditions indicate the possibility of tornado formation, a watch is issued for a geographic area that forms a rectangle (or box) approximately 100 by 250 miles on each set

Figure 1. Distribution of Georgia Tornadoes on a county basis.

of sides. When the watch is issued, all persons within the defined area are urged to watch for tornadoes and be aware that conditions are favorable for tornado formation. When a visual observation is made of a funnel aloft or a tornado on the ground, the tornado watch is changed to a tornado warning. The details concerning the tornado's reported location, direction and speed of travel are given to the public in the affected area via numerous radio and television stations. The lifetime of the average tornado is short and a finite amount of time is required to receive the sighting report, prepare and disseminate the warning. Thus, each additional minute of advance warning of a tornado's impending occurrence is of extreme value in saving lives and preventing injury to persons who otherwise may be caught unaware.

Numerous meteorological conditions must be present before a tornado will form. However, the element that must always be present for tornado formation is the thunderstorm. Although the dynamics that lead to tornado formation within the thunderstorm are not fully understood or explained, there are elements accompanying the thunderstorm such as rain, hail and electrical activity that can be sensed and measured remotely. Thus a project at Georgia Tech was proposed to determine if the forming tornado could be sensed remotely, utilizing measurements of electrical activity and other parameters of the parent thunderstorm.

B. Project History

In 1973, state officials funded a feasibility study at Georgia Tech to determine if a "signature" from a forming tornado could be detected prior to the funnel's touchdown. The study, funded from Governor Jimmy Carter's Emergency Fund, was conducted by the Applied Engineering Laboratory and the

Electronics Technology Laboratory of the Engineering Experiment Station (EES). The study group reviewed past and current literature on the general subject of tornado detection systems. These works served as a basis on which to postulate a candidate tornado detection system for empirical trial in Georgia.

A final report entitled, "A Study of Techniques for the Establishment of a Pilot Electronic Tornado Detection System for Georgia," [1] was completed in December 1973 and distributed to the Governor and other state officials. The report recommended that a pilot test system be built to determine, on an empirical basis, the validity of the tornado detection techniques found in the literature.

C. Basic System

The basic study [1] was completed in December 1973. The candidate system thought to have the highest probability of success, when developed and tested on an empirical basis, consisted of one active and three passive elements. The study recommended that as a bare minimum, a high resolution noncoherent test-bed radar system should be utilized to track the most severe cells using historically accepted radar detection techniques. It was also proposed in the planning report that an electromagnetic emissions (sferics) network be established to track the most electrically active cells and monitor the electromagnetic (sferics) burst rates associated with each.

D. Sferics Phenomenon

The general name given to the pulse phenomenon associated with electrical discharges in the atmosphere is "sferics." The word "sferics" is part of the terminology developed during early research into atmospheric electrical phenomena, and it will be used hereafter as a term to describe the electrical

discharge associated with tornadoes and severe storms. The sferics phenomenon is commonly termed "static" when heard on a regular radio broadcast during thunderstorm activity.

The direction of arrival and the total number of these sferics can be determined. Various researchers have shown that the more severe the storm, the higher the burst rate. Thus, monitoring these bursts offers a valuable insight into the phase and severity of thunderstorm development.

E. Georgia Tech Sferics System

The Georgia Tech sferics equipment was designed to operate on a center frequency of 2.8 MHz with a bandwidth of $\pm$ 300 kHz to the 6 dB point. The receiver integrates the individual sferics to form the burst count. The burst count is used as a criterion of storm severity (i.e., the higher the count, the more active the storm). The burst counter has three registers. The most sensitive register begins counting when a -70 dBm signal appears at the antenna terminals. Each of the two remaining registers begins its count at -60 dBm and -50 dBm, respectively. Thus, it is possible to derive some indication of range to the source by observing in which register the burst count is displayed. The receiver was designed to display the angle of arrival of each sferics burst over a 360-degree sector and count the number of bursts in 10 or 60 second intervals (operator selectable). In addition, four 8-digit counters were included to count the number of sferics signals occurring in each 90-degree quadrant.

An X-Y DF oscilloscope is included to supply the operator with additional bearing information. Each time a sferics signal is received, a strobe corresponding to the azimuthal angle of signal arrival is displayed on the face of the scope.

F. Receiver Placement

The original 1975 test plan included arrangements for receiver placement in Atlanta, Athens and Macon, Georgia. This configuration was chosen to provide optimum Direction Finder (DF) coverage of the area along a Columbus/Atlanta/Athens line. This 3-station configuration would also allow any one receiving station to get "covered up" by a thunderstorm without a loss of total system DF capability. The Atlanta receiver was the only sferics system operational during the Atlanta tornado. The Athens receiver was installed on the University of Georgia campus in August 1975.

G. Radar

Conventional radar can measure the location, reflectivity, vertical extent, direction and speed of movement of the thunderstorm mass. When the radar is calibrated to provide quantitative reflectivity measurements, additional data such as rainfall rate can be derived.

Doppler radar (coherent) can measure the speed of the precipitation particles along the radar beam, i.e., the movement toward or away from the radar. Since precipitation moves with speeds approximating that of the surrounding air, the radial velocity of the precipitation is a good measure of the radial component of the wind fields within the thunderstorm. A single Doppler radar cannot measure the total (three-dimensional) wind field within the thunderstorm. However, the velocity measurements that are obtained from a Doppler radar can provide valuable information about the areas of high gusts, shear, and vorticity connected with forming tornadoes. Doppler radars are still in the experimental phase and are not in use for tornado warning purposes within the State of Georgia.

H. Radar Data

The Georgia Tech weather radar used in tracking during the 1975 period was a 250 kW 10 GHz (3 cm) noncoherent unit with A-scope and plan position indicator displays. The antenna has a pencil beam with a width of 1.8 degrees, and is steerable in azimuth and elevation simultaneously. The system transmits linear polarization and has the capability of receiving both the orthogonal and parallel polarized components simultaneously.

During the 1975 tracking season, the Georgia Tech radar was located in the tracking room on the 7th floor of the Graduate Library. The radar data indicated the storm's bearing, range, and height. Top heights, echo intensity and shape, and ground speed were used to determine the storm's potential for tornado formation.

I. Tracking Operation

The tracking/plotting board is co-located with the radar. A 4 x 5 foot backlighted map with a plastic shield is used to plot most active sferics strobes and radar data. The integration of sferics and radar data on the plotting board locates the thunderstorm cells that prove to be most electrically active. Thus, the present plotting system allows thunderstorms to be tracked in almost real-time displaying their ground speed, height, geographic location, and electrical characteristics. A complete description of the sferics network and radar system will be presented in later sections.

J. Funding

Funding for the system's construction was furnished through two sources in three increments. The Board of Regents, University System of Georgia, supplied the first increment which covered the purchase of long lead-time

materials and supplies. A second increment was received from the Engineering Experiment Station's internal research fund for the purpose of system construction. A third increment was received from this same source for the purpose of system operation during the Georgia tornado season in the spring of 1975.

K. Preliminary Findings

The Atlanta tornado was the most important single event observed during the system test period. The Atlanta tornado passed within 3 miles of the Georgia Tech campus. Visual, radar, and sferics observations were made from the Georgia Tech campus of the Atlanta tornado just before, during, and after funnel touchdown. The correlation of these data with actual path locations and times of occurrence shows that the tornado was detectable 15 minutes before funnel touchdown. Detectability was based on the observation of a "hook" echo on the radar display. This echo shape is associated with the strong wind circulation in the cloud, and is a standard criterion for issuing a tornado warning.

The recorded sferics data taken before, during, and after the Atlanta tornado show marked increased sferics before the funnel touched the ground; a cessation of all sferics during the period the funnel was on the ground; and a resumed high level after the funnel left the ground. The cessation of sferics is not completely explained in the literature, and had several reputable persons using separate receiving equipment not witnessed the phenomenon, the data would have been discounted and the loss of sferics would have been blamed on equipment failure. If this phenomenon could be proven to occur during a large percentage of tornado touchdowns, it could serve an important role in the overall scheme of tornado early warning and detection.

In the case of the Atlanta tornado, the detection of the "hook" echo 15 minutes before tornado touchdown was a textbook example of a "hook" echo formation. The "hook" would probably have been missed at greater ranges due to its small size. However, the detection of the "hook" at close range indicates that the upper-level circulation associated with it would have been detectable by Doppler radar even at greater range.

L. Report Format

Sections II through V contain information on sferics and radar meteorology, and the application of radar and sferics technology to the detection of tornadoes. Sections VI and VII cover the classification of Georgia tornadoes and the analysis of Georgia Tech data on the Atlanta tornado. Sections VIII and IX discuss the Georgia Tech system and proposed additions and modifications that should be accomplished before operation during the spring of 1976.

SECTION II

THE SFERICS PHENOMENON

Studies of electromagnetic emissions from storms have been an important part of severe weather research for the last half-century. The intense wind flow within storms and the presence of both solid (hail and ice crystals) and liquid (rain) particles result in a separation of positive and negative electric charges within the storm. When the opposing electric charges become strong enough they are discharged either within the cloud or to the ground. The discharge (lightning) produces an electromagnetic signal. These signals, known as sferics, can be recorded at a distance from the storm. The rate of occurrence, strength of the signals, and source within the storm are all related to the storm dynamics.

A specific area of study of the electromagnetic signals emanating from severe storm cells has been directed to efforts at determining if one type of storm emits a particular pattern or "signature" of electromagnetic radiation with respect to another type of storm. For example, can a tornado be distinguished from a thunderstorm by close inspection of the electromagnetic signature? Such differentiation could be of major value in establishing an early warning system for protection of human life in the event of a destructive tornado.

Several recent investigations of the sferics phenomenon have been directed toward establishing definitive electromagnetic signatures of severe storms. One of the more significant investigations in this area is that conducted by Taylor [2]. His results imply that a rate enhancement in sferics activity is the most indicative parameter of tornadic activity.

Of specific importance is a so-called "burst rate" phenomenon that provides a criterion for determining the presence of a tornado in a thunderstorm.

A. The Nature of the Burst Phenomenon

A large amount of electrical activity is associated with thunderstorms, with or without severe features such as funnel clouds, hail storms, and tornadoes. All of these types of storms are strong emitters of electromagnetic energy with the heaviest concentration in the VLF portion of the frequency spectrum as shown in the graph of Figure 2.

Investigations into the signal intensity of the electromagnetic energy have failed to show that signal intensity alone can provide a source of information to differentiate between these major types of thunderstorm activity. The numerous studies and data collections conducted by Taylor, however, have produced evidence that the burst rate associated with a tornadic storm shows a significant increase over that of a nontornadic thunderstorm.

The distinguishing factor between the term "sferics" and "burst" is that a burst consists of a large number or group of sferics pulses. When sferics pulses are observed over a restricted bandwidth in the HF region the pulse rate has been observed to exceed 10^5 per second for a brief period of time. In contrast, a group of sferics, or burst, will generally have rates limited to one to three bursts per second.

The investigations of Taylor consisted of observing the number of burst rates received per unit time using various frequencies from 10 kHz to 130 MHz. The results of these efforts indicated that enhanced burst rates indicative of tornadic activity are best observed at frequencies about 1 MHz. In general, the low end of the HF band around 3 MHz is a good frequency for observing tornadic sferics.

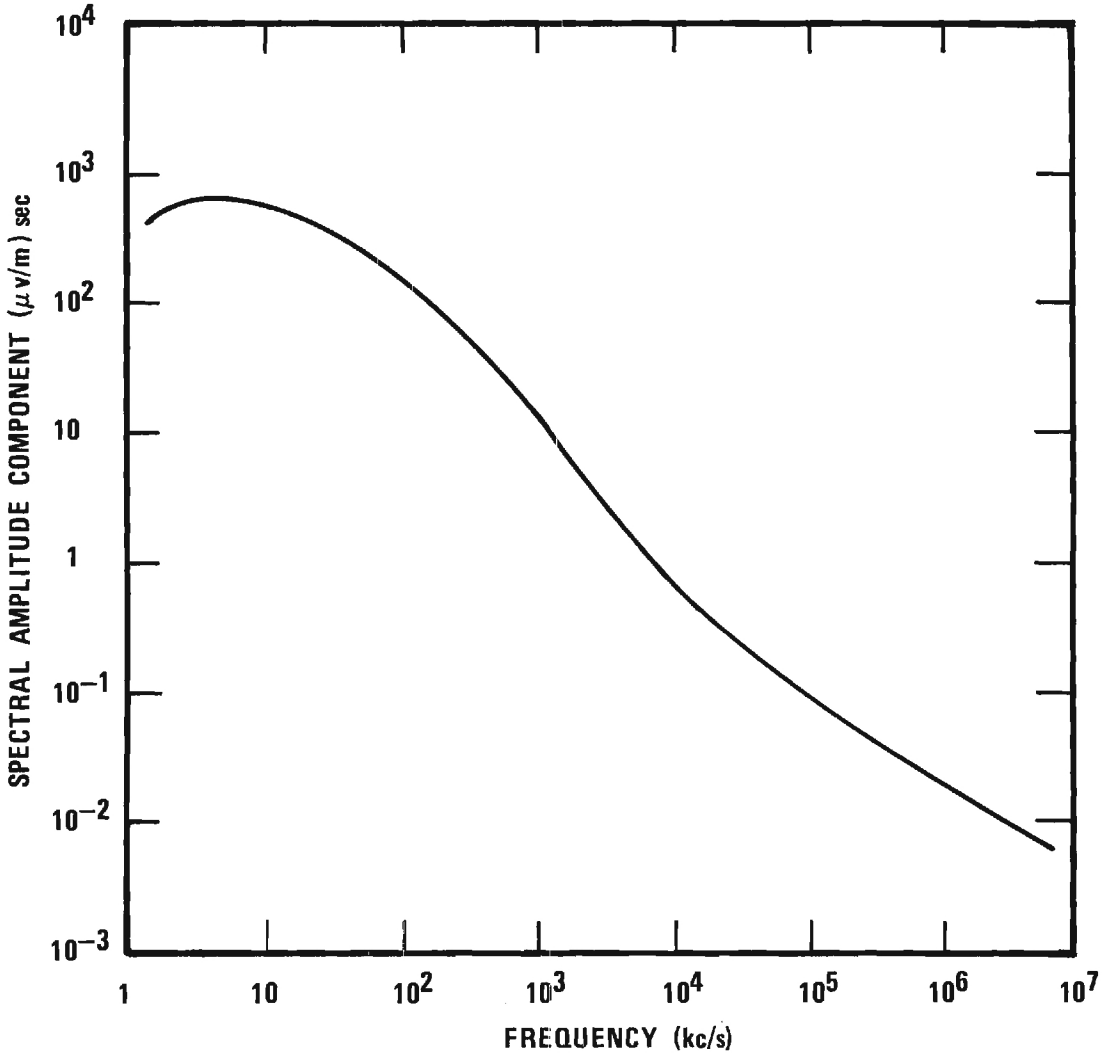

Figure 2. Frequency spectrum of the radiation components of a lightning discharge.

From ELF to MF, Taylor found that the observations were not likely to contain observable parameters sensitive to tornadic activity. Above MF, the signal attenuation losses increase significantly and ionospheric multipath effects become more severe.

The typical average field strength of these sferics signals was found to be approximately 2 volts per meter when the storm is at a distance of 40 - 50 miles from the detector, and to increase in intensity as the storm approaches. In general, the sferics are generated by cloud-to-cloud electrical discharges within the mass, although the details of the electric charge separation that produces them are not fully known.

This variation in burst rate as a function of storm type appears to be an important criterion in detecting tornadic activity within a thunderstorm. The burst rate criterion has not proved to be completely dependable for tornado detection under all circumstances. However, as will be shown later, the burst rate does indicate a good probability for detecting tornadic activity. A major uncertainty in the utility of the burst count criterion lies in the fact that most previous studies have been conducted in the midwestern United States, and at the present time there is no assurance that the sferics signature of a tornado occurring in the southeastern states would be identical to a midwestern tornado. The small amount of data collected thus far indicates that the burst count criterion is valid for the Southeast but additional study is required before any firm conclusions can be reached. The effort at Georgia Tech during the spring 1974 tornado season was one attempt to determine the validity of sferics signatures for tornado detection in the Southeast.

SECTION III

THE APPLICATION OF SFERICS TO SEVERE WEATHER RESEARCH

A number of investigators of severe weather have devised and implemented various techniques for the purpose of detecting and processing electromagnetic signals emanating from the lightning discharges that occur within severe storm cells. Instrumentation has been designed to operate at numerous frequencies ranging from VLF to VHF depending on the objectives of the particular research program. Because of the many approaches and ultimate objectives to severe weather monitoring programs, ambiguities and contradictions often seem to appear when one compares the results and conclusions of one research effort with those of others. It is likely that many of these apparent conflicts occur because of the various techniques used for data collection and subsequent processing and presentation of the sferics information.

During 1972, Taylor [2] conducted extensive tests in the midwestern states in an effort to obtain a large sampling of storm data. A major goal of this effort was to determine whether a unique signature exists for tornado-producing storms. As a part of these tests 15 radio receivers, specifically designed for reception of sferics signals, were placed in strategic areas. All receivers operated at a frequency of approximately 3 MHz. The 15 receivers were operated for a total of 66,000 hours and gathered data on 542 storms during the season. Of these storms 6 percent were later confirmed as having tornadoes, 4 percent as funnel clouds, 8 percent as hail storms, 9 percent as severe wind (non-tornadic), and 73 percent as local thunderstorms without severe weather features. The probability distribution shown in Figure 3 was derived from these data.

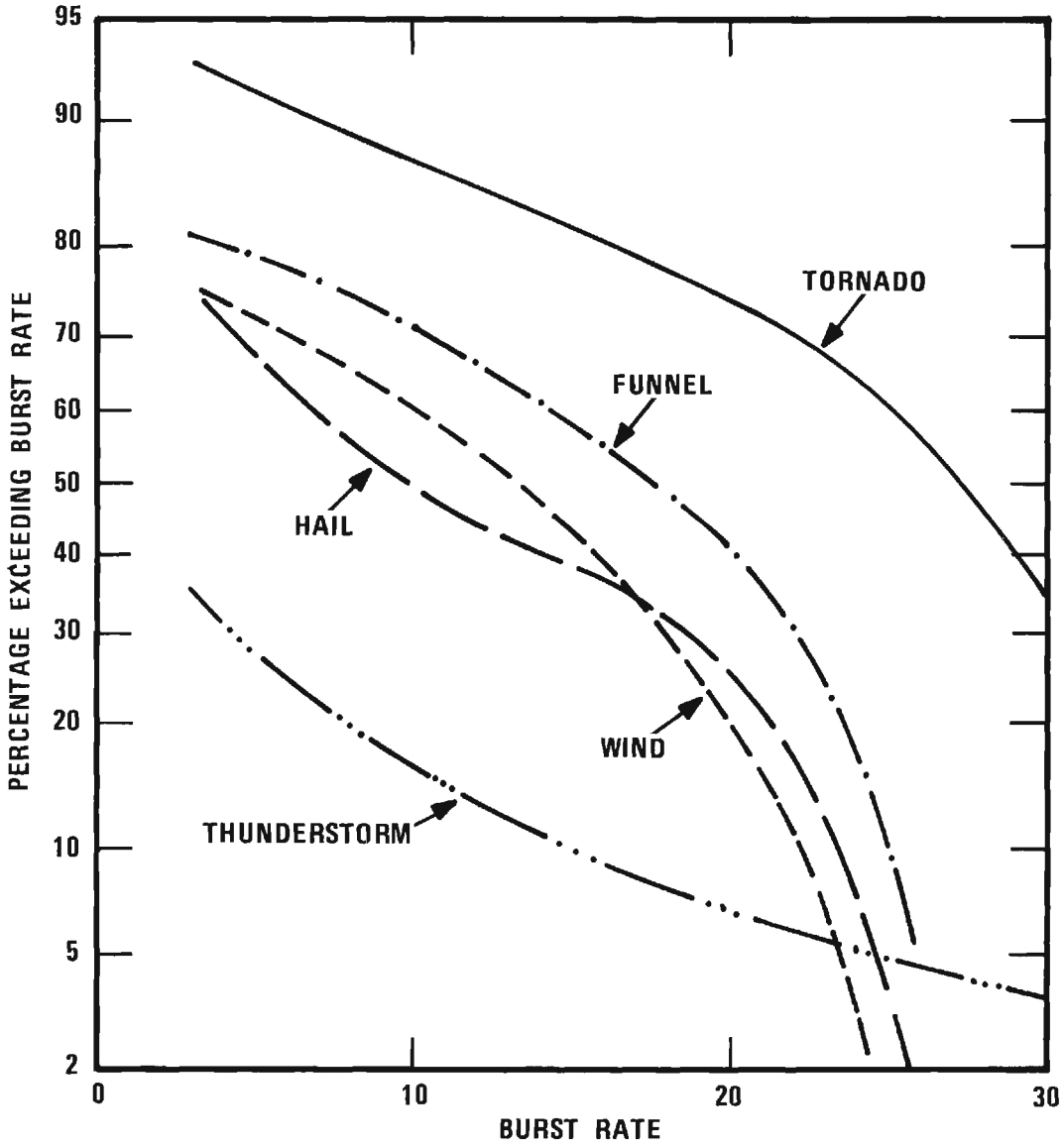

Figure 3. Probability distributions of burst rates per minute for various reported weather conditions.

The major conclusion drawn from this study was that if a burst rate in excess of 20 per minute was considered to be indicative of tornadic activity then 73 percent of the tornadoes would have been detected and 40 percent of the funnel clouds would have been registered as tornadoes. Of the hail and wind storms 27 percent would have been indicated as tornadoes, as would 6.5 percent of the local thunderstorms. From the opposite point of view, however, if a tornado warning had been issued for every high burst rate, only 25 percent of these would have been actual tornadoes or funnel clouds. This high percentage of false alarms may be due to the fact that the receivers were omnidirectional and with numerous thunderstorms covering a large geographical area the signals from all sources could partially mask the sferics signal received from any one storm cell.

In addition to Taylor's work other investigators have produced some important results. In one particular program [3] vertically and horizontally polarized signals in the VLF region of the frequency spectrum were simultaneously monitored during periods of severe weather. The average power of the received signals was computed over one-minute time frames. The resulting data showed an increase in the magnitude of the horizontally polarized signal, relative to the vertically polarized, as the severity of the storm increased. The implication of these results was that the horizontal intra-cloud lightning discharges increase more than the cloud-to-ground discharges as the storm increases in severity.

During another study [4] data were obtained on twelve tornadoes with eleven of the twelve showing a sferics pulse rate increase over nontornadic thunderstorms. In contrast, the electrical activity of thunderstorms without tornadoes was characterized by strong but isolated bursts of sferics signals.

An important implication of this research effort was that frequencies above about 1 MHz may provide far better indicators of tornadic activity, which agrees with Taylor's results.

Radio direction finding (DF) techniques have been used in a number of research efforts for the purpose of locating and tracking sferics activities. However, none of these investigations has incorporated burst rate measurements with the DF techniques. In general these programs have used equipment designed to operate at various frequencies ranging from VLF to MF with the efforts directed to both location and degree of activity of the electromagnetic signals. In some of the programs the DF system was operated in conjunction with a weather radar for the purpose of correlating the sferics activity with storm parameters derived from the radar data.

In a program conducted by General Mills for the National Weather Service (formerly U.S. Weather Bureau) [5] a radio direction-finding system, termed SPARSA (Sferics Pulse Amplitude Rate Spectrum Analyzer), was used in conjunction with a weather radar to observe the correlation between the radar and sferics data. The operating frequency of the SPARSA system was selected to be 500 kHz which was prompted in part by earlier unsuccessful efforts by the U.S. Air Force, Air Weather Service [6,7], to correlate 10 kHz sferics data with radar data and by additional supporting data from Jones and Kelley [8] which indicated that severe weather conditions could be correlated with sferics data at frequencies above the VLF portion of the spectrum. The SPARSA system utilized a rotating antenna and a 64-element sample-and-hold array to derive a voltage proportional to the sferics pulse rate for each 5.6-degree azimuth segment. The sferics-rate-voltages were subsequently applied to an oscilloscope to provide a polar plot with the position of the

line indicating the direction of arrival and the length being proportional to the sferics rate. Some of the conclusions drawn from this program include (1) severe weather as defined by the National Weather Service (NWS) does not occur without 500 kHz sferics activity, (2) most severe weather occurs during the rapid buildup of sferics activity, (3) 98 percent of the sferics activity originates in cloud regions definable as radar echoes, and (4) an increasing sferics count rate is related to the severity increase in a thunderstorm. This research program did not come to any conclusions that would indicate an ability to distinguish thunderstorms with and without tornadoes.

The SPARSA system was used later in a research effort conducted by the National Severe Storms Laboratory (NSSL) [9]. The conclusions reached by NSSL were less favorable than those reached by the previous investigators [5]. NSSL reported that the SPARSA response to damaging wind and hail events is variable; and although the SPARSA showed little or no response when thunderstorms were absent, a strong response may or may not occur when severe storms are present. NSSL further concluded that the sferics rate trends were not sufficiently regular to provide a short-period prediction of a pending storm or for discrimination of a severe event if the occurrence took place within a large storm system.

In a study conducted by Montana State University for the U.S. Forest Service [10], a VLF radio direction-finding system was designed and operated for the purpose of locating areas of severe lightning activity that would represent a potential threat for forest fires. The DF system which operated at 10 kHz used a conventional crossed loop Watson-Watt antenna and tuned radio frequency (TRF) receivers to provide a polar oscilloscope display. An incoming sferics pulse signal was displayed as a transient line radiating

from the scope center at the azimuth of arrival of the sferics signal. The length of the line was proportional to the signal strength. In addition to the polar display, a bar-chart capability was included also in the form of an oscilloscope display. In the bar-chart display any one of the four quadrants could be selected with the given quadrant being divided into 30 sectors of 3 degrees each. Each sferics signal arriving on a bearing within the selected quadrant was recorded as one event in its appropriate sector. The total number of events in each sector was displayed as an amplitude on the oscilloscope. The field tests of this lightning location system included the placement of one DF system in Seattle, Washington, and a second system in Medford, Oregon. It was hoped that triangulation could be used to locate areas of heavy lightning activity accurately over a large area of the northwestern portion of the United States, but the program encountered many problems.

Attempts at triangulation over an area of 10^6 square miles proved to be difficult because of (1) an inability to achieve visual or other confirmation of suspected areas of heavy lightning activity, (2) a problem of obtaining geographical maps with suitable detail and accuracy, and (3) polarization errors. In regard to polarization errors, it was determined that VLF daytime errors of up to 15 degrees could exist whereas nighttime errors could be as high as 40 degrees. The triangulation problem and a design/implementation problem with the bar-chart display resulted in very little positive output from this research effort.

SECTION IV

RADAR STUDIES OF METEOROLOGICAL TARGETS

Just as sferics can indicate storm severity on the basis of high burst rate counts, radar is an invaluable tool to those involved in meteorological research. The microwave signal transmitted by the radar is reflected by the hydrometeors (raindrops, hail, ice crystals) associated with the storm mass. The aviation industry, both private and commercial, depends on radar as a severe weather avoidance aid, and operational meteorologists depend on radar to show the movement of weather systems accompanied by precipitation. Those involved in severe weather research use radar as a remote sensor to study the dynamic processes that lead to the formation and growth of thunderstorms.

The basic meteorological radar usually consists of a transmitter/receiver system, a pencil beam antenna steerable in azimuth and elevation, an indicator that displays range and elevation (Range Height Indicator) and an indicator that displays range and azimuth simultaneously (Plan Position Indicator). A basic system having the features described can tell the meteorologist the location of the embedded severe cells within range of the radar, the area covered by precipitation, the speed of movement of the weather mass, and the vertical extent of the storm. The speed and direction of movement, area of precipitation, and cell top heights can serve as an indicator of the storm's severity. Radars with reflectivity measurement capability add another important parameter that can be used to determine storm severity. Numerous studies link areas of tornado occurrence with areas of high radar reflectivity (i.e., heavy rainfall or hail).

A. Rainfall Measurement

A convenient form of the radar equation for meteorological applications [11] is:

$$\overline{P}_r = 0.468 \frac{P_t \lambda^2 G^2 \theta^2 h \eta}{r^2} \quad (1)$$

where

$\overline{P}_r$ = average power received by the radar (watts)

P_t = power transmitted by the radar (watts)

λ = radar wavelength (meters)

G = antenna gain along the main axis (dimensionless)

θ = half-power beamwidth, horizontal or vertical (degrees)

h = length of the radar pulse (meters)

η = reflectivity, cross section per unit volume (inverse meters)

r = range to the resolution cell (meters).

The important parameter in this equation is the reflectivity η, which is equal to the scattering cross sections of all the raindrops within the radar resolution cell divided by the total volume of the cell. When the drops are small in size compared with the radar wavelength λ, the scattering cross section derived from electromagnetic theory is proportional to the sixth power of the drop diameters. It is convenient to define a quantity Z, called the reflectivity factor, which is equal to the total of the sixth powers of all the drop diameters. Thus if the drops having diameters D_1, D_2, D_3, etc., are present in number concentrations N_1, N_2, N_3, etc., respectively, then the reflectivity factor Z is given by

$$Z = N_1 D_1^{\,6} + N_2 D_2^{\,6} + N_3 D_3^{\,6} + \ldots . \quad (2)$$

The reflectivity factor is related to the reflectivity η by

$$\eta = \frac{\pi^5 |K|^2 Z}{\lambda^4} \qquad (3)$$

and has units of cubic meters. The parameter K is related to the dielectric constant of water.

Two assumptions implicit in the formulation of the radar equation should be noted. Equation (1) implies that the scattering or absorption of the radar signal by the precipitation is very small compared to the radar signal strength. If this assumption is not valid (for example, in very heavy rain) then signals returned from deep within a storm can give erroneously low values of reflectivity. Equation (1) also assumes that the raindrops (or ice crystals) are distributed uniformly within the radar resolution cell. This assumption is generally valid for meteorological measurements except near the edge of a storm or near a sharply defined rain or hail shaft.

The rainfall rate R, commonly expressed in millimeters per hours, is defined as the total volume of the raindrops multiplied by their fall speed. For the distribution described above the rainfall rate is given by

$$R = 1.89 \times 10^6 \{N_1 V_1 D_1^3 + N_2 V_2 D_2^3 + N_3 V_3 D_3^3 + \ldots\} \quad . \qquad (4)$$

Thus the exact relation between Z and R depends on the distribution of drop sizes. A considerable body of research has documented Z-R equations appropriate to various types of rain, including thunderstorm rain. Many of these are given by Battan [12]. It should be noted that these formulations apply also to ice crystals or snow, with a different value of $|K|^2$ for ice, and D representing the equivalent melted diameter.

In cases of hail or heavy rain in which the drops may be too large (relative to the wavelength) for Equations (2) and (3) to be valid, one cannot

relate the reflectivity to rainfall rate so easily. In these cases (and for operational purposes in general) one uses the reflectivity or the "equivalent reflectivity factor" Z_e, defined as $(\eta\lambda^4/(\pi^5 |K|^2)$, as a relative measure of storm intensity. The National Weather Service uses a particular value of Z_e, for example, as one of its criteria for issuing severe weather warnings.

B. Practical Limits of Radar Measurements

The measurement of meteorological parameters by radar is subject to limits imposed by the radar design and by the atmosphere. The most obvious is the size of the volume in space that can be resolved by the radar. This so-called resolution cell is approximately a cylindrical volume of radius $0.0175\ r\ \theta$ and length (along the beam) $h/2$. Echo power represents an average in this volume, and the dimensions of the cell define the accuracy of measurements of storm geometry. Because the volume of the cell increases as the square of the range, the assumption of uniform distribution of scattering elements in the beam becomes more uncertain. Also, because the radar sensitivity is defined by a minimum detectable power in the receiver, the minimum detectable reflectivity increases as the square of the range.

Attenuation, neglected in the formulation of Equation (1), can be significant in heavy rain, or hail. It can be a major factor in quantitative reflectivity measurements, and must be considered when computing rainfall rates. Even in cases where quantitative measurements are not required, attenuation can cause distortion of echo shape, in that the echo on the far side of a precipitation or hail shaft may appear erroneously weak. Examples of attenuation in very heavy rain (40 mm/hr) are 1 dB/km for 3-cm radars and 0.012 dB/km for 10-cm radars such as the National Weather Service WSR-57.

All radars are plagued by "clutter," which is loosely defined as signal echoes from anything other than what one wants to detect. In the case of weather observations, clutter includes echoes from the ground, trees, buildings, aircraft, and birds. At long ranges some of these echoes can be eliminated by raising the beam slightly in elevation; others are overwhelmed by the much larger echo from the weather target. At close range, perhaps as far as 20 - 30 miles, ground clutter can be a problem. The clutter can be "blanked out" by range gating techniques, or the clutter can be suppressed selectively through appropriate data processing. The latter approach is preferable, of course, as the removal of the closest 20 miles of coverage destroys valuable data on the low-altitude weather structure.

Other limits on the accuracy of radar measurements are due to the effects of variations in the atmospheric refractive index, which may cause the radar beam to deviate from the normal line of sight. These effects tend to be difficult to predict or measure, but are generally much less significant than other factors in the observation of severe storms.

SECTION V

THE TORNADO SIGNATURE AS DETECTED BY CONVENTIONAL PULSE RADAR

Studies have been conducted for the past 30 years in an attempt to link observable radar parameters to severe thunderstorm and tornado formation. These studies have yielded five major radar-detectable signatures which have been accepted as valid indicators of severe weather. These are (1) "hook"-shaped echoes displayed on the PPI, (2) precipitation-free "vaults" displayed on the RHI, (3) echoes with Z (or Z_e) exceeding 10^5 mm^6/m^3, (4) top height measurement, and (5) thunderstorm cell rotation and, in some cases, converging or diverging cells. None of these indicators is absolute and any one could be missed by a radar observer occupied with tracking multiple thunderstorms on his display.

A. History of "Hook" Echo Detection

One of the first records of radar being used for the detection of a tornado appeared in June 1953 by G. E. Stout and F. A. Huff [13]. They reported that while a performance test was being run on their APS-15 (3 cm) radar on 9 April 1953 between 4:45 p.m. and 8:00 p.m. CST, the operator noticed a "hook" echo accompanying a heavy precipitation return. Several hours later it was learned that a tornado had occurred at a point corresponding to where the "hook" had been located on the PPI, 35 miles north of the radar site in Illinois. The tornado caused 3 million dollars damage to property. Correlation of radar scope data and the tornado path confirmed that the "cyclonic curl" or "figure-6 hook" displayed on the PPI was the tornadic signature.

Since the initial discovery of the "hook" phenomenon in 1953, hundreds of other cases of "hook"-shaped echoes associated with mesoscale cyclonic circulation (tornado formation) have been documented. Figure 4 is a photograph of the radar PPI from television station WHIO, Dayton, Ohio, the day of the Xenia, Ohio, tornado. (The ellipticity of the range marks is caused by a nonlinear sweep in the monitor.) Range marks occur at 20-mile intervals in Figure 4 and the classic "hook" can be seen 18 miles southeast of Dayton, Ohio, on the southwest corner of the parent thunderstorm located east of the city. Figure 5 shows the "hook" after the initial formation. The range on the radar has been changed to display one range mark each 10 miles and Xenia appears at the tip of the "hook."

B. "Hook" Formation Theories

There are several theories of how the "hook" echo forms. Fulks [14] constructed a tornado model which attempted to explain the occurrence of the "hook" echo in the southwest corner of the thunderstorm cell when it is moving on an eastward track. Fulks' model hypothesized wind shear acting on the large convective tower to produce the cyclonic flow that gives rise to the development of the "hook."

Fujita's theory of "hook" development [15] assumed a rotating updraft core that interacts with the ambient wind to give the core a translational motion relative to the principal cloud mass. The radar detectable "hook" appears as the displaced rotating core draws precipitation particles out from the cloud. Fujita further concluded that the "hook" echo is an indication of the pre-existing vortex concentrated in the storm core.

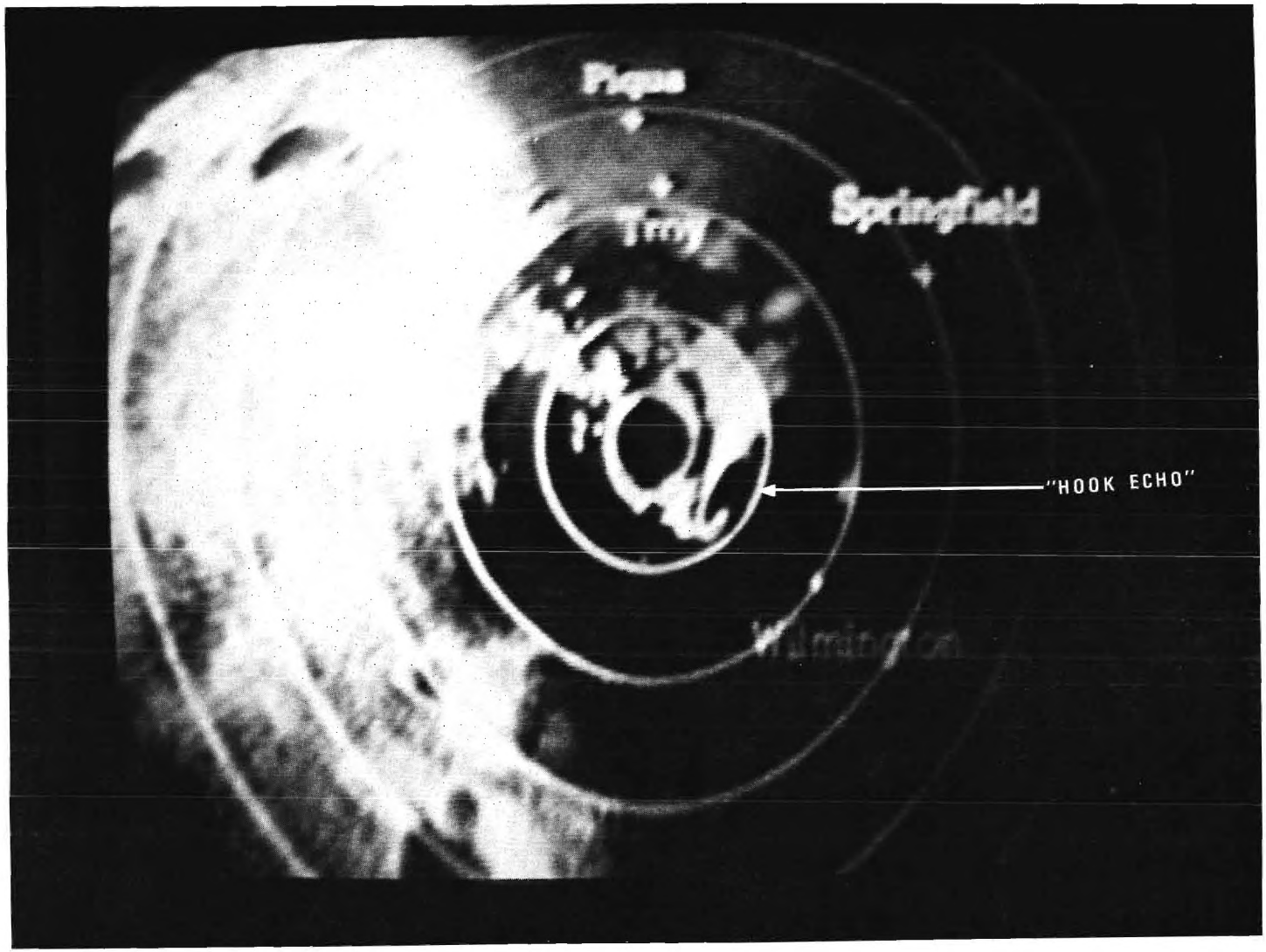

Figure 4. The Xenia, Ohio, tornado "hook" displayed on the WHIO-TV radar with 10-mile range marks. The ellipticity and stretch of picture caused by monitor problems.

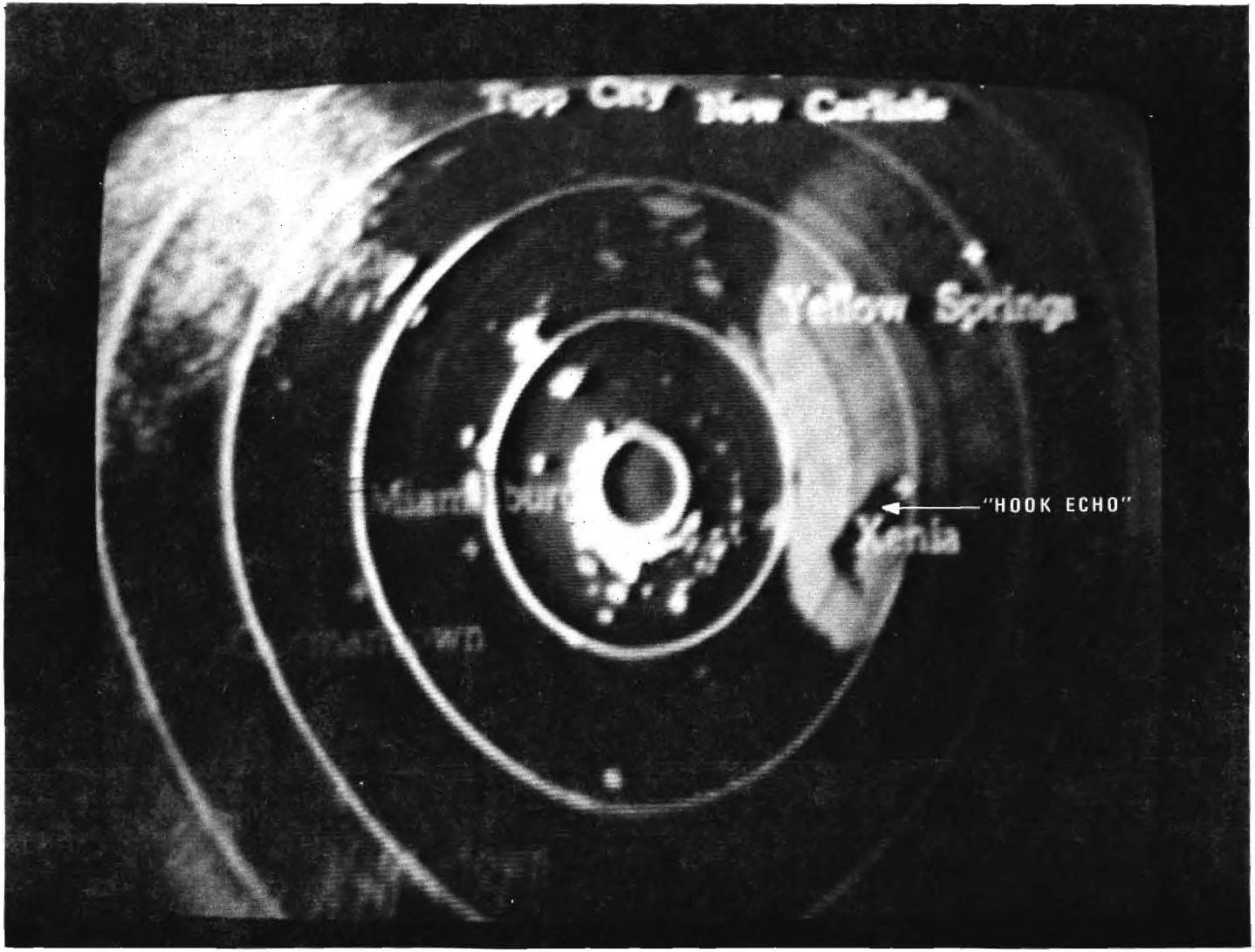

Figure 5. The Xenia, Ohio, tornado "hook" displayed on the WHIO-TV radar with 10-mile range marks. The ellipticity and stretch of picture caused by monitor problems.

C. Practical Limits of "Hook" Echo Detection

The radar parameters are important if "hook" echoes are to be properly resolved at moderate and long ranges. The pulse width must be sufficiently short and the antenna beam sufficiently narrow to ensure adequate spatial resolution of the echo. However, the most important link in the system is the operator. There is no assurance that the operator will recognize the "hook" at great ranges (i.e., 100 nmi).

The operator may fail to recognize the "hook" because his attention is divided between the numerous cells on the display other than the one producing the tornado, or the size of the precipitation-free area within the "hook" may physically appear too small to resolve when the PPI is scanning long ranges. For example, on a PPI scope face measuring 12 inches across, with the scan from the center to the edge representing a range of 125 nmi, a precipitation-free vault area described by a 5 x 5 square mile area, at a range of 100 nmi the area would measure approximately 1/4 x 1/4 inches. Under stress the radar operator may miss completely a "hook" surrounding this area. More important, a "hook" at these ranges may appear as one of numerous irregularities in the precipitation patterns on the scope.

The literature suggests that the "hook" is visible usually at radar look elevations less than 10,000 feet, but sometimes as high as 20,000 feet. At greater elevations the radar return forming the apparent finger on the "hook" merges with the returns from heavier precipitation suspended aloft to close the hole within the "hook" on the radar display. The precipitation-free holes within the "hook" may vary in size. The Xenia tornado "hook" shown in Figure 5 measures less than 5 miles in its longest dimension. Numerous researchers report that the vault area may be as small as 1 or 2 miles across. Studies

of historical radar PPI photographs taken during tornado occurrence confirm that of the majority of tornadoes studied, few had vaults exceeding diameters greater than 2 nmi. Thus, it may be concluded that the "hook" is a fairly reliable indicator of tornado activity if the radar can resolve small areas at long ranges and the operator is able to recognize the "hook" embedded in precipitation.

D. Georgia Tornadoes

Figure 6 (A-P) demonstrates the problem of tornado detection on the basis of "hook" echo recognition alone. Radar PPI photographs were obtained from the National Weather Service (NWS) for the periods when 15 tornadoes occurred in Georgia as reported in the Storm Data Summary published by the NWS. The time (Greenwich Mean Time) of the photograph appears on the 24-hour clock in the upper right-hand corner of the photograph. The time shown in the caption under each photograph corresponds to the Eastern Standard Time (EST) when the tornado was reported to have occurred. In Figure 6, the locations of the tornadoes have been purposefully deleted in order to illustrate the difficulty of locating "hook" echoes on a cluttered PPI display. The photographs in Figure 7 (A-P) show the location of each tornado. "Hooks" are apparent in several of the photographs; however, in many cases the quality of the photographs or radar resolution is too poor to allow the small precipitation-free area within the "hook" to be immediately distinguished.

The difficulty of locating precipitation-free areas in the photographs, due to film and possibly radar resolution, suggests several observations. It may be inferred that most of the tornadic thunderstorms in Georgia have small precipitation-free vaults on the order of less than 2 miles across at the

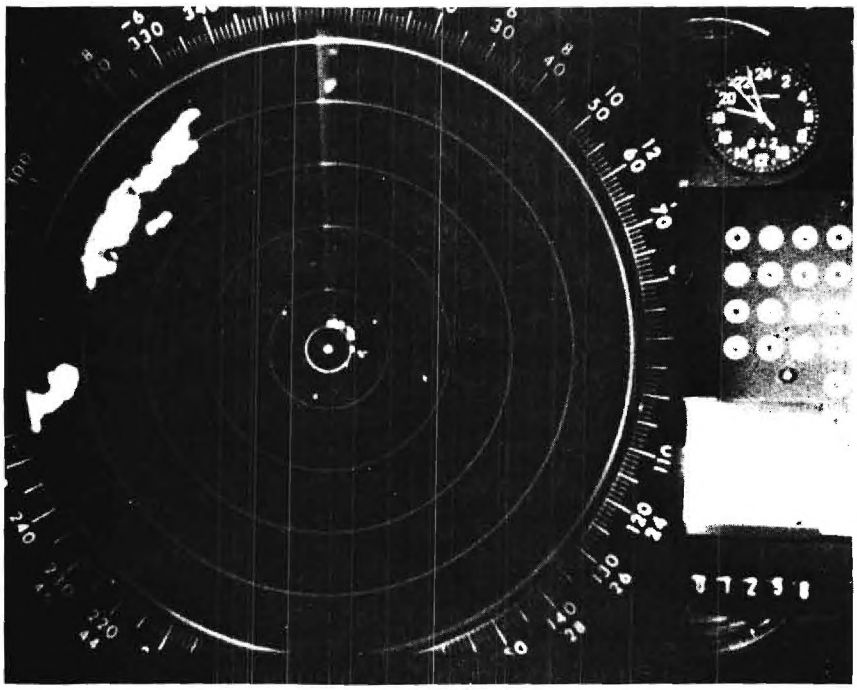

(a) Radar scope photograph from Waycross of tornado occurring in Bainbridge on 1–12–75 at 1:45 p.m. EST.

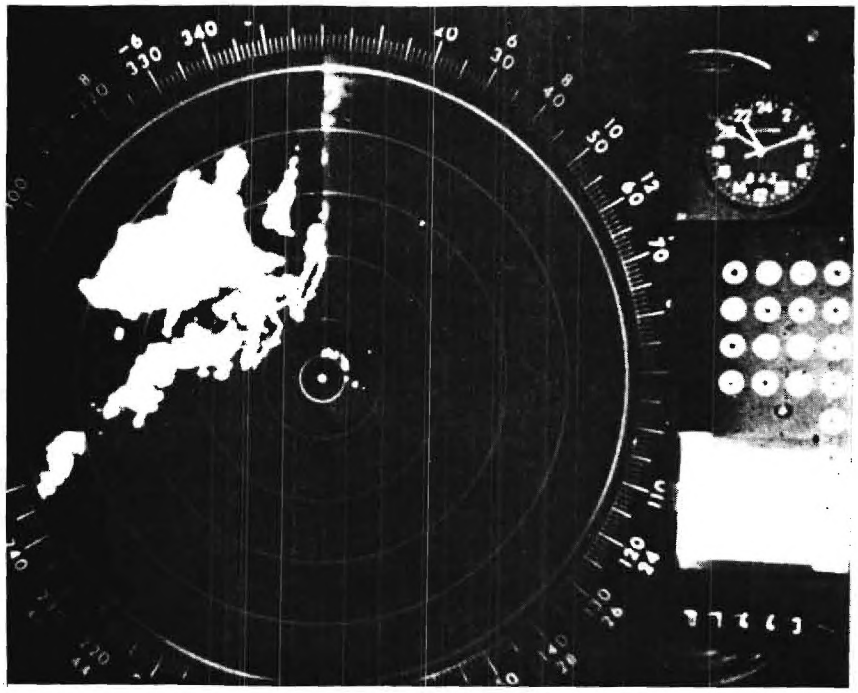

(b) Radar scope photograph from Waycross of tornado forming at 4:50 p.m. Occurrence was in Lyons on 1–12–75 at 5:15 p.m. EST.

Figure 6. Photographs of National Weather Service radar during periods of known tornado occurrence with tornado locations intentionally omitted.

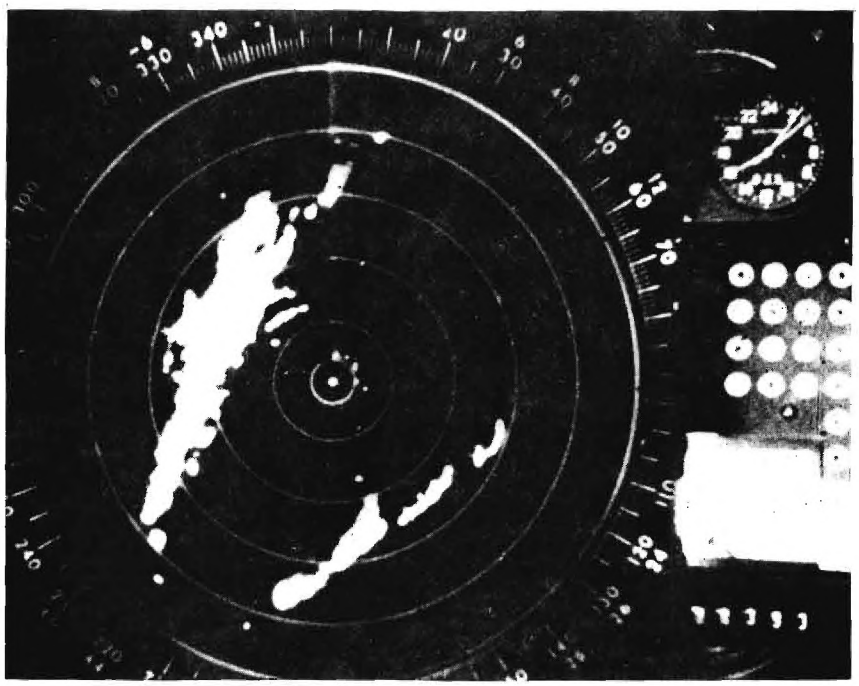

(c) Radar scope photograph from Waycross of tornado occurring in Nashville on 1–25–75 at 11:06 a.m. EST.

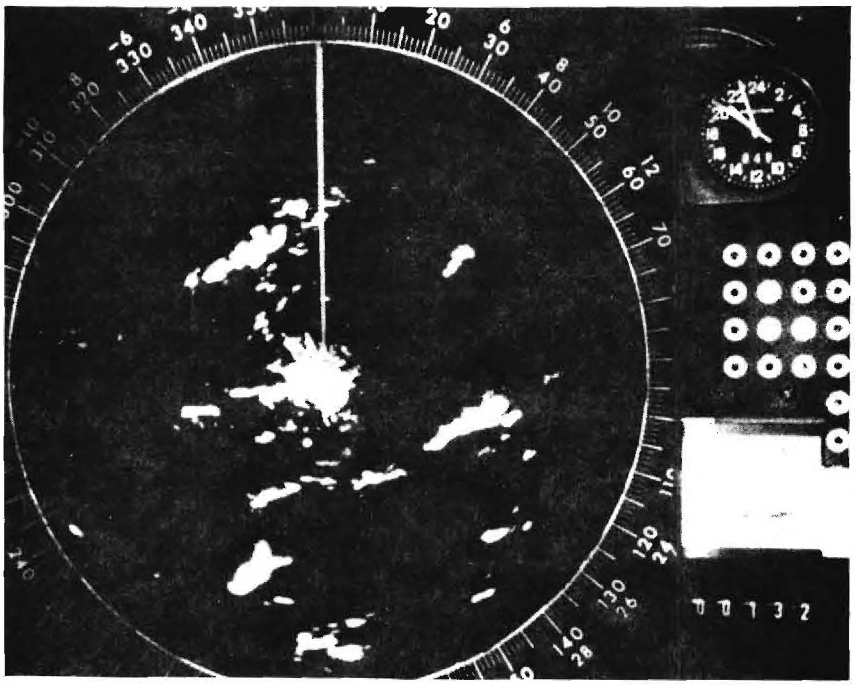

(d) Radar scope photograph from Athens of thunderstorm at 3:51 prior to tornado occurrence at 4:07 p.m. EST at Fort Valley on 2–18–75.

Figure 6 (Continued),

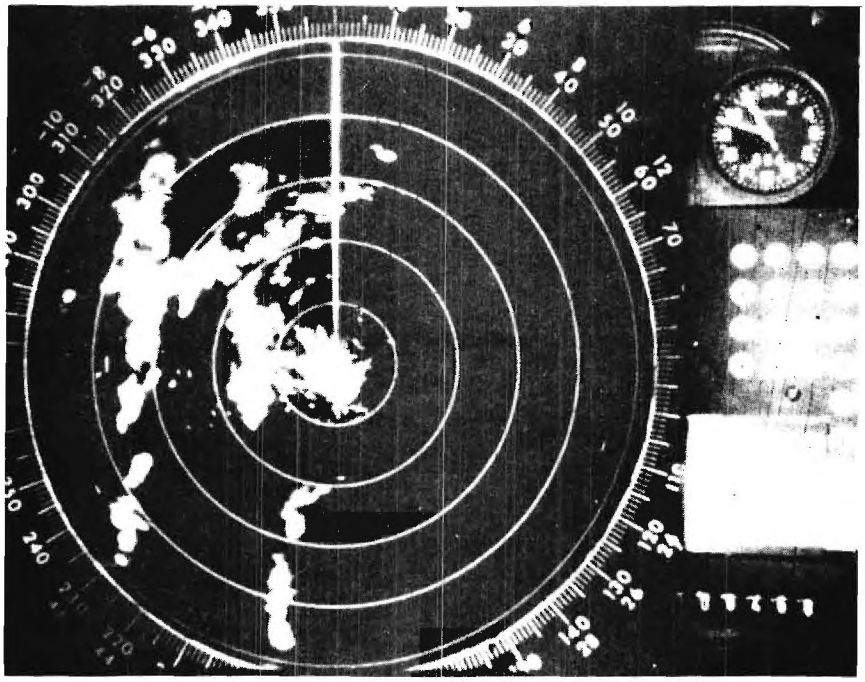

(e) Radar scope photograph from Athens of tornado occurring in Douglas County area on 2–23–75 shortly before 6:00 p.m. EST.

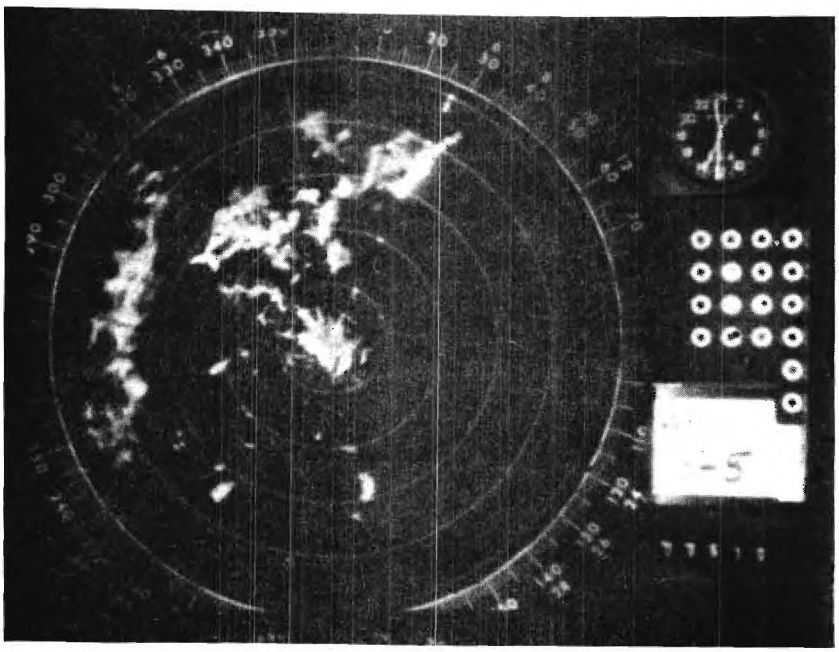

(f) Radar scope photograph from Athens of tornado occurring in Cobb County on 2–23–75 at 6:30 p.m. EST.

Figure 6 (Continued).

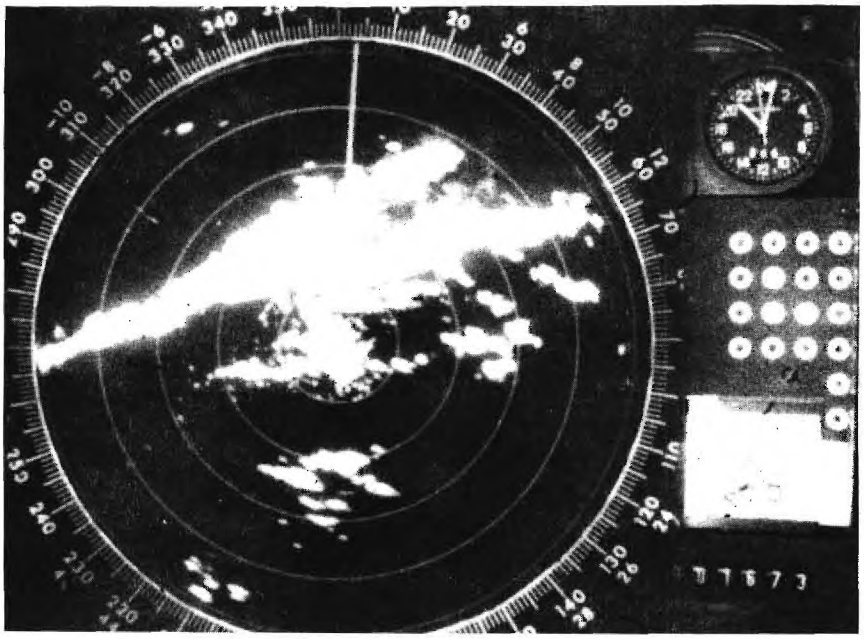

(g) Radar scope photograph from Athens of tornado occurring in Coal Mountain on 3–7–75 at 4:00 p.m. EST.

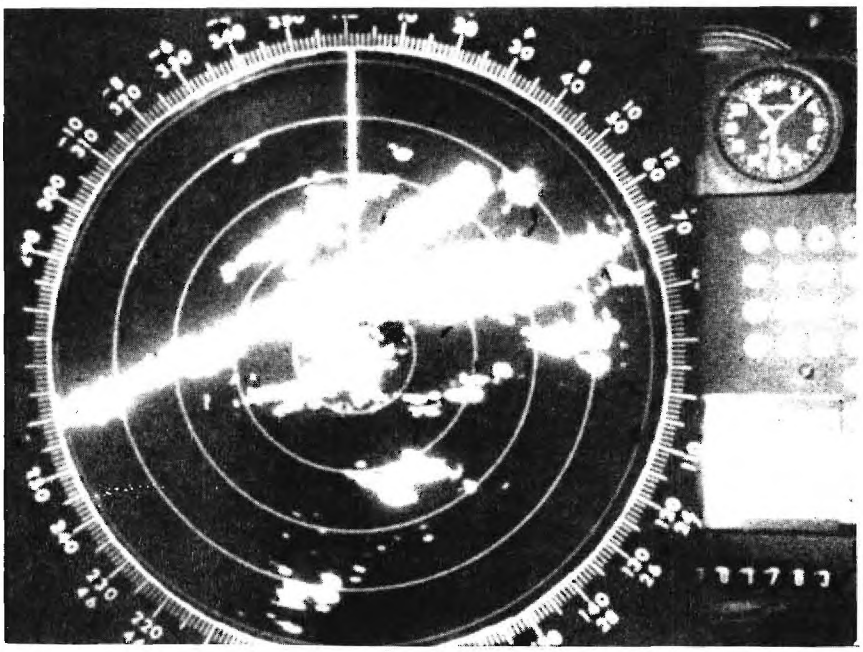

(h) Radar scope photograph from Athens of tornado occurring in Cobb County on 3–7–75 at 4:30 p.m. EST.

Figure 6 (Continued).

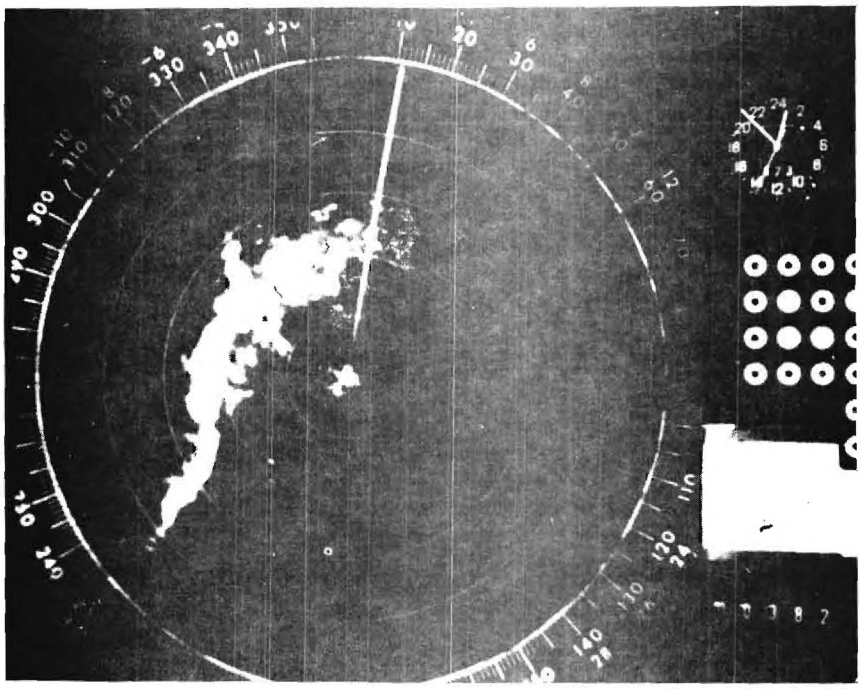

(i) Radar scope photograph from Athens of tornado occurring in south Fulton area on 3–13–75 at 7:50 p.m. EST.

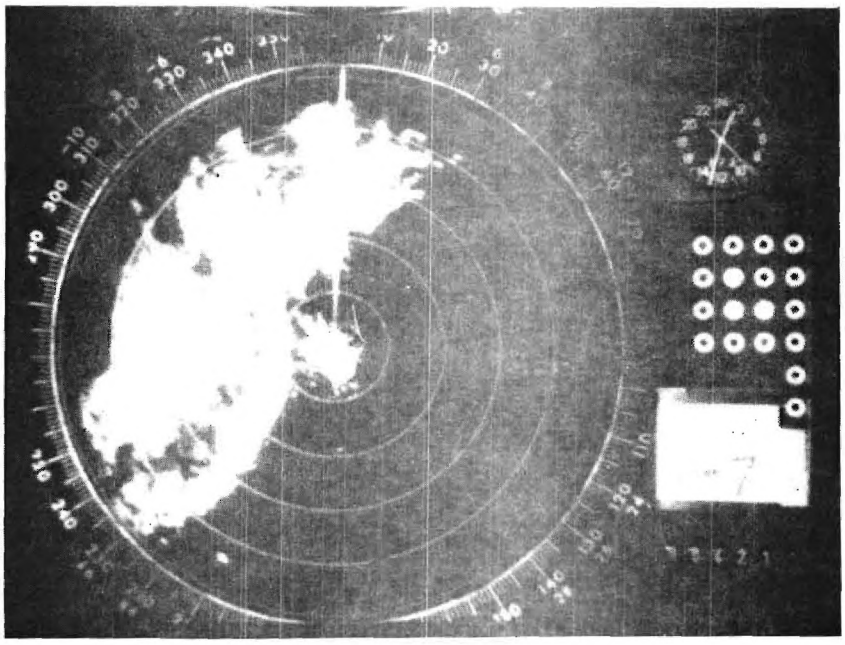

(j) Radar scope photograph from Athens of tornado occurring in Alpharetta on 3–13–75 at 8:33 p.m. EST.

(Figure 6 (Continued).

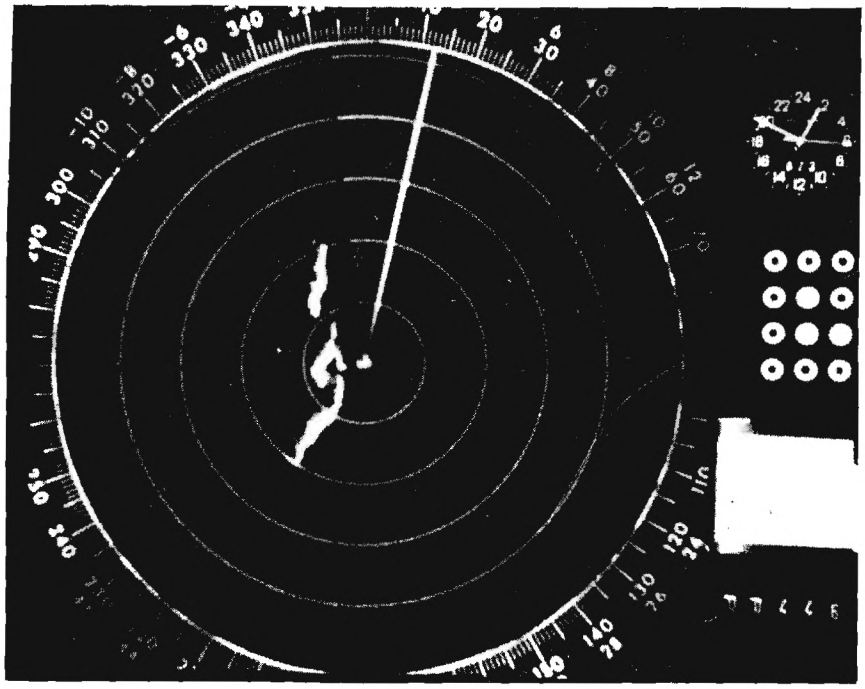

(k) Radar scope photograph from Athens of tornado occurring in Athens area on 3–13–75 at 8:50 p.m. EST.

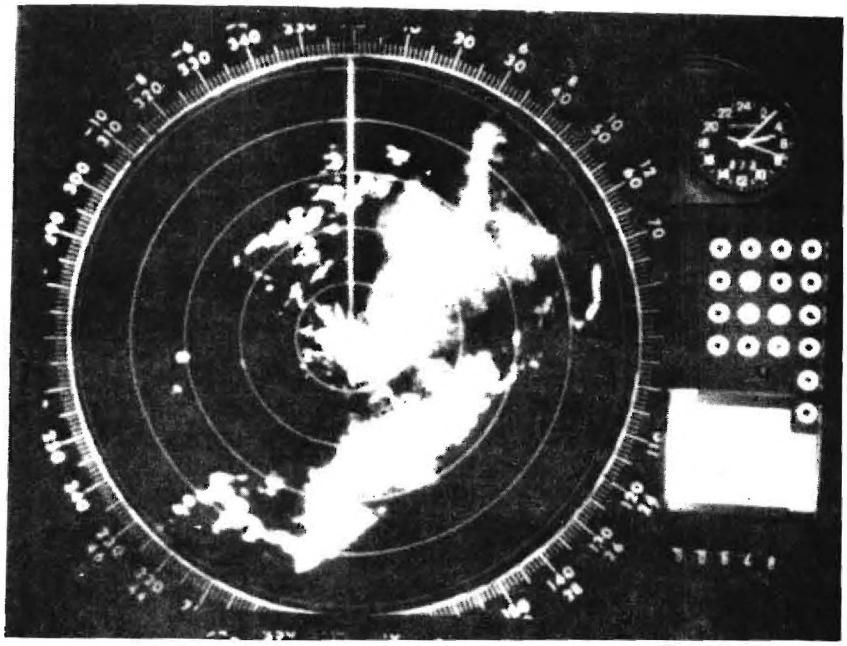

(l) Radar scope photograph from Athens of tornado occurring in Byromville on 3–14–75 at 12:07 a.m. EST.

Figure 6 (Continued).

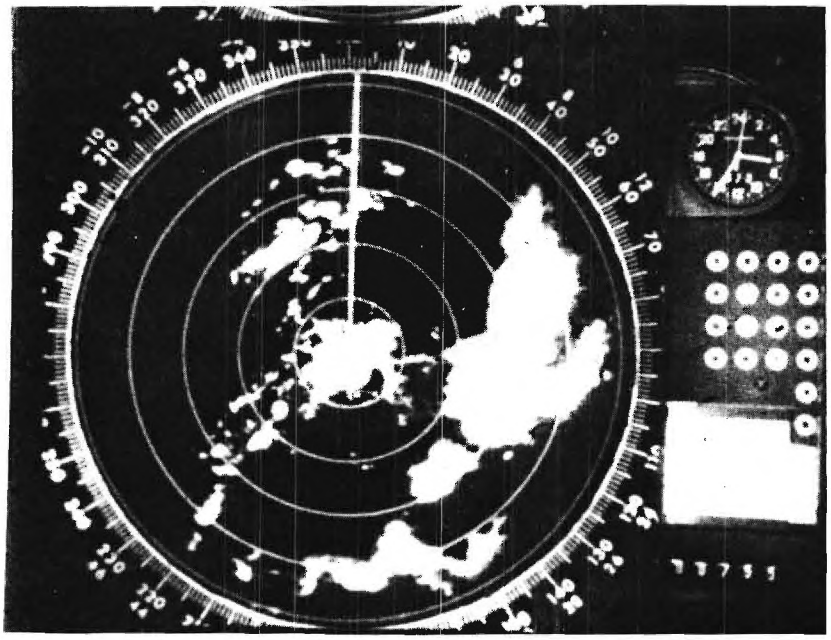

(m) Radar scope photograph from Athens of tornado occurring in Washington County on 3–14–75 at 1:35 a.m. EST.

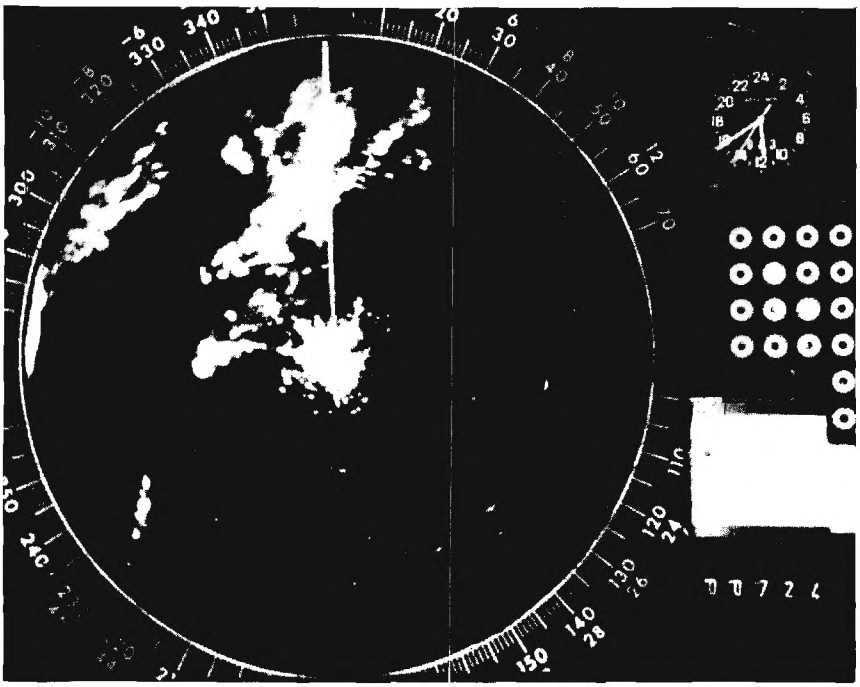

(n) Radar scope photograph from Athens of tornado occurring in Atlanta on 3–24–75 at 6:29 a.m. EST.

Figure 6 (Continued).

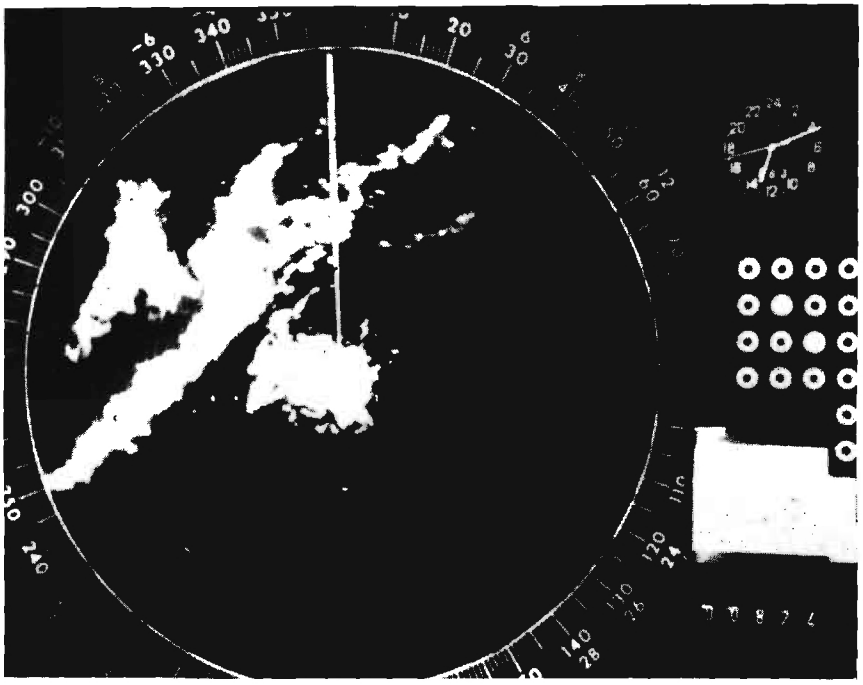

(o) Radar scope photograph from Athens of tornado occurring in Shannon area on 3–24–75 at 8:40 a.m. EST.

Figure 6 (Concluded).

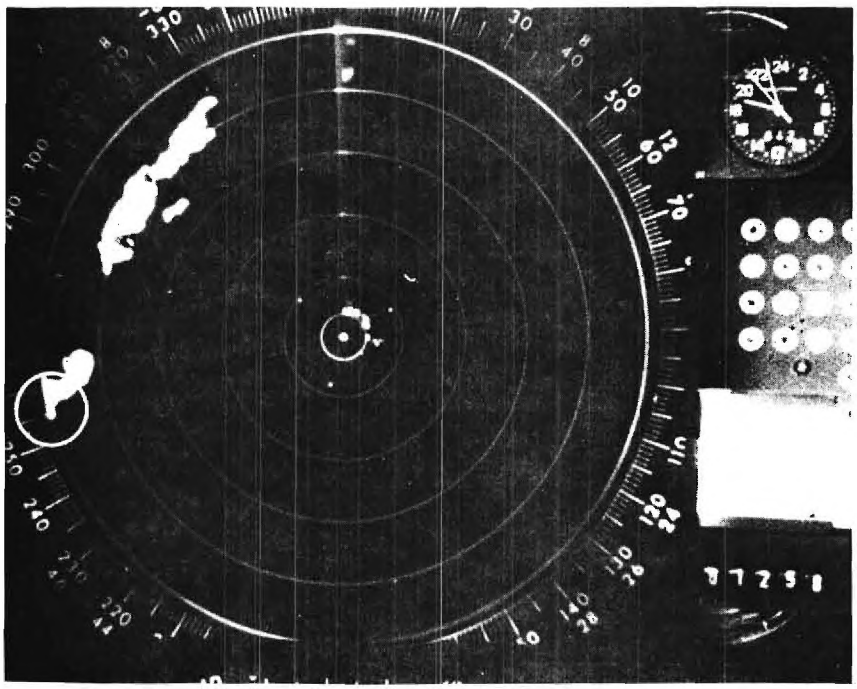

(a) Radar scope photograph from Waycross of tornado occurring in Bainbridge on 1–12–75 at 1:45 p.m. EST.

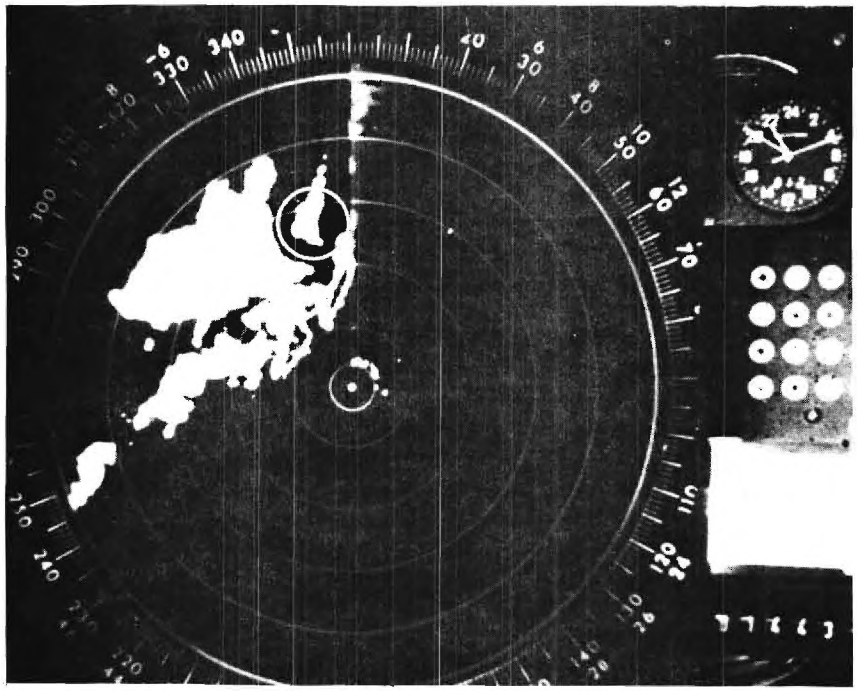

(b) Radar scope photograph from Waycross of tornado forming at 4:50 p.m. Occurrence was in Lyons on 1–12–75 at 5:15 p.m. EST.

Figure 7. Photograph of National Weather Service radar during periods of known tornado occurrence with tornado locations shown.

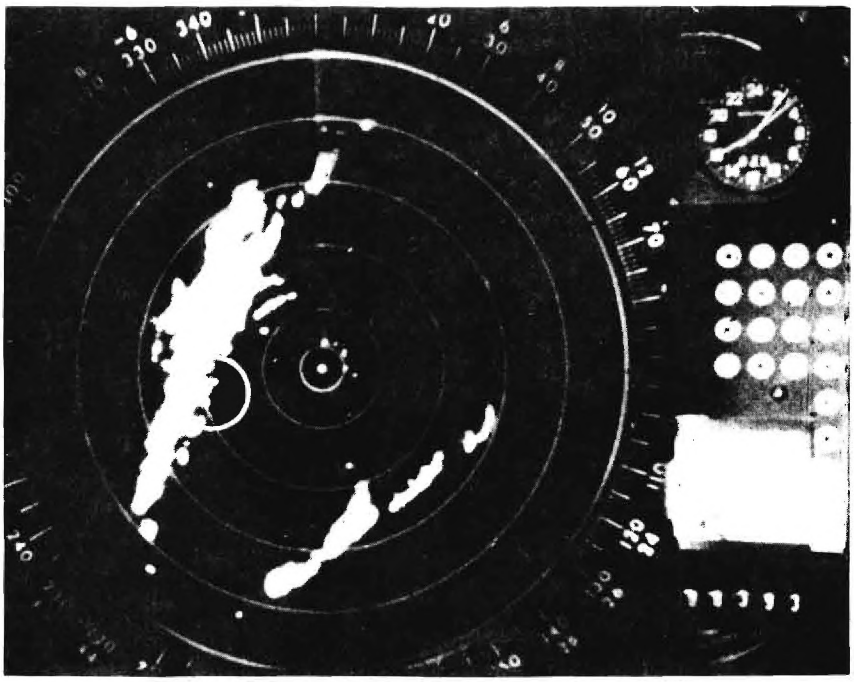

(c) Radar scope photograph from Waycross of tornado occurring in Nashville on 1–25–75 at 11:06 a.m. EST.

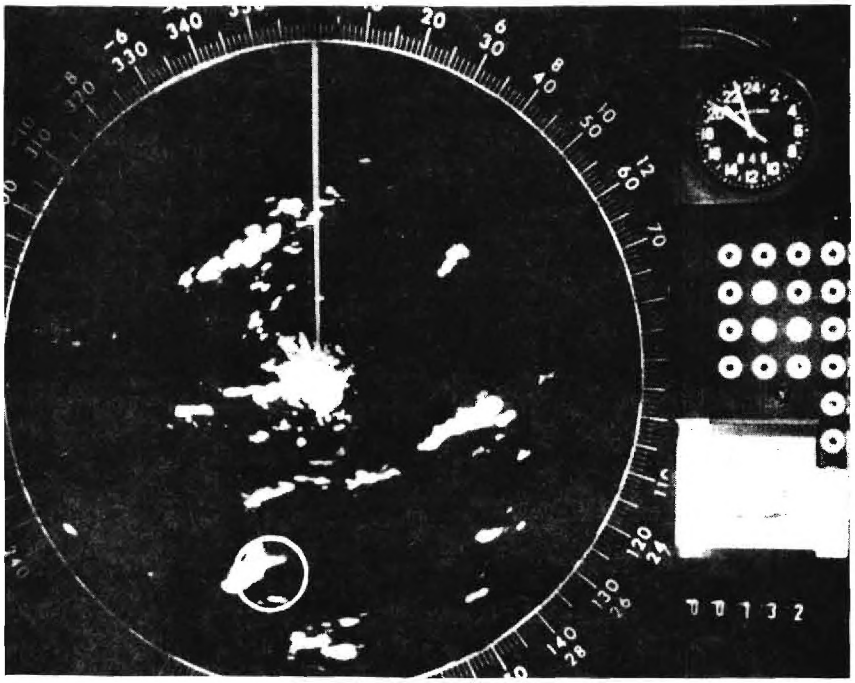

(d) Radar scope photograph from Athens of thunderstorm at 3:51 prior to tornado occurrence at 4:07 p.m. EST at Fort Valley on 2–18–75.

Figure 7 (Continued)

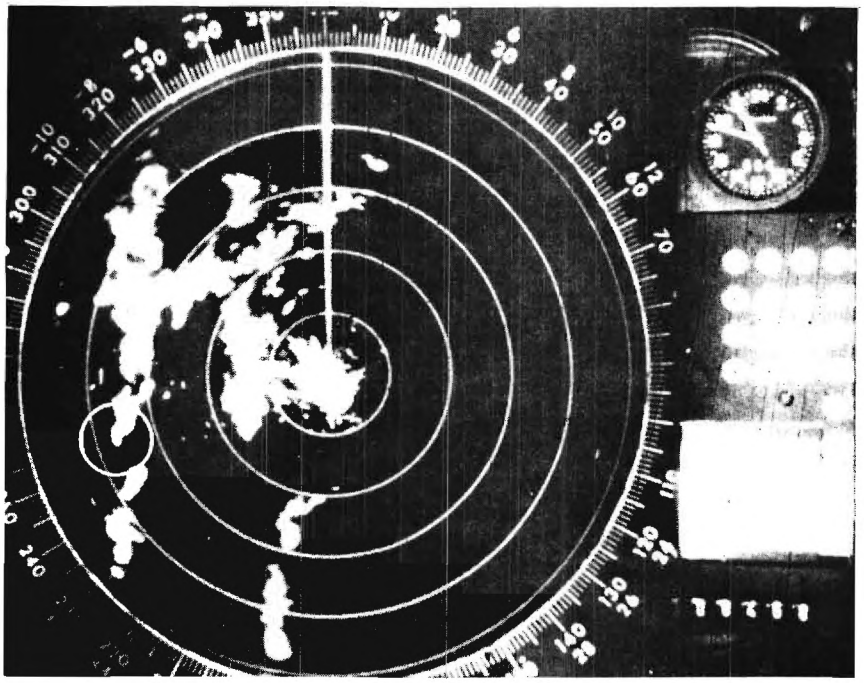

(e) Radar scope photograph from Athens of tornado occurring in Douglas County area on 2–23–75 shortly before 6:00 p.m. EST.

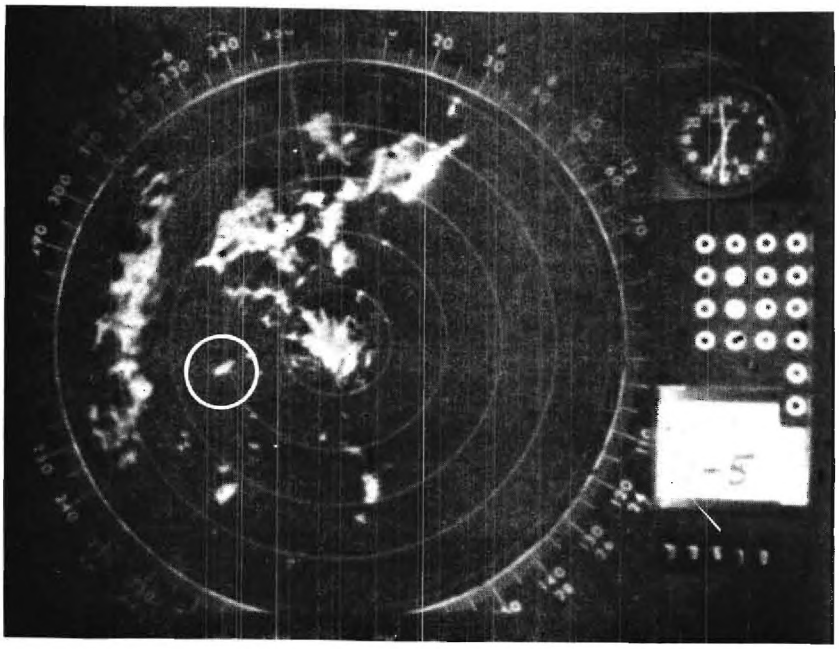

(f) Radar scope photograph from Athens of tornado occurring in Cobb County on 2–23–75 at 6:30 p.m. EST.

Figure 7 (Continued)

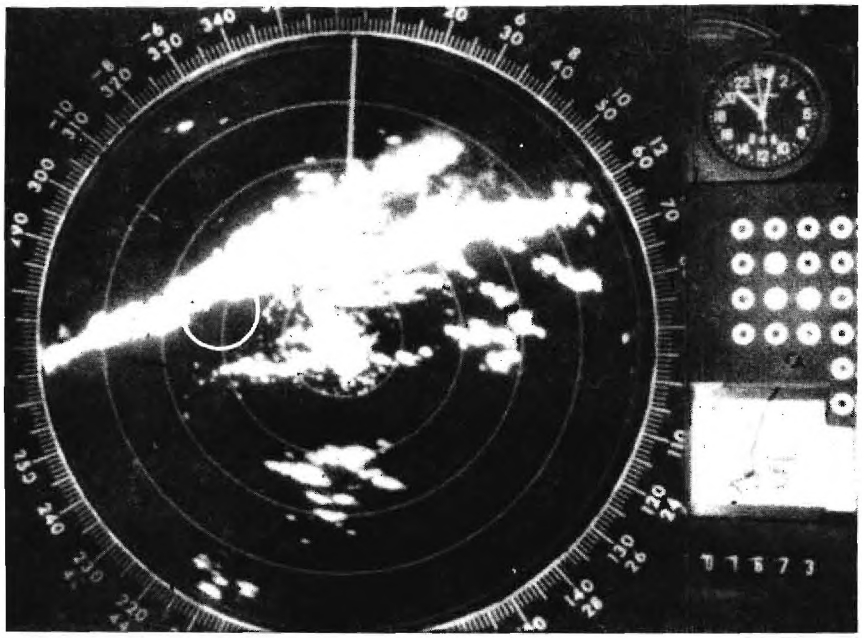

(g) Radar scope photograph from Athens of tornado occurring in Coal Mountain on 3–7–75 at 4:00 p.m. EST.

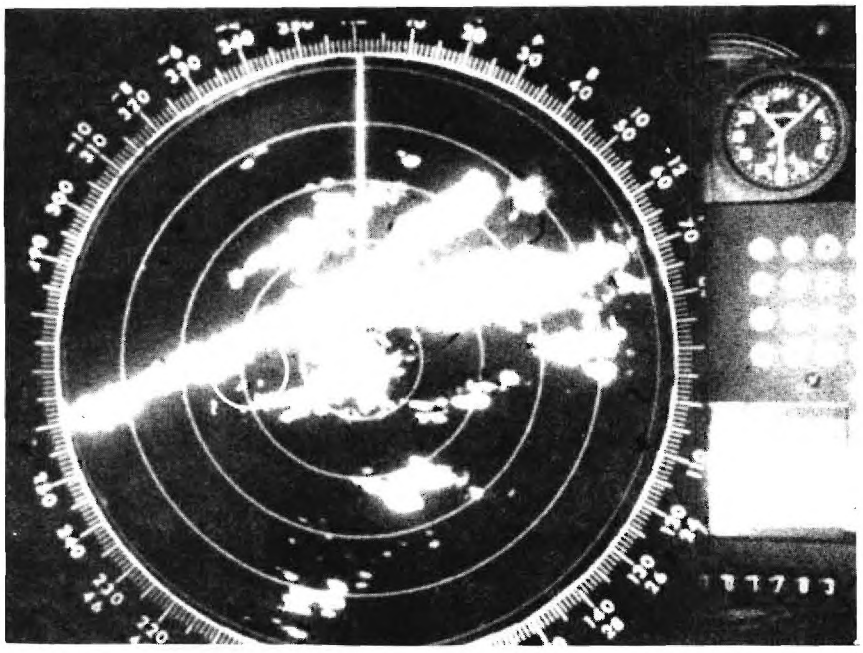

(h) Radar scope photograph from Athens of tornado occurring in Cobb County on 3–7–75 at 4:30 p.m. EST.

Figure 7 (Continued)

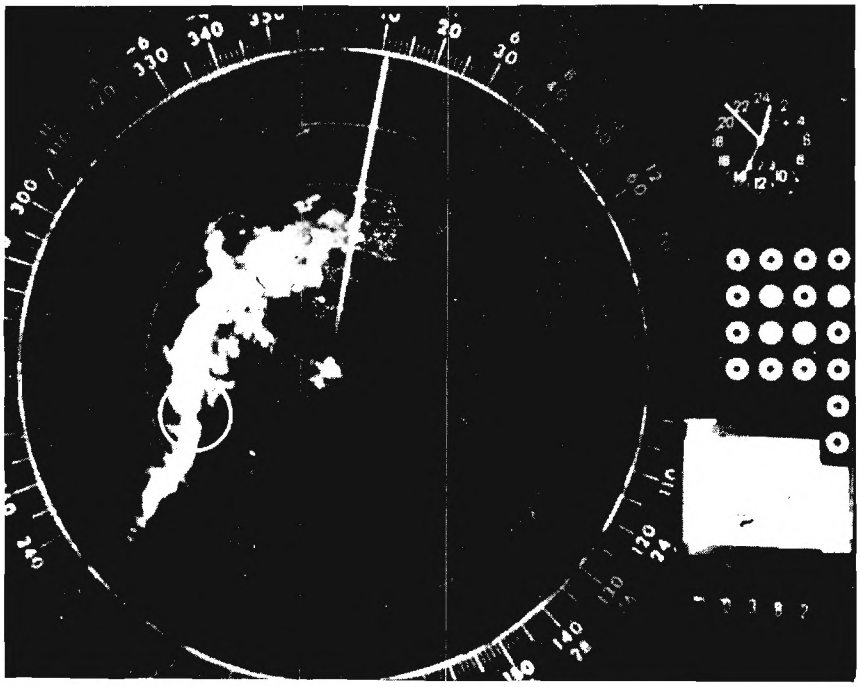

(i) Radar scope photograph from Athens of tornado occurring in south Fulton area on 3–13–75 at 7:50 p.m. EST.

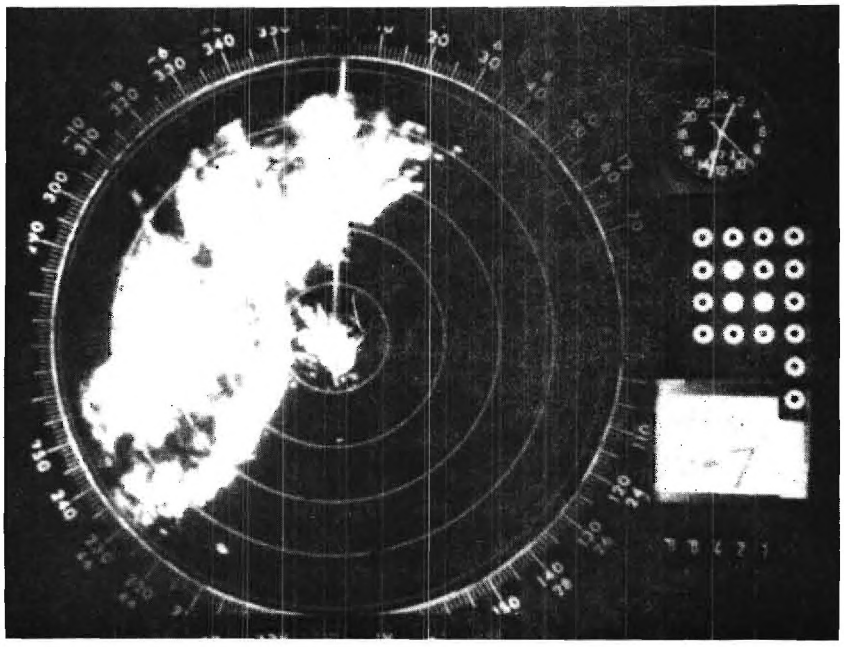

(j) Radar scope photograph from Athens of tornado occurring in Alpharetta on 3–13–75 at 8:33 p.m. EST.

Figure 7 (Continued)

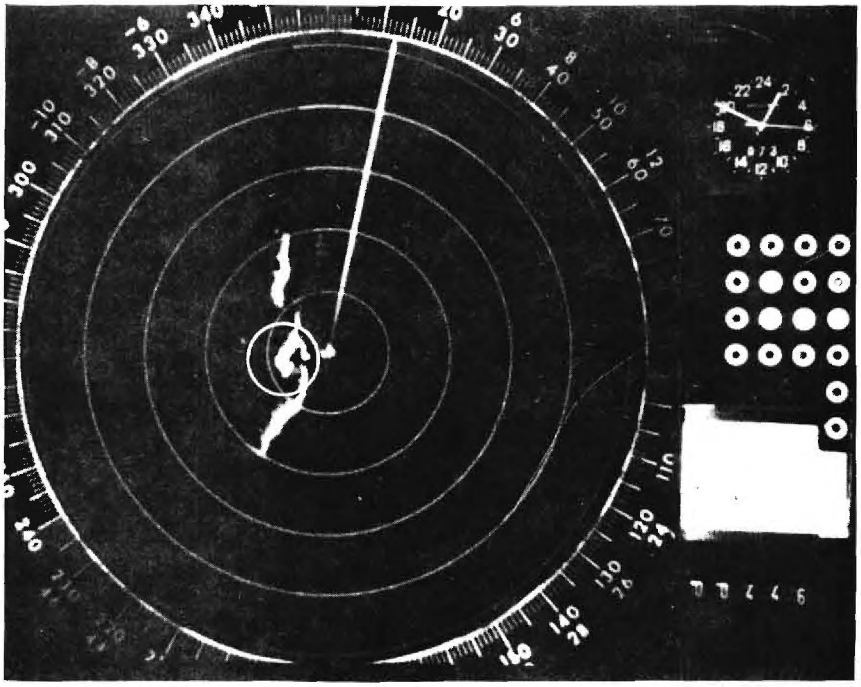

(k) Radar scope photograph from Athens of tornado occurring in Athens area on 3–13–75 at 8:50 p.m. EST.

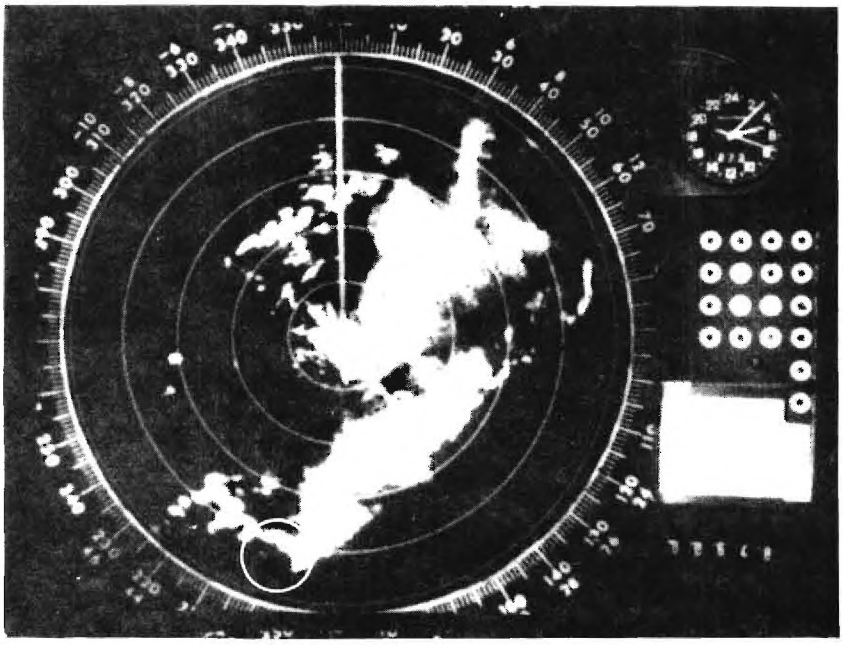

(l) Radar scope photograph from Athens of tornado occurring in Byromville on 3–14–75 at 12:07 a.m. EST.

Figure 7 (Continued)

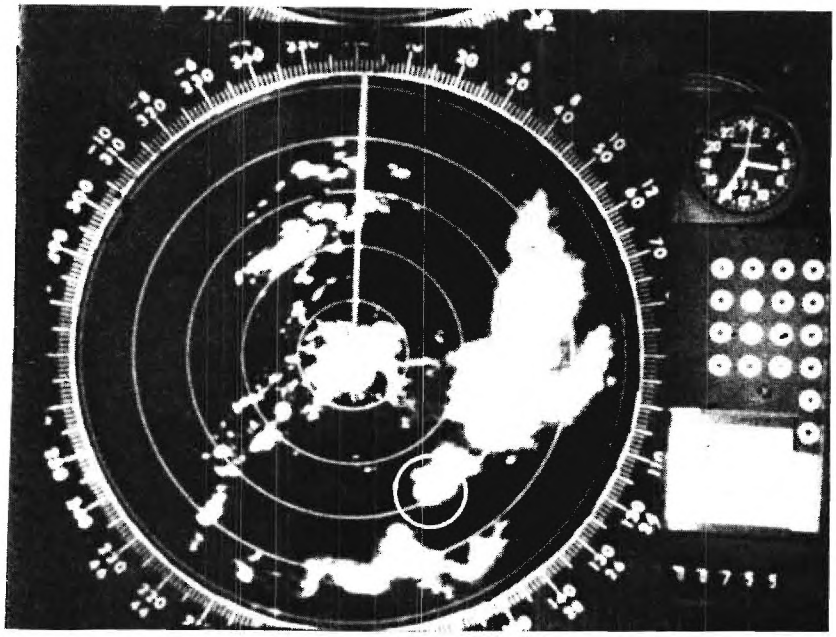

(m) Radar scope photograph from Athens of tornado occurring in Washington County on 3–14–75 at 1:35 a.m. EST.

(n) Radar scope photograph from Athens of tornado occurring in Atlanta on 3–24–75 at 6:29 a.m. EST.

Figure 7 (Continued)

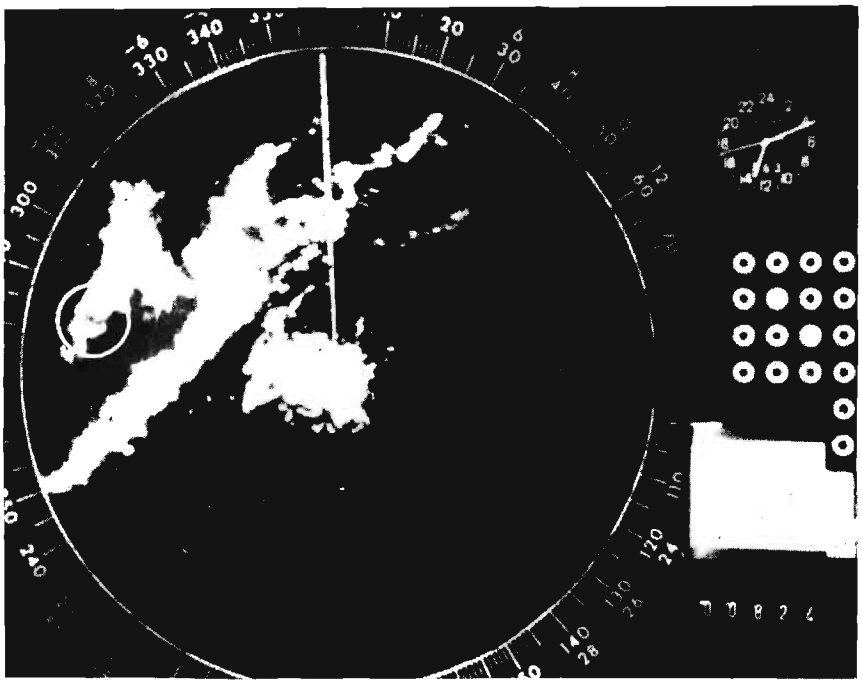

(o) Radar scope photograph from Athens of tornado occurring in Shannon area on 3–24–75 at 8:40 a.m. EST.

Figure 7 (Concluded)

1,000 to 5,000 foot level. (This was certainly the case with the Atlanta tornado observed at ranges of less than 10 miles with the Georgia Tech radar, where the vault area was less than 2 nmi in diameter at all times.) Thus, it can be demonstrated that total dependence on visual recognition of the "hook" echo at moderate-to-long ranges is not a dependable method of tornado detection unless the "hook" is large. However, when other conventional radar discriminants are employed, a higher probability of radar detection of the tornado is assured.

E. Vault Areas on the RHI

The Range Height Indicator (RHI) furnishes the operator a picture of the vertical extent of the storm in much the same manner as the PPI furnishes data on the storm's horizontal extent. The RHI display is generated by scanning the antenna in elevation while scan is stopped in azimuth. The precipitation-free "vault" area displayed as a function of elevation is a small sector of the same precipitation-free area that forms the "hook" echo in the azimuthal plane. The RHI measurement serves as a useful technique to check areas of apparent "hook" formation to determine if there is a substantial organized updraft. The organized updraft indicated by the echo-free vault, or "weak echo region," has been shown to be a distinctive feature of storms containing hail [16].

F. "Tops" Measurements

Numerous studies have shown a direct link between severe weather and the vertical extent reached by the storm. One such study, "A Study of Texas Thunderstorms," by Leipper and Sanford [17] in 1961 demonstrated that the severity of a storm increases when the vertical extent of the storm passes

a level of 32,000 feet. Their findings showed that the model value of echo height for the rain classification is 32,500 feet; 42,500 feet for the storms with hail less than 1/2 inch in diameter; 47,500 feet for storms producing damaging winds at the surface. The storms with exceptionally high first growth tops were generally the most severe. In addition, it was found that storms with more than one hailfall tended to have hailfalls well before the maximum tops were reached while storms with one hailfall had the hailfall slightly after the storm reached maximum height. Other studies of similar nature support these findings with minor differences due to local seasonal and meteorological conditions.

G. Rainfall Measurements

The relationship between radar signal level backscatter and rainfall rate was discussed in the previous section. A measure by radar of reflectivity profiles within the thunderstorm permits one to estimate the locations of severe turbulence. The actual amount of precipitation suspended depends on the updraft speed, availability of moisture and the duration of the updraft. Barclay [18] defined the severe turbulence zone affecting aircraft operation as the area within the thunderstorm where $Z = 10^5$ mm^6/m^3 or greater plus a 5-mile buffer around it. (Barclay assumes that the echo has reached a height likely to produce severe weather.) Ward, Meeks, and Kessler [19] found that radar echoes from storms producing hail and tornadoes almost always exceed $Z = 10^5$ mm^6/m^3. These findings and others verify that reflectivity profiles with $Z \geq 10^5$ mm^6/m^3 aloft are indications of the onset of severe weather when the storm has built to sufficient levels through the troposphere and possibly into the stratosphere.

H. Rotating and Merging Cells

Newton and Katz [20] found that convective rain storms generally moved with a primary component to the right of the 700-mb wind direction. Newton and Frankhauser [21] also found that severe weather phenomena tend to follow a path to the right of the direction of the mid-tropospheric winds. Others have found that thunderstorms that form tornadoes tend to rotate about a vertical axis. Browning and Fujita [22] have shown that when a severe thunderstorm or tornado-cyclone cloud begins rotation, the echo tends to diverge at an angle of about 25 degrees from its original direction of travel or from the other echoes in the vicinity. Fujita [15], in his analysis of the radar films of a tornado-producing storm which occurred 26 May 1963, found that there was strong divergence between the nonrotating echo and the rotating echo that spawned the tornado. The nonrotating echo continued to track on an east-northeast course while the diverging rotating echo assumed an east-southeast course.

Radar echoes that converge have also been reported with the occurrence of tornadoes. Stout and Hiser [23] in their study on a tornado-producing storm that occurred 28 May 1954, reported that as two echoes converged at a 30-degree angle to the axis of travel the intensity of the larger echo to the north increased by 4 dB. Simultaneously, a tornado formed at the approximate interface of the two cells. The same phenomenon was observed by Georgia Tech radar operators during the Atlanta tornado, which will be discussed in Section VII.

I. Summary

There are 5 major criteria that may be measured with conventional meteorological radars. These criteria may occur in different combinations and their detection may lead to early tornado warning. "Hook"-shaped echoes are

fairly easy to recognize on the PPI if the radar has the capability to resolve the small precipitation-free area within the "hook." This task can be difficult when the weather mass is at moderate-to-long ranges, due to the physically small size of the displayed "hook."

The RHI is an important tool in determining the vertical extent and amount of the precipitation suspended over the vault in storms usually producing tornadoes. The operator, through the proper use of the RHI, can discriminate between the false "hooks" appearing in irregular shaped clouds and the true "hook" with heavy precipitation suspended overhead.

Reflectivity measurements tend to confirm that certain cells may spawn tornadoes if other primary considerations such as speed of cell movement and extreme "top" heights are met. Reflectivity factors greater than 10^5 mm^6/m^3 usually are accompanied by severe weather consisting of hail and possibly tornadoes, assuming the storm has met other criteria.

Divergence, convergence and rotation of echoes may indicate tornado formation. The history of the cell movement may suggest cyclonic activity within the core area of the larger cell being observed.

These criteria and others are utilized by radar operators charged with the responsibility of severe storm and tornado warning functions. The success in applying these criteria to the early detection of tornadoes is presently a function of radar resolution capability and operator ability to integrate the numerous events occurring on his indicator into a meaningful pattern indicative of severe weather.

SECTION VI

SHORT TERM TRENDS IN THE OCCURRENCE OF GEORGIA TORNADOES

The short term trends in tornado occurrence in Georgia are of interest to persons conducting tornado research and those involved in the warning function. The researcher needs tornado trend data in order to ensure that field operations are scheduled to coincide with the most probable time of tornado occurrence. Those charged with disseminating the warnings to the public must be aware of short term trends of tornado occurrence in order that major fluctuations from the expected norm can be recognized. The fluctuation can indicate an entirely new warning system may be required if there is a shift in tornado occurrence to a time of day when the general public may be out of touch with presently used warning systems. Thus, an effort was made to present a general study of the short term trends for use by both groups, based on the best data available to Georgia Tech analysts.

A. Data Source

The data for the base period of 1953 through 1969 were taken from the U.S. Weather Bureau publication entitled, "Georgia Tornadoes" [24]. The reporting procedures, quality of data, and changes in the tornado criteria, if any, during the reporting period are unknown. The data used to derive short term trends between 1970 and June 1975 were taken from two National Weather Service sources: (1) the publication, "Storm Data" [25], and (2) "Tornado Data Sheet" prepared by local meteorologists for transmission to those compiling "Storm Data." A sample of the tornado data sheet for February 1975 is shown as Figure 8. The two-source approach was used to verify the accuracy of the data. There are no existing data that might indicate the number of

TORNADO DATA SHEET

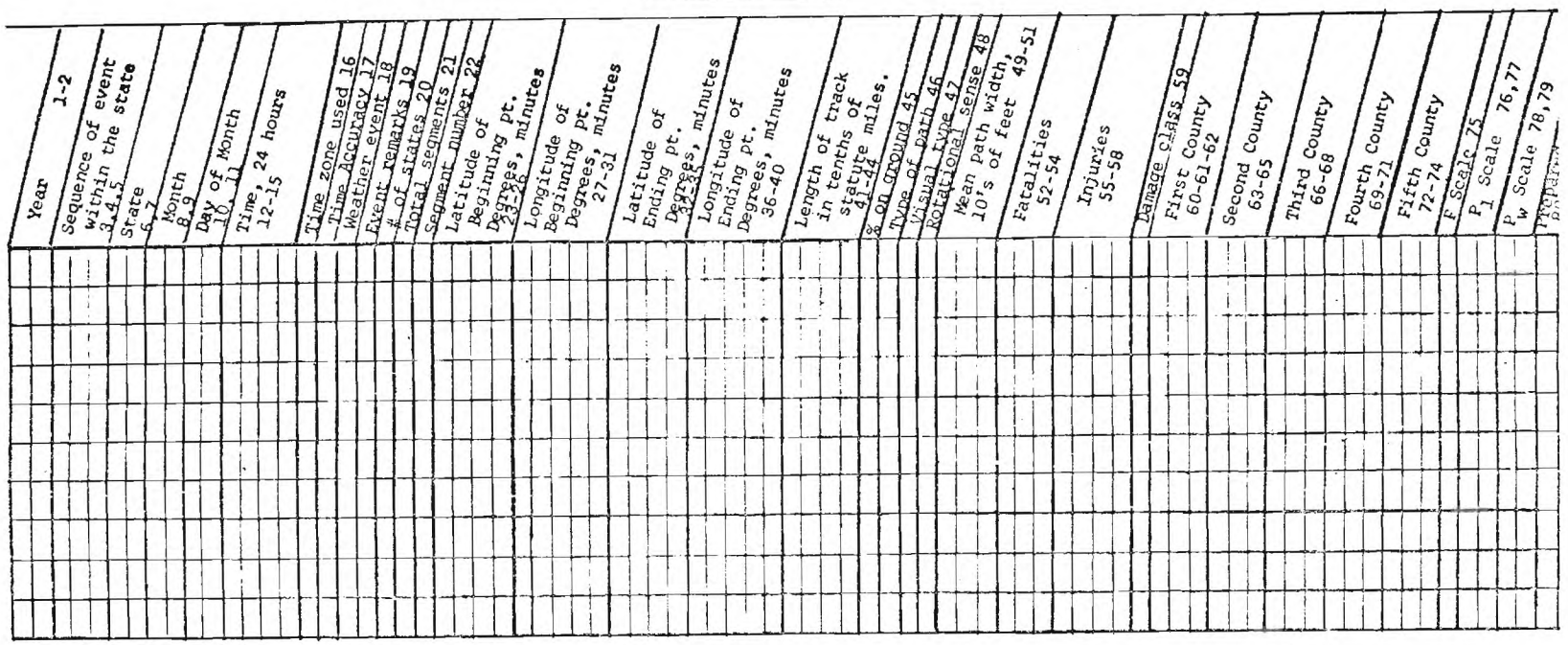

Col 16	Col 17	Col 18	Col 19	Col 45	Col 46	Col 47	Col 48
1-EST	1-±15 min	1-Tornado	1-With large hail	0-100%	0-Straight	0-ropelike	1-Cntrclockwse
2-EDT	2-±30 min	2-Funnel Cld	2-With heavy rain	1-10%	1-sinusoidal	1-cone shape	2-Clockwise
3-CST	3-±45 min	3-Waterspout	3-With 1 & 2	2-20%	2-L turn loop	2-eleph trunk	blank if unknown
4-CDT	4-±1 hour	4-Wspt movg ashore	4-No rain or hail	.....	3-30° to left	3-thin column	
5-MST	5-±75 min	5-Torn movg ovr large		9-90%	4-45° to left	4-mdt column	Col 80
6-MDT	6-±90 min	body of water		blank if	5-60° to left	5-thick column	1-SC from clippings
7-PST	7-±105 min	6-Hail >3/4"		unknown	6-R turn loop	6-obscrd by R+	2-SC from survey
8-PDT	8-±2 hour	7-Winds 50 K or greater			7-30° to right	7-no vsbl sign	3-NSSFC from Storm Data
9-GMT	9->2 hours	8-Hail aloft >3/4"			8-45° to right		4-Other
		9-Extreme turb.			9-60° to right		

Figure 8. Master data sheet used by National Weather Service to record tornado occurrence.

tornadoes occurring in the state but not reported by the public. Therefore, the total sample data base consists of data concerning only verified tornadoes. These data sources were used to derive general conclusions concerning the trends of tornado occurrence.

Radar plan position indicator film taken at NWS radar stations in Athens and Waycross, Georgia, during tornado occurrence was analyzed in conjunction with this study. The radar films cover only the time periods of tornado activity within range of the respective radars during the period from January through May 1975. The films were analyzed in an attempt to determine if the "hook" phenomenon, core rotation, thunderstorm convergence and divergence could be detected on a consistent basis before touchdown.

B. Tornado Occurrence in the State

Between 1953 and 1969 approximately 305 tornadoes [24] were reported in Georgia. The data analyzed for the period January 1970 through June 1975 include 192 tornadoes. (Funnel clouds reported by the public are counted as tornadoes.) These data imply that Georgia during the past five and one-half years has experienced 63 percent of the total tornadoes reported during the previous 17-year period. Stated another way, the average number per year was 17.9 between 1953 and 1969, but increased to 34.9 between 1970 and 1975. A general comparison of the long and short term data bases indicates not only an increase in the average number of tornado occurrences during the 1970 - 1975 period, but also a shift in the seasonal trends from those established between 1953 and 1969.

The yearly distribution of the tornadoes occurring between 1970 and 1975 is shown in Figure 9. Figure 10 shows the distribution by month of the tornadoes occurring during the 1953 - 1969 period. A fairly well defined

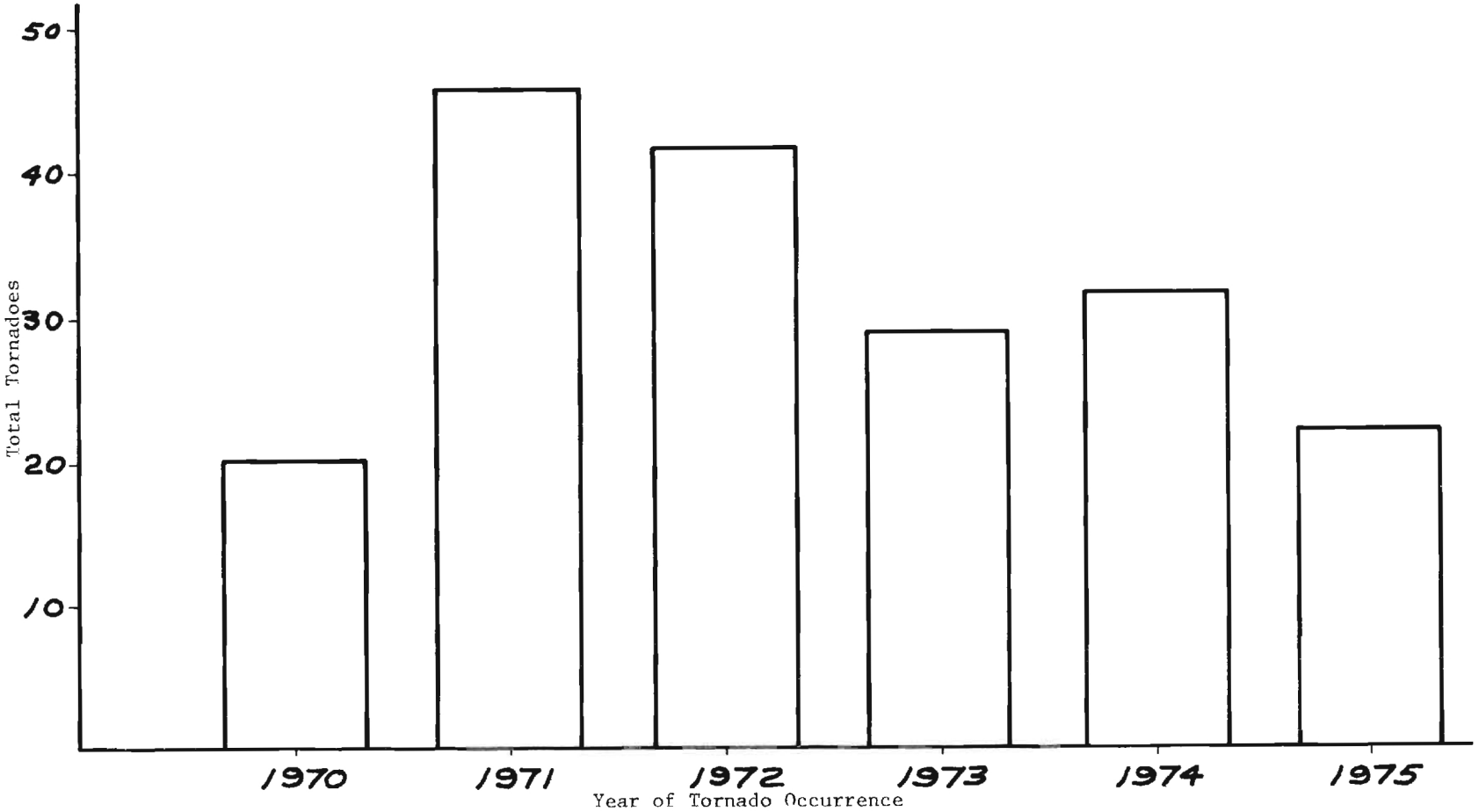

Figure 9. Yearly distribution of tornadoes occurring in Georgia, 1970 through June 1975.

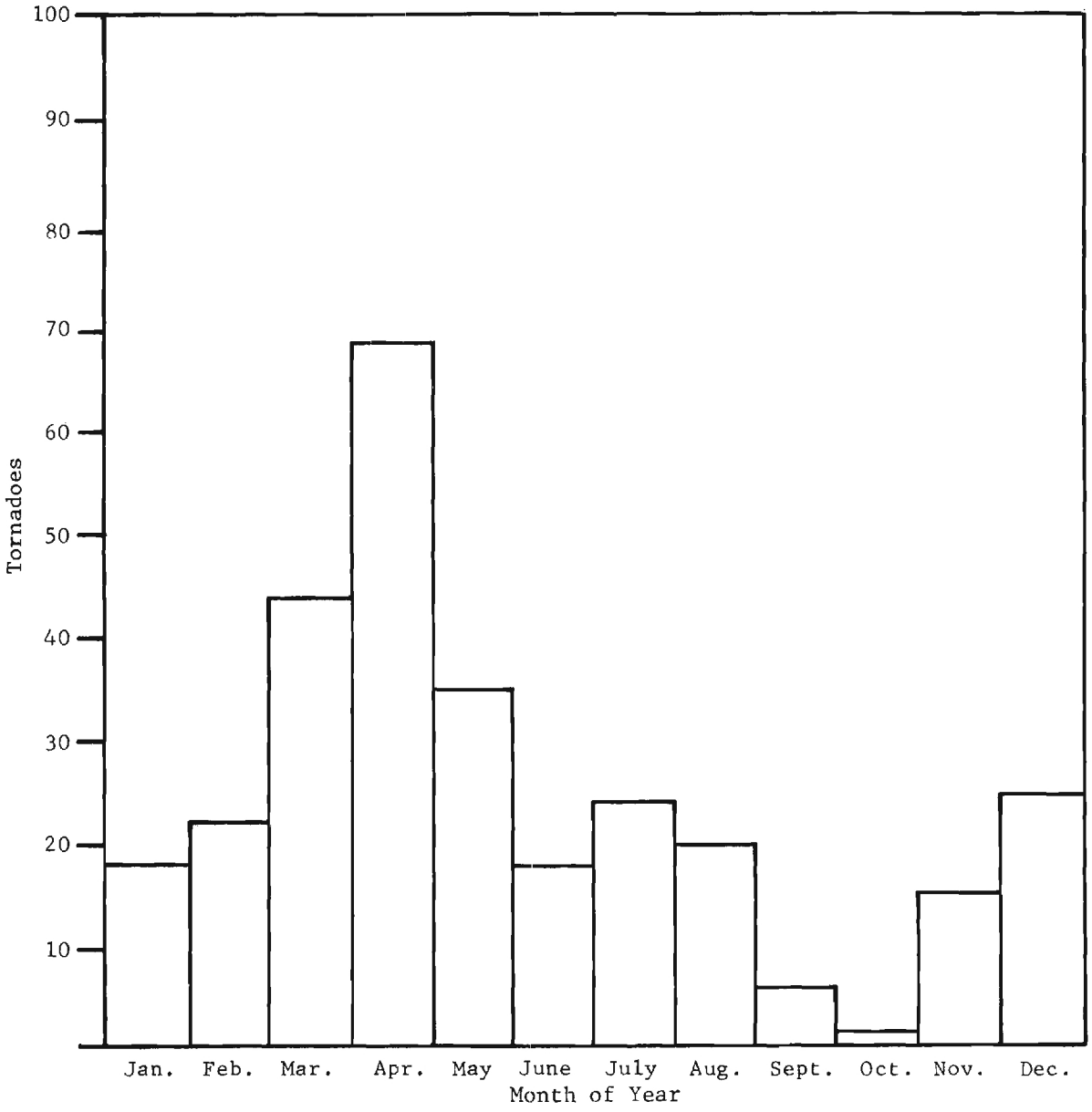

Figure 10. Monthly distribution of tornadoes occurring in Georgia during the years 1953 - 1969 as compiled by the National Weather Service.

maximum of tornado occurrence is during March and April. Figure 11 shows tornado occurrences by month for the 1970 - 1975 data base. These data show a general shift of tornado occurrence from the March/April time frame to the earlier months of the year. This trend can probably be linked to the unusual seasonal variations that have occurred during the past several years. Nevertheless, the trend is significant and should be considered in future plans for tornado research and for dissemination of warnings.

Figure 12 shows the hourly distribution of tornadoes in Georgia during the 1953 - 1969 period. This figure indicates a primary peak around 5:00 p.m. EST and a secondary peak around 9:00 a.m. Figure 13 shows a similar distribution for the 1970 - 1975 data, and reveals a distinct shift in tornado occurrence to earlier hours of the day. The indicated accuracy of the 1970 - 1975 data is shown in Figure 14. There were 155 tornadoes (81 percent of the cases) during this time period for which the time of occurrence was specified within $\pm$ 15 minutes. The shift in time of occurrence (Figure 13) is small in terms of hours, but it could define the type of warning system that should be employed to warn both rural and urban residents. For example, if the majority of tornadoes occur during the hours that persons will normally listen to the radio and watch television, the present warning system may be the most cost effective approach for public warning purposes. However, if the majority of tornadoes occur during the periods when the public is asleep, at work, or generally away from the radio and television, then a variety of concepts in warning systems may be practical, especially in urban areas.

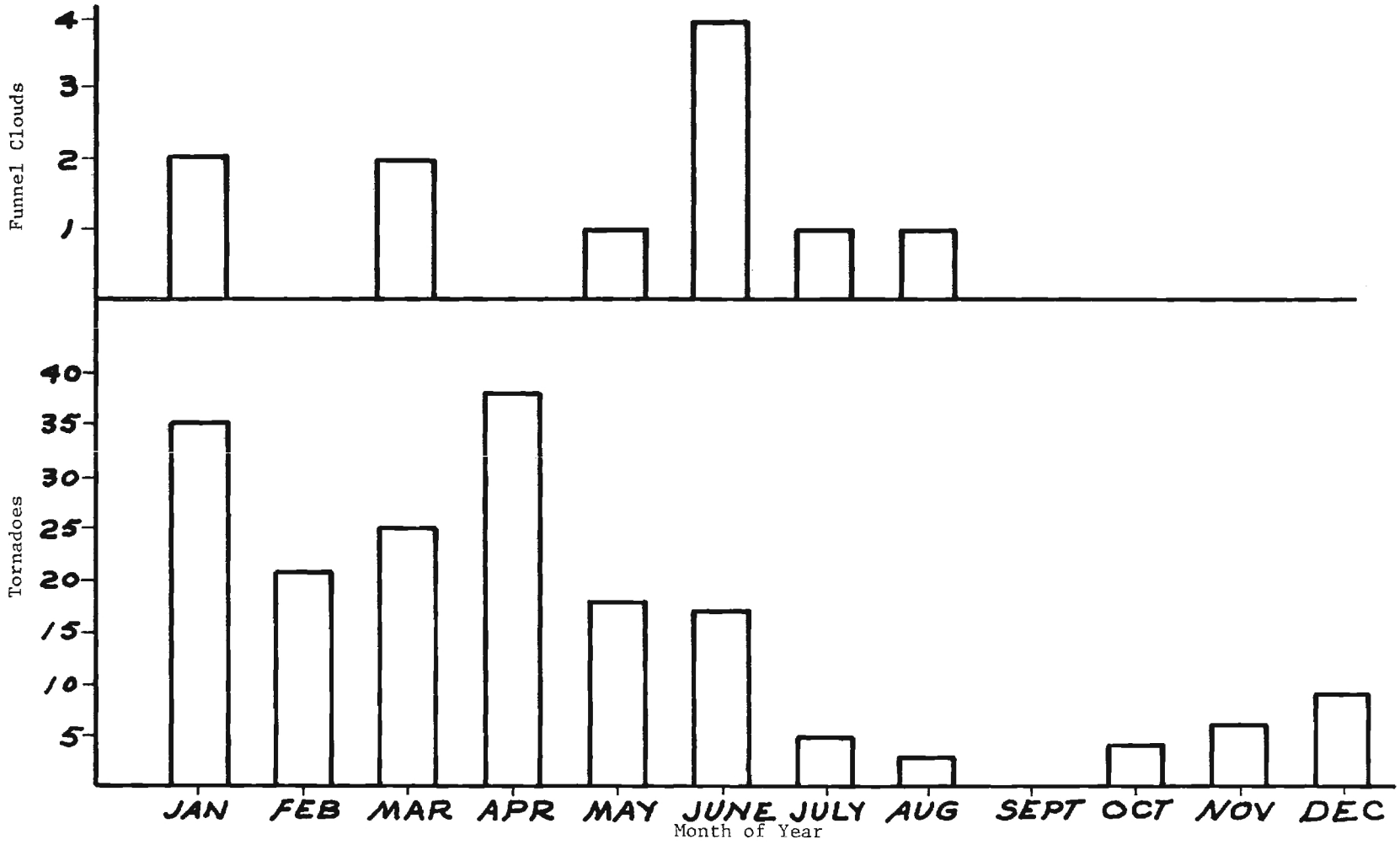

Figure 11. Monthly distribution of tornadoes occurring in Georgia, 1970 - June 1975.

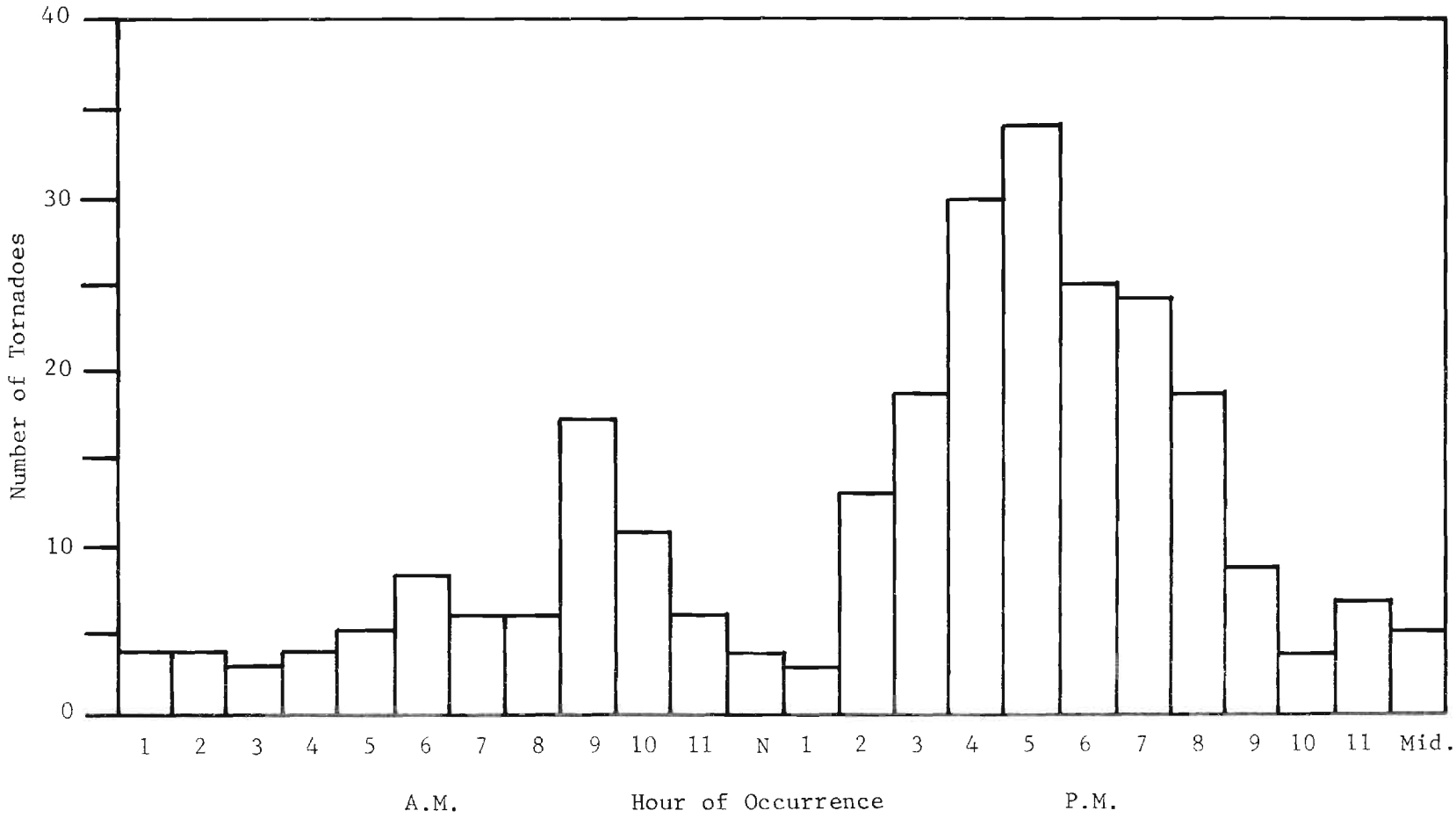

Figure 12. Hourly distribution of tornadoes occurring in Georgia, 1953 - 1969, as supplied by the National Weather Service.

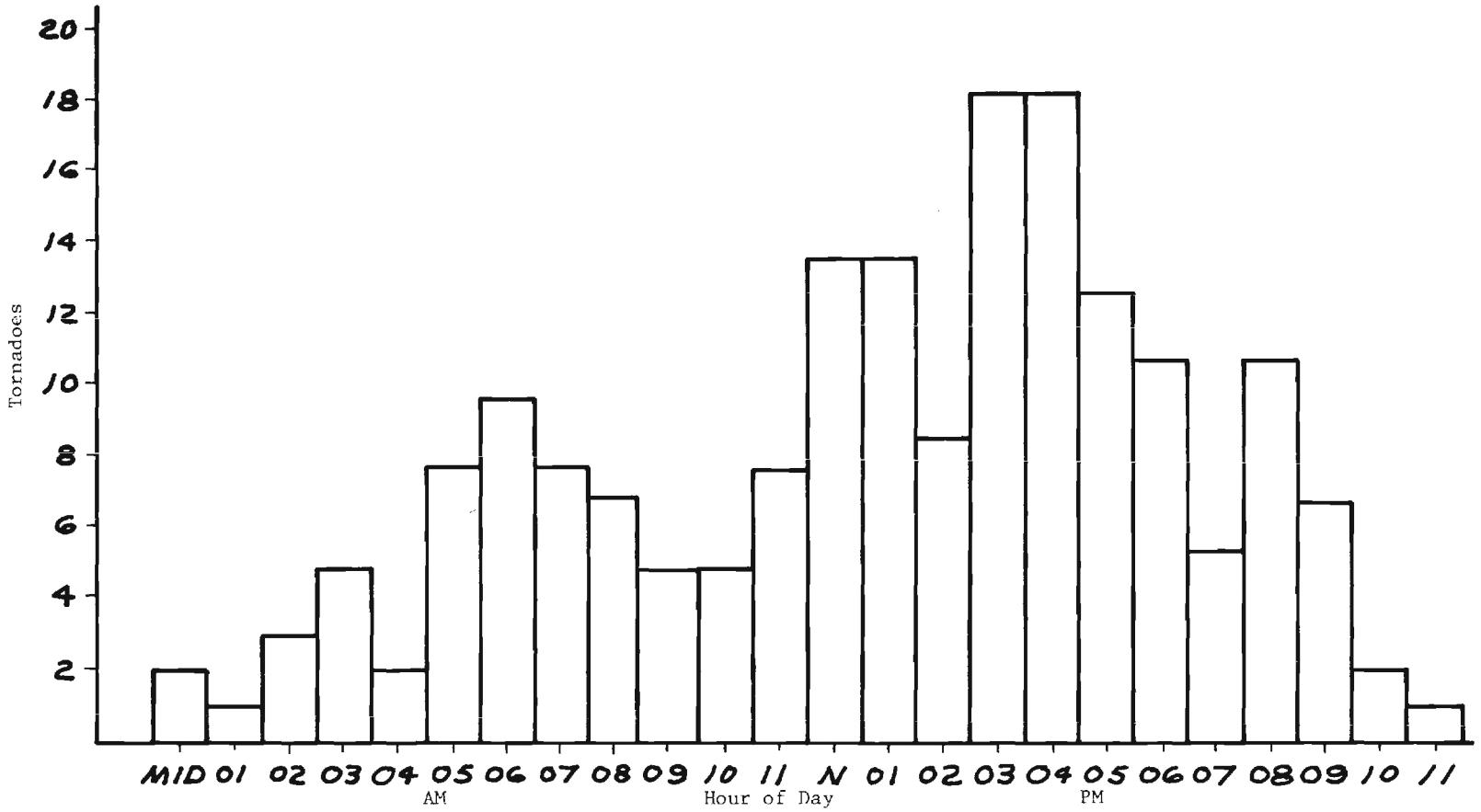

Figure 13. Tornado occurrence in Georgia for specific hours of the day during the 1970 through June 1975 time period.

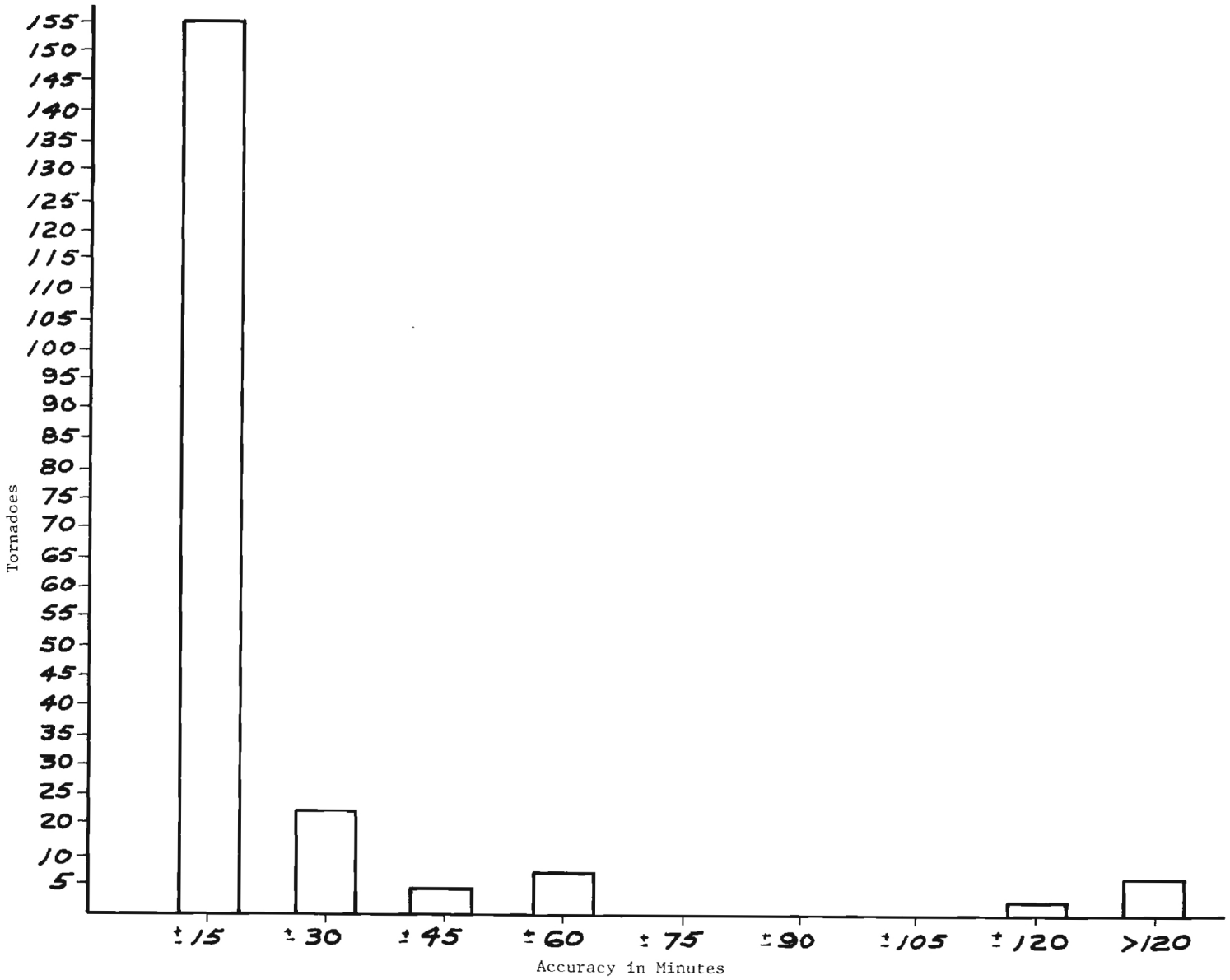

Figure 14. Averaged indicated accuracy of times of occurrence of tornado data 1970 - June 1975.

C. Path Length, Direction, and Speed of Movement

The data concerning tornado movement in Georgia are not reliable enough to subject them to detailed analyses; therefore, only general observations concerning these parameters will be made. Historical data concerning path length may be very accurate as in the case of the Atlanta tornado where NWS officials made detailed on-site inspections. The path length in other cases may be estimated by a non-trained observer or from incomplete damage surveys.

Figure 15 shows the total number of tornadoes occurring between 1970 and 1975 as a function of their reported path length. A general conclusion that might be drawn from these data is that approximately 62 percent of the tornadoes occurring in Georgia stay on the ground for distances of less than five miles. There is no consistently tabulated data available on the ground track speed of tornadoes in Georgia (although radar films and wind data for the 700 mb level could be used to derive these data when time and funding permit). A range of speeds from 35 to 60 knots is representative of the best-documented tornado occurrences in 1975. With a 35-knot minimum ground speed, a tornado with a path length of 5 miles would be on the ground approximately 9 minutes. A tornado traveling at 60 knots over the same distance would be on the ground approximately 5 minutes. Thus the data imply that 62 percent of Georgia's tornadoes were on the ground 10 minutes or less.

The time taken by an observer to call the local National Weather Service office, and a sighting report to be relayed to the primary radio or television warning station, at best could take 3 minutes even when an oral "phone patch" warning is made. A warning could take 5 minutes when teletype is used. Because a tornado can cover a path as long as 5 miles in this interval, both an early detection and rapid warning system are critical.

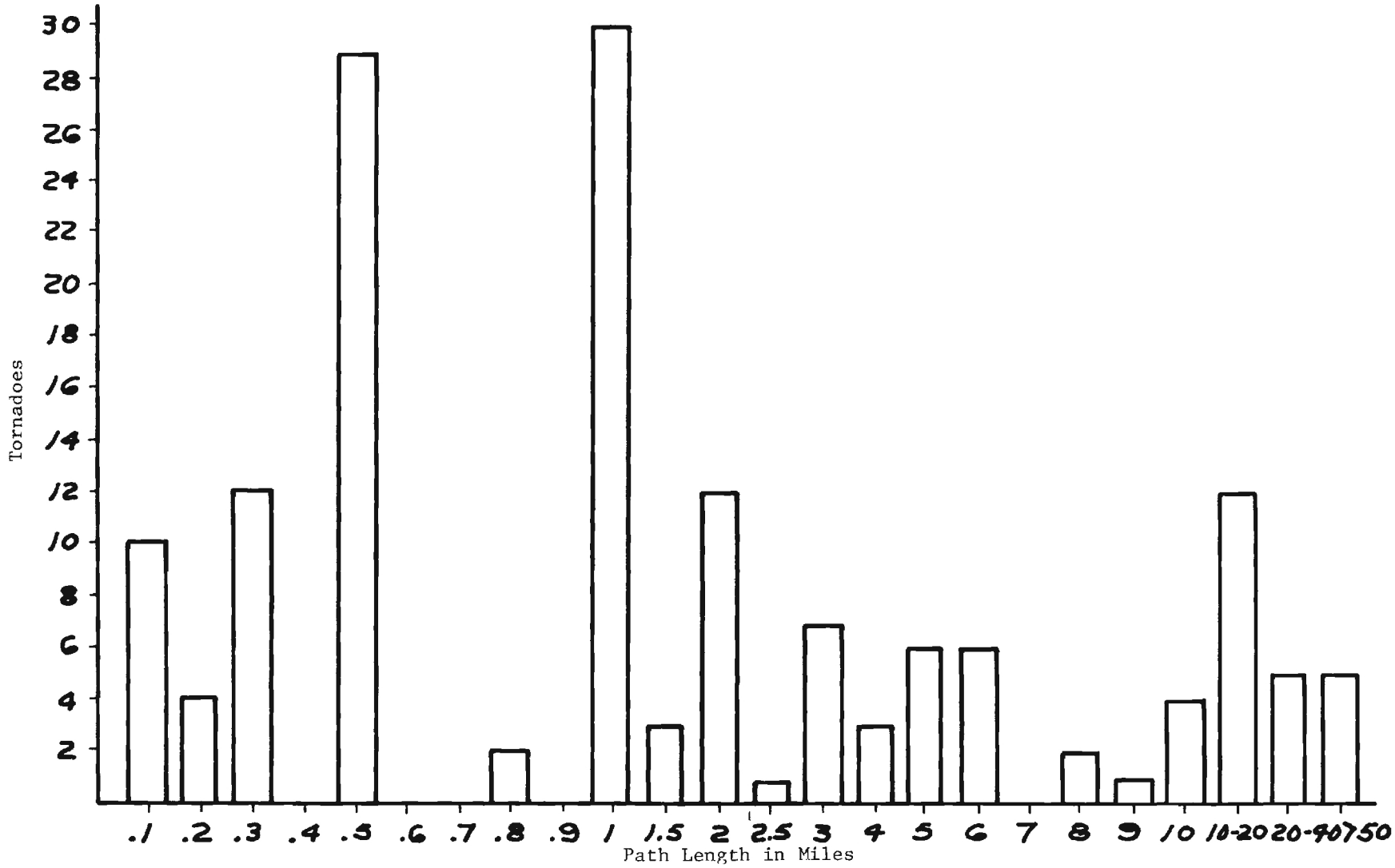

Figure 15. Average path length of tornadoes occurring in Georgia for the period 1970 - June 1975.

The direction of movement was computed on the great circle using the start and end points in longitude and latitude taken from the NWS tornado data sheets for 1970 - 1975. These data are uncertain in some cases for the same reasons noted for path length data. Figure 16 shows the computed path lengths, the direction of travel and the year of occurrence for tornadoes reported in 1970 - 1975. Path length is scaled in nautical miles while the year of occurrence is shown as the number within the circle marking the first point of touchdown. The direction of movement of the tornadoes occurring during the period is predominantly to the north-northeast. Although a mean direction of travel could be computed, it was not because of the discrepancies found in the data.

D. Anomalies

It is interesting to note that relatively few tornadoes occur along the "fall line" running generally from August through Macon to Columbus. Another area of few reports is the extreme southeast corner of the state, but this absence of reports is explainable by the fact that much of the area is uninhabited pine forest and swampland. The fall line anomaly is harder to explain because a number of towns exist in this area and any tornadoes would be reported. A study of this phenomenon may disclose an important geophysical factor in tornado dynamics, or simply a lack of consistent reporting procedures from the area.

E. Radar Film Analysis

Radar film taken of NWS weather radar displays during periods of tornado occurrences was obtained for the months of January through May 1975. These films were obtained for the Centreville, Alabama (CKL), Athens, Georgia

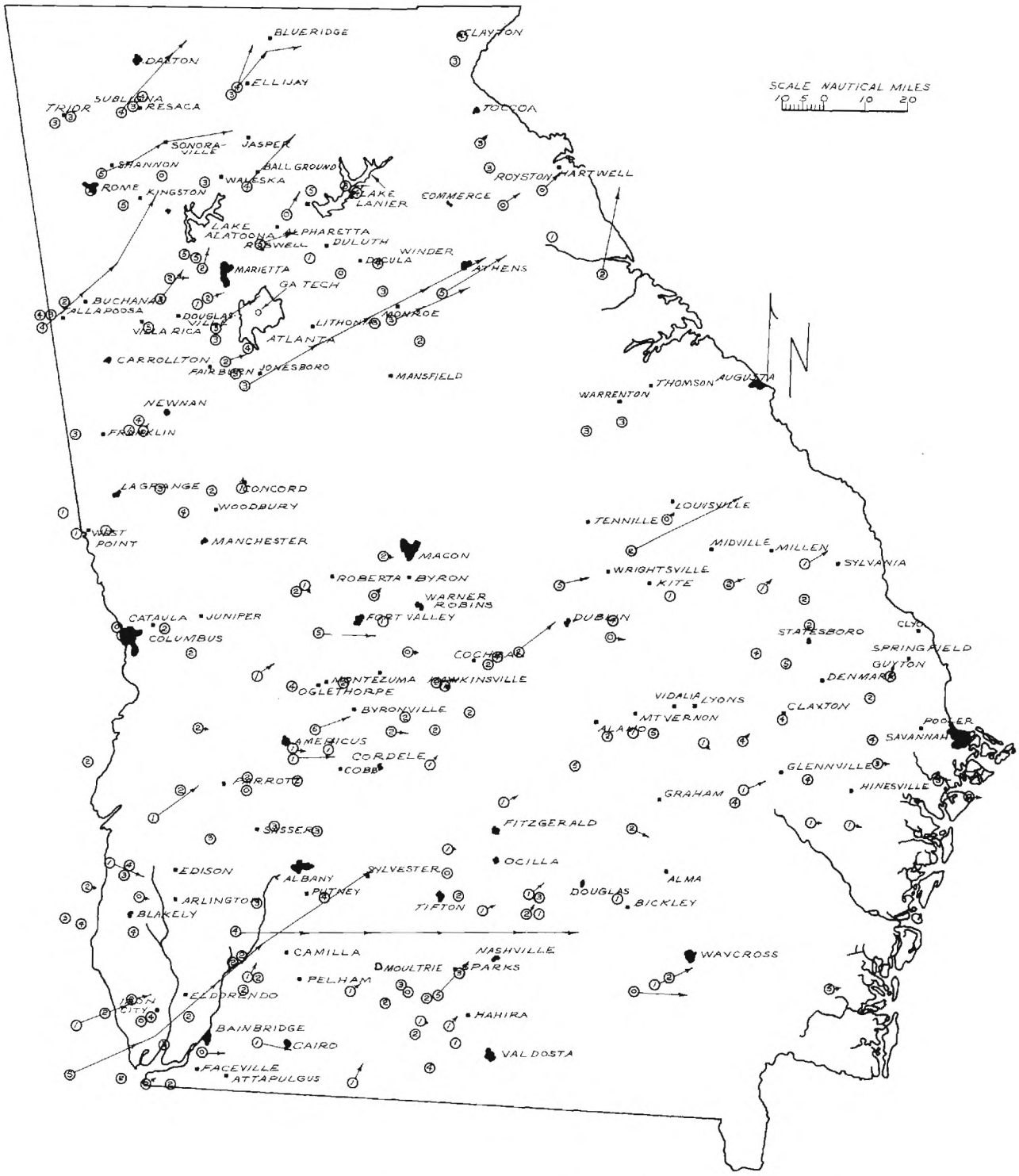

Figure 16. Computed path lengths and direction of travel for tornadoes occurring in Georgia, 1970 - June 1975. The last digit in circle represents year of occurrence and circle represents first point of touchdown.

(AHN), and Waycross, Georgia (AYS), radar stations. The film was analyzed on a frame-by-frame basis during the time periods of known tornado occurrence for the Bainbridge, Fort Valley and Lyons tornadoes. These tornadoes were chosen for further study because they are typical of the tornadoes occurring in Georgia. The Bainbridge, Fort Valley, and Lyons tornadoes had well documented ground tracks of 105, 10.3, and 2 miles, respectively.

The compressed time radar scope photographs of each tornado occurrence were studied to determine if there was (1) rotation and splitting of the echo as reported by Fujita [15], and (2) convergence or merging of cells with the tornado occurring at the interface of the cells as reported by Stout and Hiser [23]. Cell rotation, convergence, and splitting were found to occur in several of the cases studied.

Figure 17 is a composite of compressed time photographs of the National Weather Service AYS radar scope during the period when a tornado went from Bainbridge through Seminole, Decatur, Mitchell, Worth, and Turner Counties on 1 January 1975 between the hours of 12:45 p.m. and 3:00 p.m. The AYS radar has contouring provisions which display areas of heavy precipitation within the thunderstorm as a dark hole within the echo. The contoured main core of the parent thunderstorm begins detectable rotation in "textbook" fashion at 2:15 p.m. EST as the cell is centered near the 100-mile range mark on a bearing of 270 degrees from the radar. Rotation in the core of the parent thunderstorm is apparent during the next hour. During the 2:15 p.m. to 2:50 p.m. EST time period, the cell appears to rotate one-quarter of a turn, increasing speed such that the core has rotated one-half turn by 3:15 p.m. Ground speed of the tornado-producing thunderstorm was approximately 30 knots and the top heights are unknown. While rotation of the core was

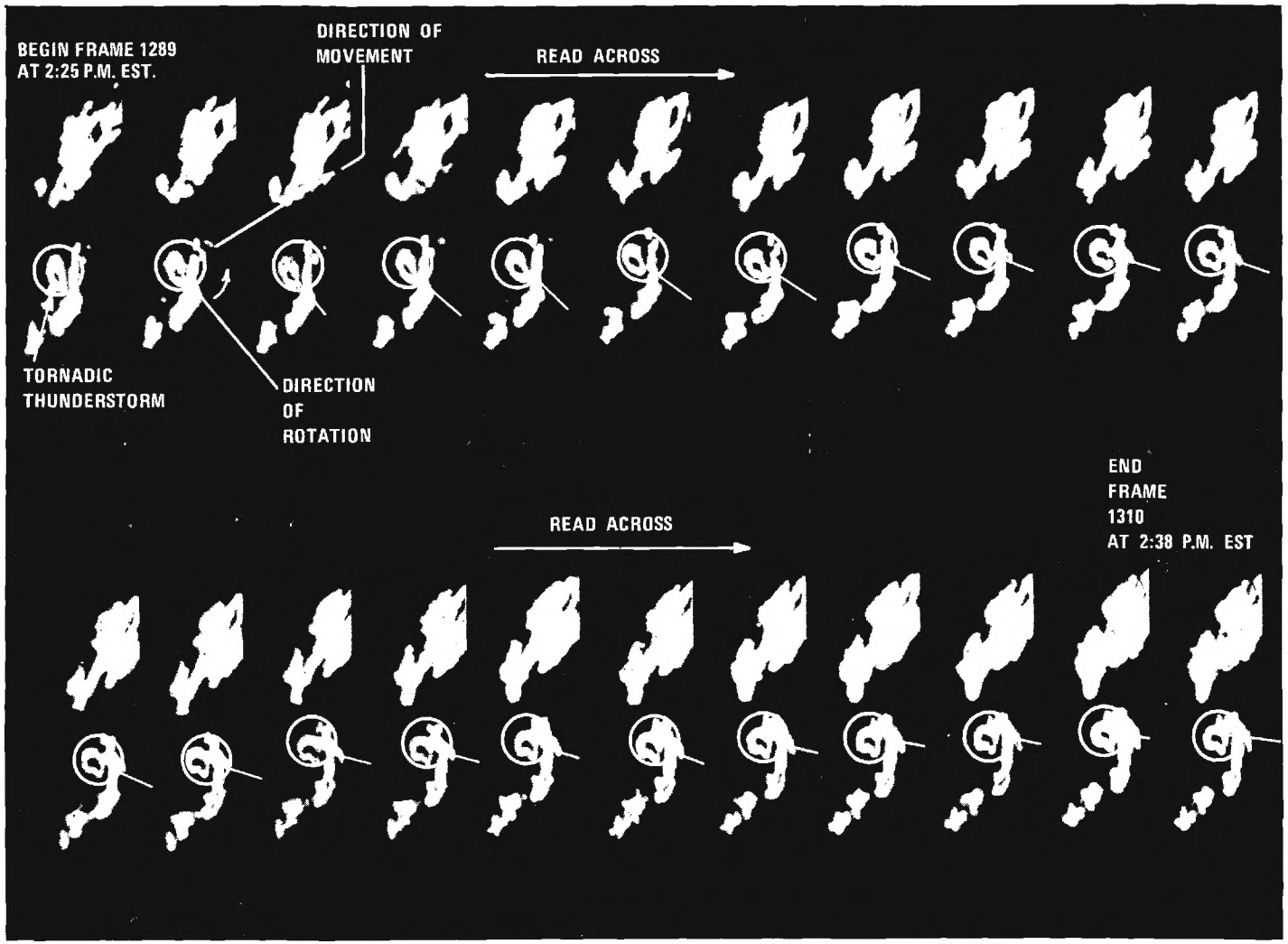

Figure 17. Frame-by-Frame analysis of Bainbridge tornado showing rotation within thunderstorm between 2:15 and 3:15 p.m. EST, January 1, 1975 moving at 50 mph over a path of 105 miles. Core rotates approximately 1/4 turn in 15 minutes. Rotation is dramatically demonstrated by viewing entire radar film for period between 2:15 p.m. and 3:15 p.m. EST.

observed, the thunderstorm appeared to move in the same direction as other thunderstorms in the area, indicating little or no steering influence from higher altitude winds.

A different phenomenon was observed to occur on 18 February 1975 during the Fort Valley tornado shown in Figure 18. The parent thunderstorm was observed from the AHN radar. The storm moved on an approximate heading of 70 degrees at a point 95 miles from AHN on a bearing of 195 degrees from north. A smaller echo 20 miles south of the tornado-producing thunderstorm was observed to move due north toward the large thunderstorm at 3:50 p.m. EST. The smaller echo continued a northerly course and merged with the large thunderstorm about 4:00 p.m. EST. Records show that the first officially reported tornado damage occurred at 4:08 p.m. The correlation between the time of tornado occurrence and merging echoes is consistent with the type of observations made by Stout and Hiser [23]. There are several meteorological explanations for the observed echo motion. However, for purposes of advance detection of tornadoes, the important point is that the wind flow anomaly, revealed by the movement of the small cell, marks the large storm as potentially severe at least 15 minutes prior to tornado touchdown.

The Lyons, Georgia, tornado occurred at 5:15 p.m., 12 January 1975. The film examined was taken by the AYS radar located approximately 58 miles to the south on a bearing of 184 degrees from Lyons. Figure 19 shows that at approximately 4:30 p.m. the thunderstorm that produced the Lyons tornado appeared to move rapidly ahead of an associated mass, and by 4:50 p.m. (see Figure 7B) a well defined "hook" is beginning to form on the southwest edge of the thunderstorm. Shortly after 5:00 p.m. another echo can be seen merging from the south with the large thunderstorm to the north. During echo merging

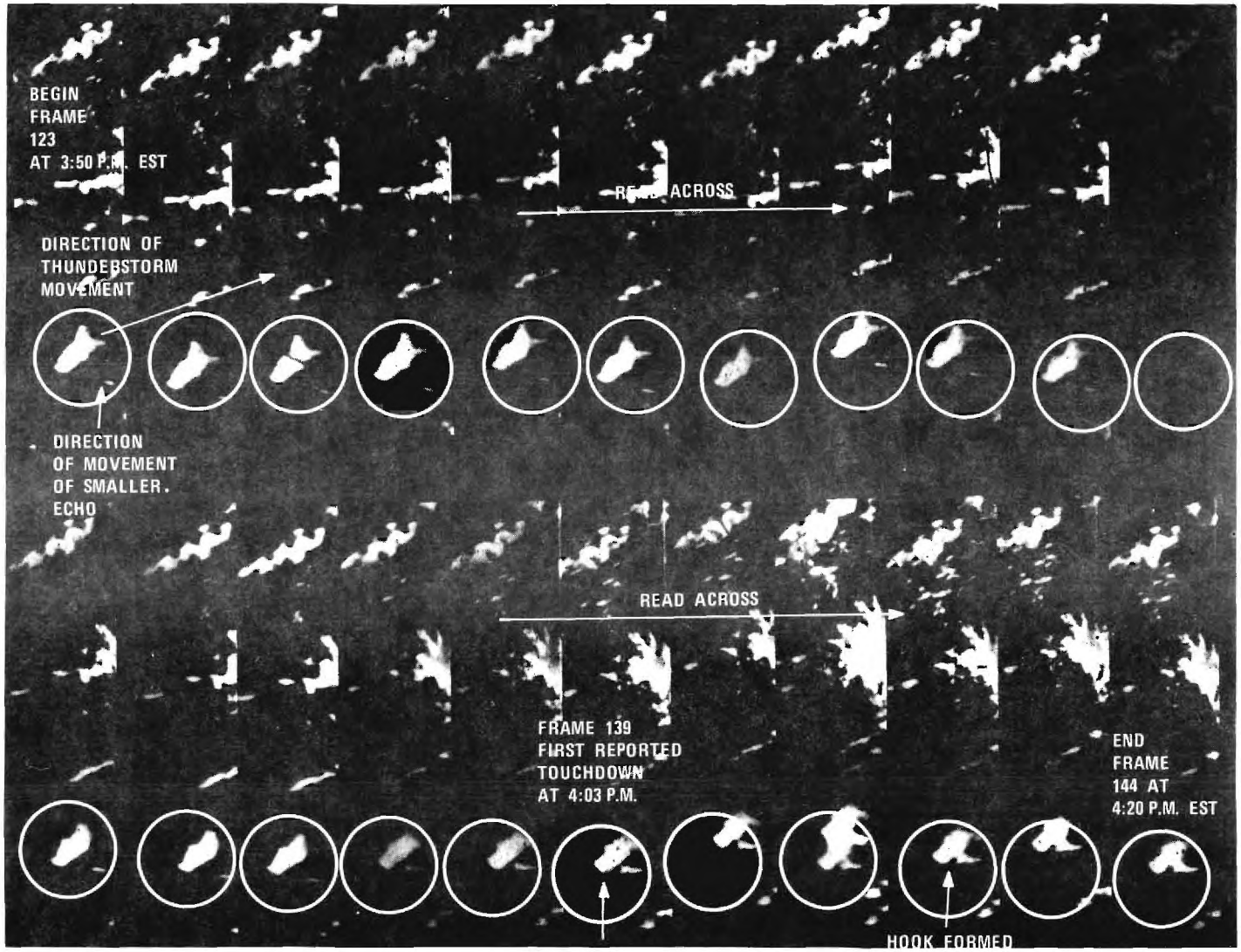

Figure 18. Frame-by-Frame analysis of Fort Valley tornado showing cross wind merger of precipitation echo with the main echo during 3:50 - 4:10 p.m. EST time frame on February 18, 1975 as observed from Athens radar without contouring. Smaller echo moves with low level winds from south to north. Tornado touchdown occurs just before merger between main thunderstorm and smaller echo to the south.

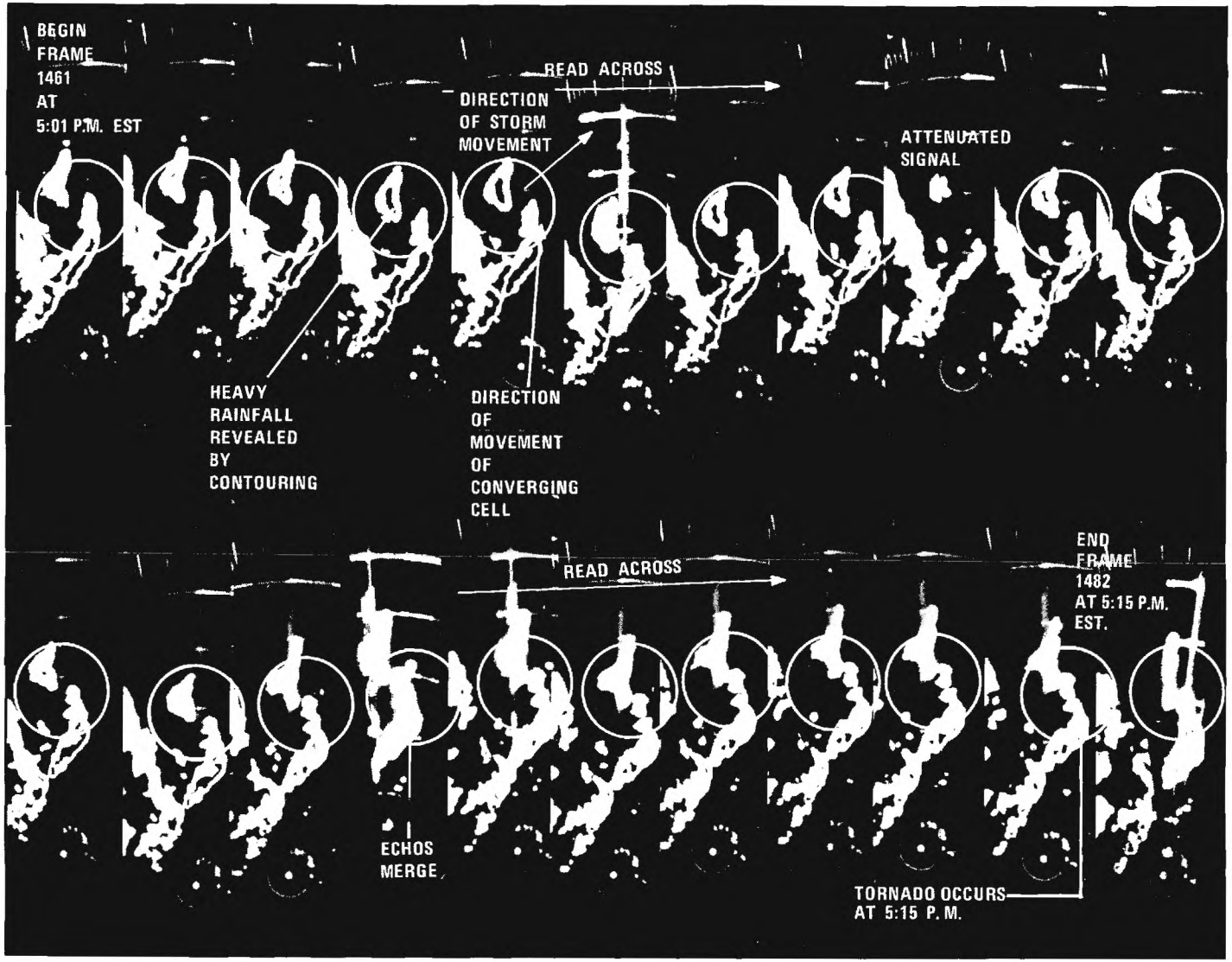

Figure 19. Frame-by-Frame analysis of Lyons, Georgia, tornado showing merger between echos between 4:30 - 5:00 p.m. time frame on January 12, 1975 as observed by Waycross radar with contouring. Tornado producing thunderstorm moves away from main mass then merger occurs with converging echo to the south as tornado touchdown occurs at 5:15 p.m.

the tornado was reported to have occurred. Again, several meteorological explanations could be made about the echo motion. The important point is that the "hook" formed and the merging began before damage from the tornado was reported.

F. Sferics Observations of Nontornadic Storms

The sferics records for the Atlanta tornado are the only sferics data that will be presented. Additional data taken on 18 thunderstorms observed during the March to June period are not presented since supporting data from NWS and other sources are insufficient to provide the needed correlation between the sferics data and actual meteorological occurrences.

Normalized sferics activity for these 18 thunderstorms exceeded 100 bursts per minute only when local corona conditions were present. One exception, however, was a storm on 16 May that produced 50 mph winds and hail at Winder, Georgia. This storm produced a burst rate of 205 counts per minute for a 5-minute period. The cause of the one high intensity spike is unknown, although the possibility of funnel cloud formation during the time has not been ruled out. Wind damage and a reported tornado occurred at the Winder, Georgia, airport a short time after the peak occurred. The data taken on the 18 nontornadic thunderstorms indicate in general the burst rate will be lower than in the tornadic case observed.

G. Summary

The rate of tornado occurrence appears to have increased during the past 5-year period over an earlier 17-year sample period. A trend appears to have been established during the past 5 years that would indicate tornadoes are occurring during periods when the public is out of contact with the normal

channels of warning. Thus the need for new approaches to public warning systems is suggested.

Studies of the path lengths indicate that a majority of tornadoes occurring in Georgia are short in duration, the average path length being less than 6 miles. However, this fact does not affect the amount of damage done when a community lies in the path of a short-lived tornado.

Examination of National Weather Service radar film shows detectable deviations in the normal direction of movement in thunderstorm echoes tens of minutes before tornado damage is reported. Echo divergence and "hook" echoes were also seen to occur before tornado formation. While there are several possible meteorological explanations for the effects observed, the important point is that there seems to be a circulation pattern present, possibly unique to tornado formation, tens of minutes before funnel touchdown. With advanced radar data processing this unique signature may be detectable consistently with a low false-alarm rate.

SECTION VII

THE ATLANTA TORNADO

The tornado that passed through northwest Atlanta at 7:30 a.m. EDT on 24 March 1975, was one of the best documented tornadoes in Georgia during the 1975 tornado season. The Georgia Tech tracking radar and basic sferics monitoring equipment were operational during the occurrence. Georgia Tech's radar operators were eye witnesses to the tornado and Georgia Tech personnel flew over the ground track later in an aircraft to confirm the point of touchdown, path length and width. Thus it is possible to present an in-depth discussion of the Atlanta tornado.

A. Synoptic Situation

At 8:00 a.m. EDT (7:00 a.m. EST) on 24 March 1975 a rapidly moving cold front, extending out of a deep closed low pressure system over Iowa, was moving into northwest Alabama (Figure 20). A severe squall line ahead of the front was just entering the extreme northwest corner of Georgia and moving eastward about 35 knots. Figure 21 depicts the time history of the barometric pressure occurring at the Georgia Tech nuclear reactor the morning of 24 March. As the front approached, the barometric pressure dropped from 29.8 to 29.72 inches between 2:00 a.m. and 6:00 a.m. EDT. A further drop in pressure of .01 inch was recorded during the period of tornado passage. The rain-induced pressure maximum associated with a squall line occurred between 9:15 and 9:30 a.m. A strong southerly flow of warm moist air at the surface was producing a few scattered thunderstorms over north Georgia ahead of this squall line.

The Georgia Tech tracking system was activated at 3:00 a.m. EDT, 24 March 1975. The operational elements of the system were: (1) the 3-cm weather

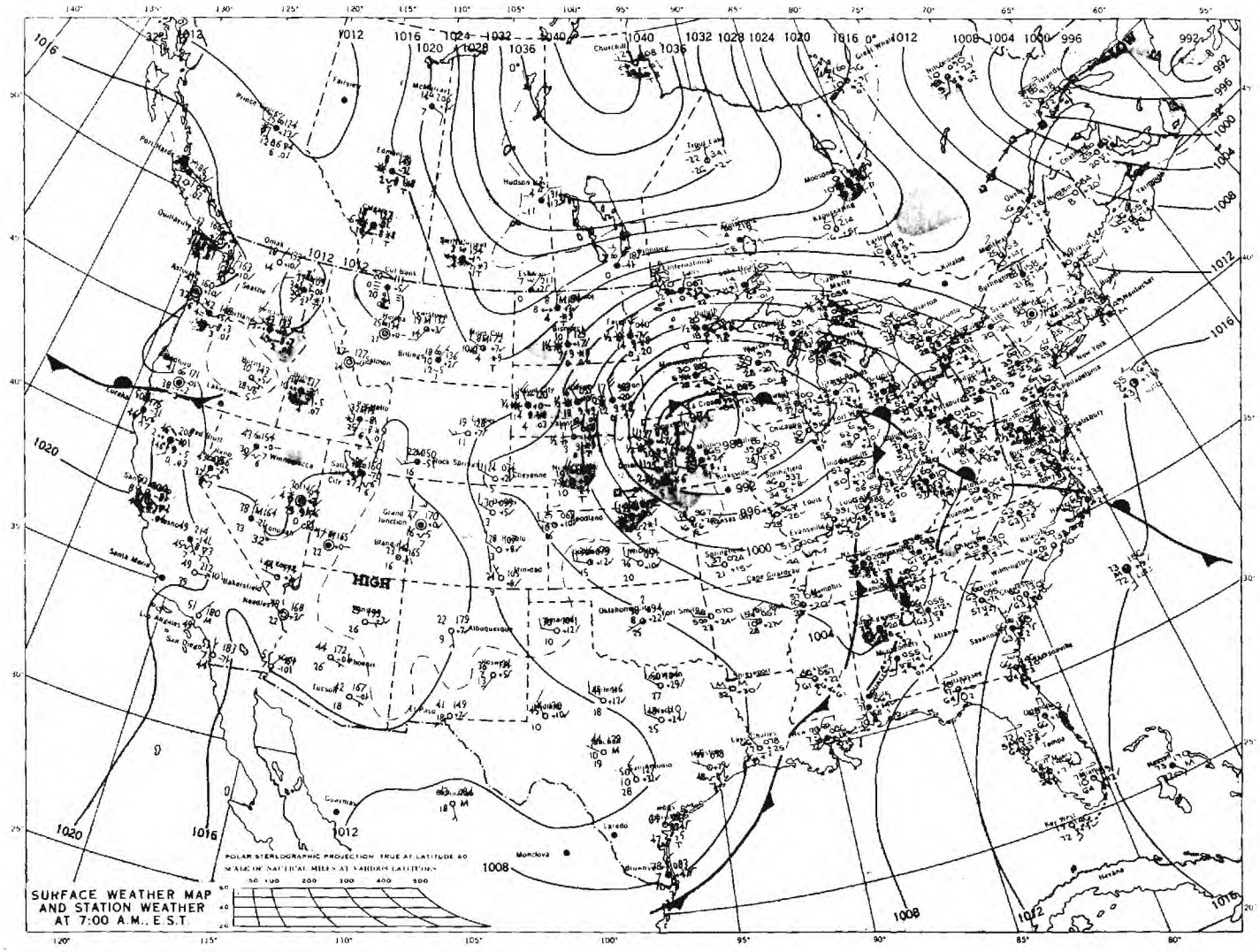

Figure 20. Surface weather map at 8:00 a.m. EDT (7:00 EST) 30 minutes after the Atlanta tornado occurred.

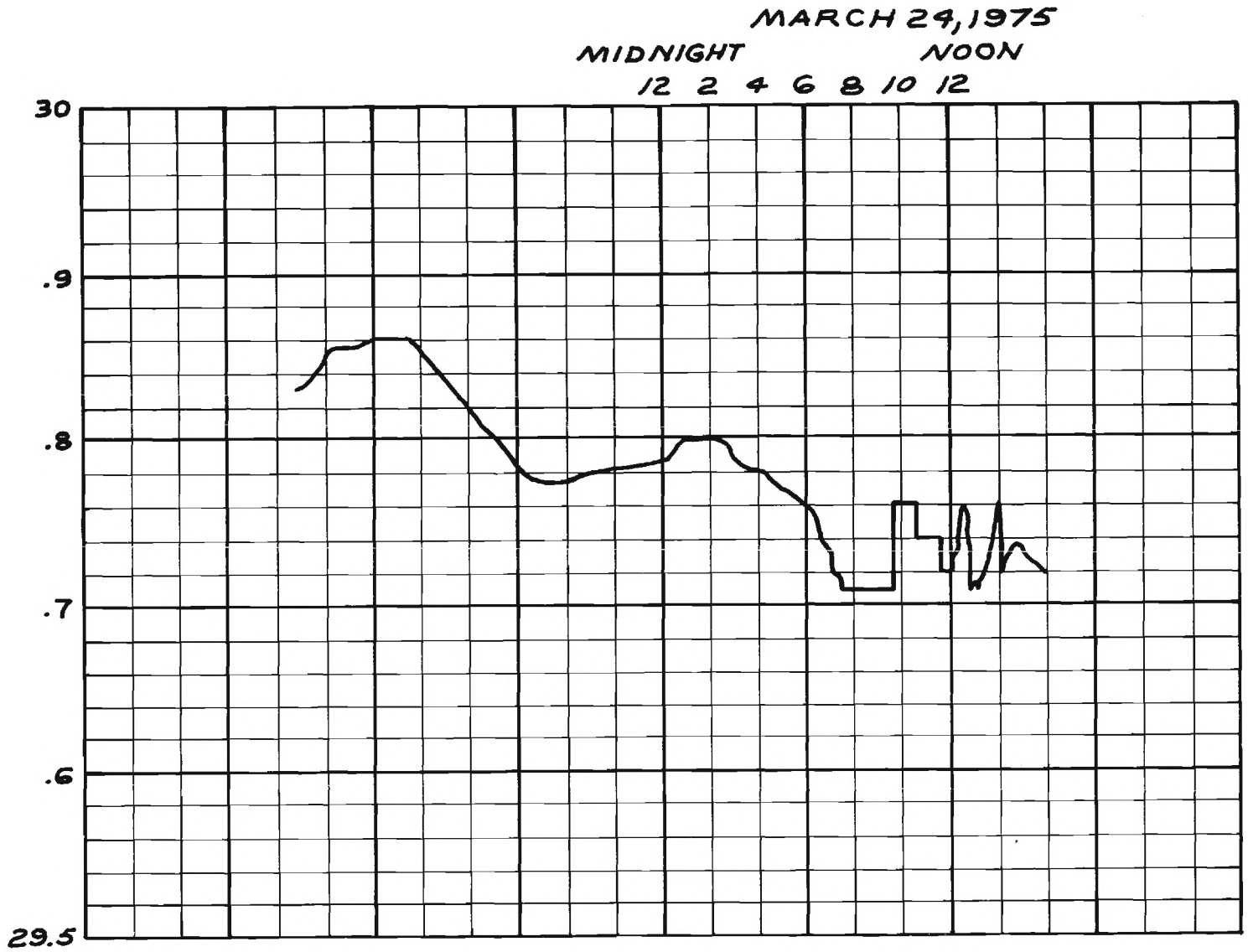

Figure 21. Time/History trace of the barometric pressure taken on the Georgia Tech campus March 24, 1975, between the hours of 5:30 - 11:00 a.m. EDT.

radar located on the Graduate Library, (2) a high-frequency direction finder sferics station on the Physics Building, and (3) several non-directional sferics receivers with burst counters and audio monitors located in the Electronics Research Building Communications Laboratory. Several lines of thunderstorms moving from southwest to northeast along an approximate heading of 30 degrees were tracked before the thunderstorm that produced the Atlanta tornado was detected.

The Georgia Tech radar indicated the presence of a tornado associated with an approaching thunderstorm at 7:15 a.m. EDT. The tornado touched down at 7:30 a.m. west of town and moved toward the northeast through the northwestern part of Atlanta at about 50 knots, causing very heavy damage. In its 400-yard wide path were both industrial and residential property including the Governor's mansion. About an hour and a half after the tornado had passed, a squall line with strong gusty winds and heavy rain passed through the city.

The thunderstorm that spawned the Atlanta tornado presented an ideal case for sferics/radar studies. This thunderstorm moved toward Atlanta at an almost constant speed between 6:00 and 8:00 a.m. EDT, well ahead of any other thunderstorms in the area. Because the storm was isolated, it is assumed that all high-amplitude sferics signals recorded during the 6:00 - 8:00 a.m. time period were from this thunderstorm. The bearings obtained from a direction-finder sferics station on the Physics Building during thunderstorm approach tend to confirm this assumption. Data to be presented later in this section demonstrate the research value of observing an isolated tornado-producing thunderstorm at extremely close range. It is doubtful that such significant results would have been obtained if this thunderstorm had not been isolated and near the Georgia Tech campus.

B. Radar Observation

Figure 22 is a time history reconstruction of the thunderstorm that spawned the Atlanta tornado. Radar films from Centreville, Alabama (CKL), and Athens, Georgia (AHN), and data from the Georgia Tech radar were used in the reconstruction with echo intensity contouring shown only for the Centreville coverage due to the fact that the WSR-57 at Athens had no contouring provisions. This thunderstorm formed in South Alabama, 200 miles south-southwest of Atlanta about 4:00 a.m. EDT. The mature storm crossed into Georgia at a speed of approximately 50 knots just before 6:00 a.m. Two major cells topping 45,000 feet with extremely heavy precipitation could be detected within the storm at this time. Convergence between these two cells began between 6:00 and 6:30 a.m.

The Georgia Tech radar operators first began tracking the thunderstorm at 6:15 a.m. EDT when the most easterly cell was 49 nmi on a bearing of 238 degrees from Georgia Tech. The closest cell was designated as target No. 10 and the converging cell was designated No. 13. The reconstructed ground track of cell location derived from Georgia Tech radar data, with time and top height data, is shown in Figure 23. (An elevation correction was made for an error caused by antenna leveling problems.) Cell No. 10 had moved to a range of 43 nmi at 235 degrees azimuth by 6:24 a.m. Cell No. 13 is not shown until later. Cell No. 10 was topping 40,000 feet at 6:51 a.m. and was 22 nmi from the radar at 228 degrees. Cell No. 13, topping 43,000 feet, appeared near Cell No. 10 at 6:55 a.m. Cells Nos. 10 and 13 merged at 6:59 a.m. in such a manner that neither could be distinguished as separate targets on a basis of reflectivity profiles.

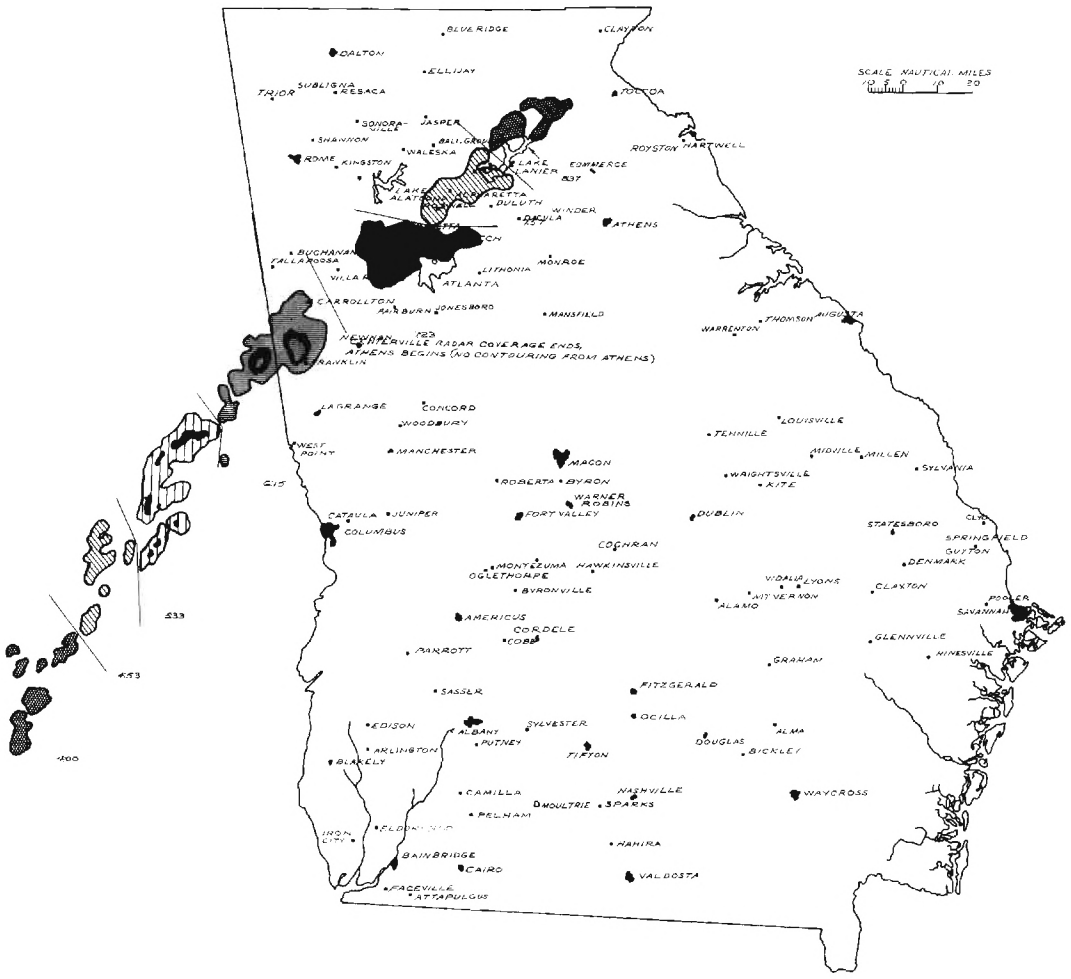

Figure 22. Time/History reconstructed composite radar history of the thunderstorm that developed into the Atlanta tornado.

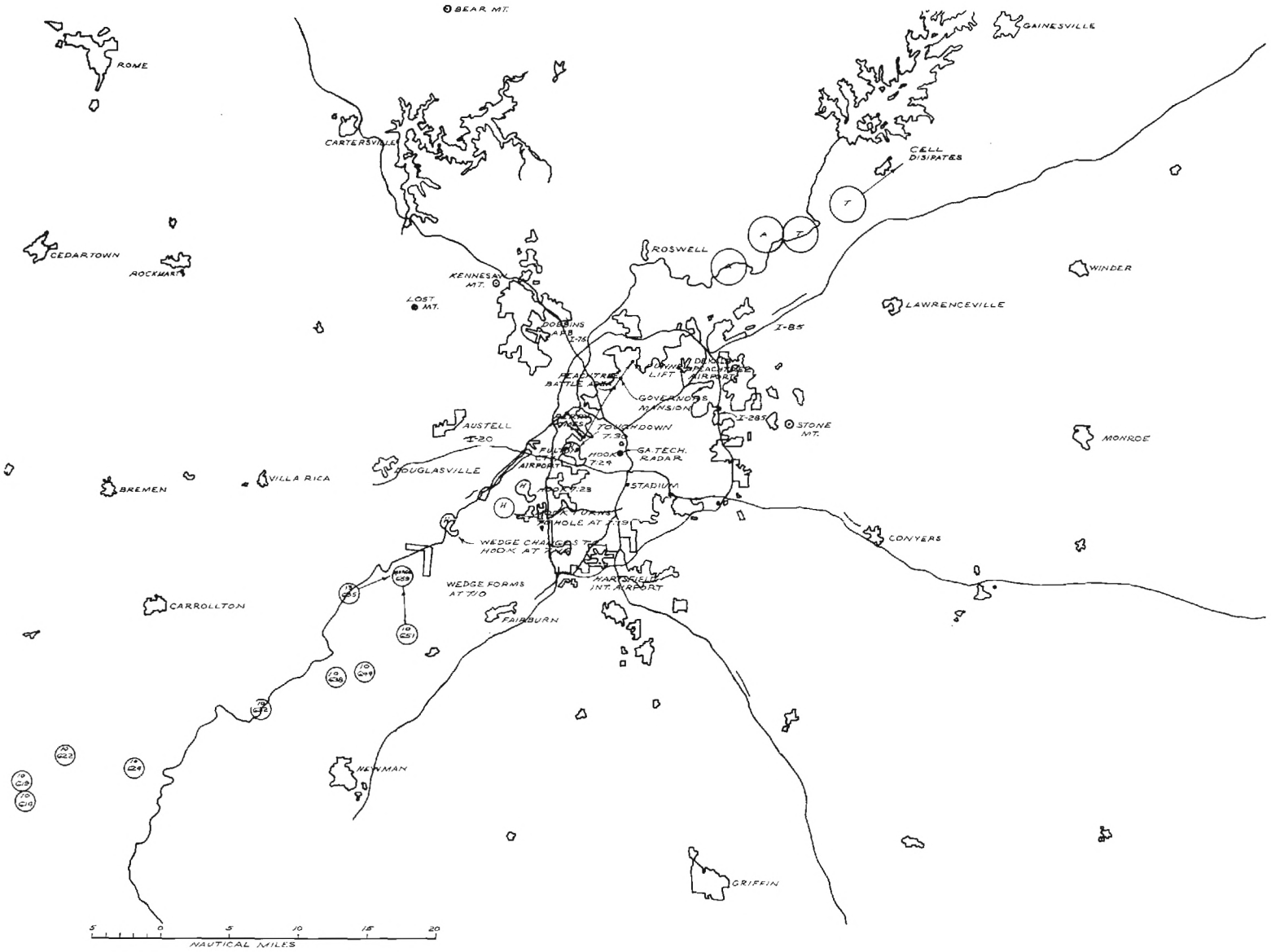

Figure 23. Cell movement diagram depicting location of the cores, top heights, and time of observation.

At 7:10 a.m. the radar antenna was lowered to an elevation angle of approximately 2.0 degrees which corresponds to a beam height of 3,000 feet at a range of 15 nmi. A wedge of extremely high reflectivity was noted to form on the PPI at this time at a range of 15 nmi and a bearing of 225 degrees. The sides of the wedge formed a perfect straight edge; each side being no longer than 2 nmi with the tip of the wedge aligned along the axis of the storm's movement.

The wedge was observed to form a hook at 7:15 a.m. at a range of 14 nmi. The antenna was raised to 3 degrees in elevation, giving a beam elevation of 6500 feet at 14 nmi. At this height the "hook" apparently merged with the general precipitation echo within the thunderstorm, as it could not be discerned. When the antenna was lowered to the 1-degree position, the "hook" was again clearly defined. The vault area within the finger of the "hook" measured a diameter of no more than 2 nmi across. The tip of the "hook" closed to the main area of precipitation at 7:20 a.m. forming a hole in the return. The approximate diameter of the hole was 1 nmi at a range of 10 nmi with the elevation angle still less than 1 degree. The "hook" was clearly discernible again by 7:29 a.m. at a range of 4 nmi on a bearing of 260 degrees with the antenna elevation angle at 1.3 degrees. The "hook" echo persisted until approximately 7:33 a.m. EDT when power was lost on the Georgia Tech campus.

C. Visual Observation

Visual observation of the tornado was concurrent with the latter part of the radar observations. The observer was on the 7th floor roof of the Graduate Library within voice range of the radar operator. No precipitation fell before or during the tornado at the radar site. The "hook" had been

visible on the radar for a period of 10 minutes before the observer went to the door overlooking the roof at approximately 7:25 a.m. EDT. He observed an unusually large cloud-to-ground discharge of lightning at an approximate bearing of 250 degrees. The discharge approximated a cylinder with a diameter of a ball point pen held at arm's length. The 7:26 - 7:28 a.m. time of occurrence would have placed the discharge very near (± 1 nmi) the location where the funnel first touched the ground just south of the Perry Homes area. The lightning stroke was a very intense bluish color with no points of deviation from the vertical axis. Later in the evening other witnesses, calling on a local radio talk show (non-Georgia Tech personnel), commented on the intensity and unusual appearance of the stroke. This stroke was the only form of natural electrical activity observed from the Georgia Tech vantage point on the southeast side of the storm.

The tornado appeared as a dark cloud with a diameter of 10 degrees within the field of view and was observed about 7:27 - 7:29 a.m. at a bearing of approximately 250 degrees. It extended to the ground from the cloud base of approximately 1,000 feet. The walls of the dark cloud were vertical, but no characteristic funnel shape was observed at any time. Green flashes appeared within the vortex between 7:28 and 7:33 a.m. These flashes are thought to be due to broken power lines rather than to any natural electrical phenomena, as power to the Georgia Tech campus was disrupted about this time.

An attempt was made to visually correlate the tornado's actual location with the radar "hook" echo. The tornado vortex appeared to lead the hook by approximately a mile, but no accurate optical angle measurements were available to confirm this finding. Power was lost at Georgia Tech momentarily at approximately 7:33 a.m. Auxiliary power was restored almost immediately, but

the high-voltage generator for the radar transmitter could not be restarted until 7:48 a.m., at which time the "hook" was no longer visible and the main mass of the thunderstorm had moved north of the radar site.

The thunderstorm continued to move north-northeast on a bearing of 38 degrees. Moments later when the storm was south of Buford, Georgia, another "hook" echo was seen to form at 8:04 a.m. at a range of 18 nmi and azimuth of 38 degrees. No further tornado activity occurred, however, and shortly thereafter the thunderstorm rapidly dissipated.

D. Sferics Observations

During the period before and during the Atlanta tornado two Georgia Tech sferics receivers were in operation as was a DF receiver without burst count capability and a military R-390 receiver used to aurally monitor sferics burst. A receiver supplied by William L. Taylor [2] for incorporation by Georgia Tech into a NASA sponsored severe weather monitoring project was also in operation the morning of the Atlanta tornado.

The data in Figure 24 present averaged burst rate counts from 1:30 to 10:45 a.m. EDT on the morning of 24 March 1975. Six 1-minute burst rate counts were averaged to produce one point on the plot. This technique serves to smooth the curve and is useful in showing the trend of the burst rate as a function of time. More detailed data will be presented to demonstrate the very high counts that can and do occur within a single 1-minute counting interval. Figure 24 shows that the burst count remained at a fairly low rate as the isolated thunderstorm approached the city. Burst counts remained below 50 counts per minute prior to 6:30 a.m. An examination of the minute-by-minute data prior to 6:30 shows that there were no high, single-count events

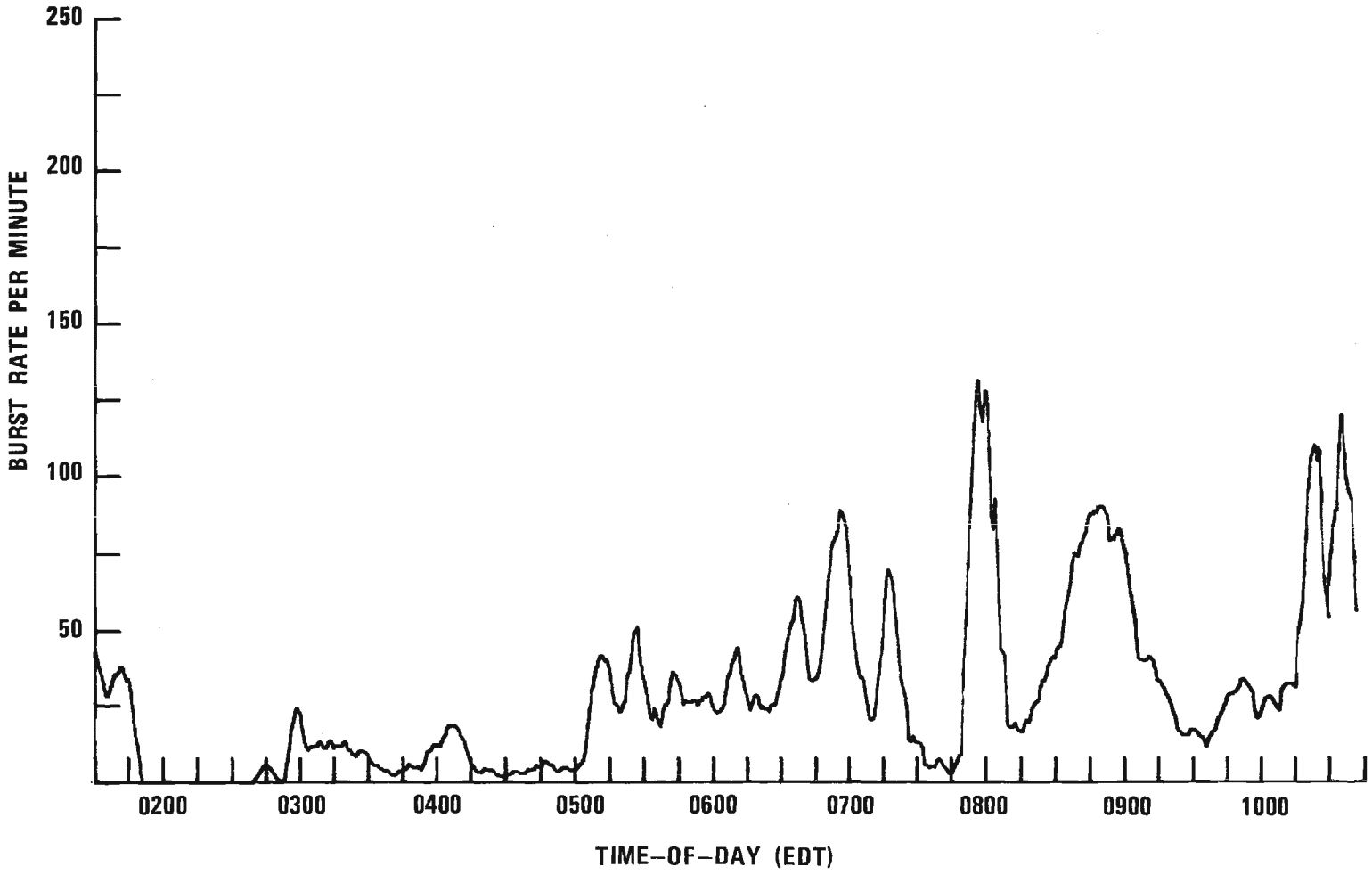

Figure 24. Long-term averaged sferics data for the severe weather of March 24, 1975.

during this period. At approximately 6:30 a.m. the burst rate increased significantly, with several periods of very intense activity occurring between 6:30 and 10:45 a.m. The burst rate showed a marked increase at 6:55 a.m. and at 7:10 a.m. with a significant decrease between these two time intervals. During the period that the tornado was on the ground, the burst rate dropped to a very low value.

The observations of the sferics equipment operator during this time period are also quite significant. The operator noted that prior to touchdown a high level aural output, in the form of "static," was emanating from the co-located R-390 communications receiver that was tuned to the same frequency as the sferics receiver. At the time of touchdown, when the burst count dropped to a very low value, the aural output from the communications receiver became "very quiet."

It is believed that this "quiet" phenomenon occurred as a result of the funnel's acting as a "short circuit" between cloud and ground, thus serving to discharge the accumulated electrical energy through a low resistance path and to prevent any subsequent buildup of static charges during the time that the funnel was in contact with the ground. This factor is an important finding if it can be shown that sferics levels always decrease when the funnel is on the ground. Subsequent operational periods will be necessary to confirm that this phenomenon is repeatable.

One possible reason that this effect is not often observed is that few observations are made as close as 4 miles to an active tornado spawned by an isolated thunderstorm. Normally, sferics observations would be made on a line of active thunderstorms, of which one might produce a tornado. If such a line contained 10 equally active cells and if the tornado-producing cell

ceased sferics emission during the period that the funnel was on the ground, the total sferics count would be reduced by only 1/10. Such a decrease would be difficult to detect without precise directional data. Through the use of highly directional burst counting equipment in future experiments the sferics cessation phenomenon may be observed again, and thus may offer a dependable remote warning mechanism to indicate funnel touchdown.

E. NOAA Receiver Data

A sferics receiver, designed by W. L. Taylor of the National Oceanic and Atmospheric Administration (NOAA) was co-located with the Georgia Tech sferics receiver during the period of the Atlanta tornado on 24 March 1975. The NOAA receiver shown in Figure 25 was on loan to Georgia Tech for inclusion in a severe weather instrumentation package developed by Georgia Tech under a contract with NASA-Goddard, Greenbelt, Maryland.

Sferics burst data are presented by the NOAA receiver in the form of four front panel lights of different colors. These status lights (white, green, yellow and red) indicate the magnitude of the burst rate. The white light indicates low burst, green medium, yellow intermediate, and the red light indicates a high burst rate that may be associated with the probability of tornadic activity as was presented in the graph of Figure 2, Section II.

The manner in which the burst rate lights indicated severe weather activity on 24 March is shown with the Georgia Tech burst rate data in Figure 26. Figure 26 presents 6-minute averages of burst count between 6:39 and 10:45 a.m. Figure 27 presents the burst rate data on a minute-by-minute

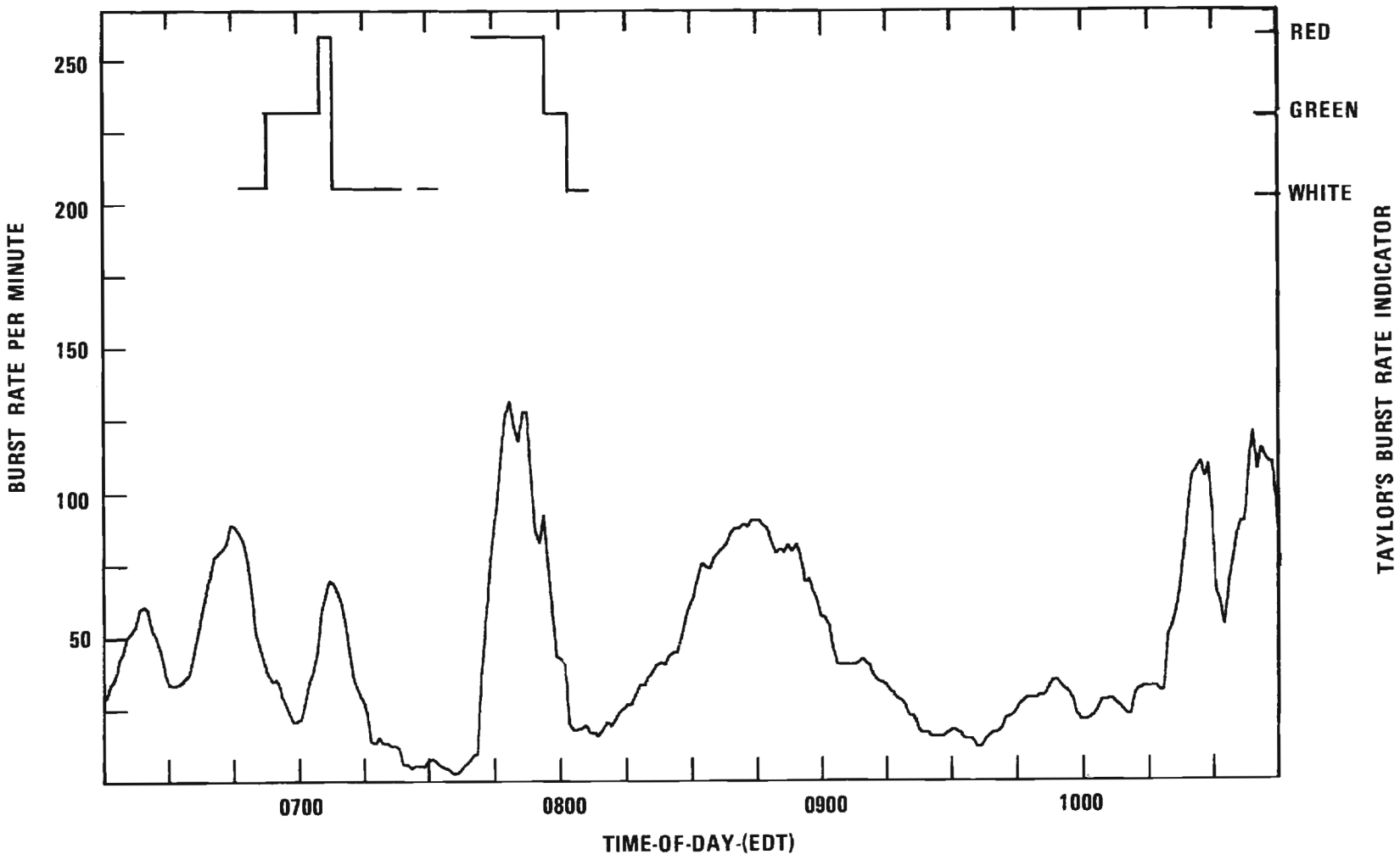

Figure 25. Averaged sferics activity for the severe weather of March 24, 1975.

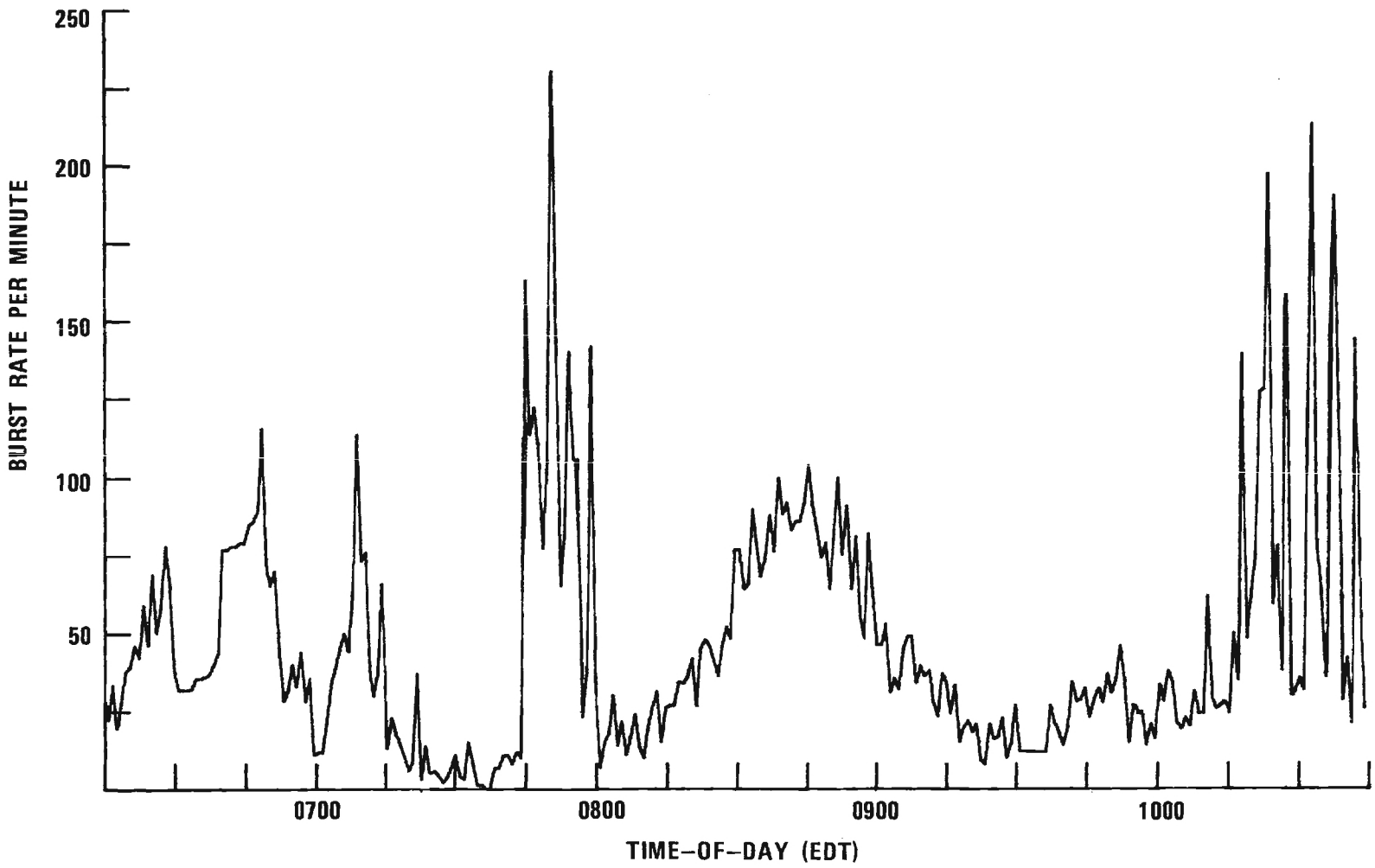

Figure 26. Discrete data for severe weather of March 24, 1975.

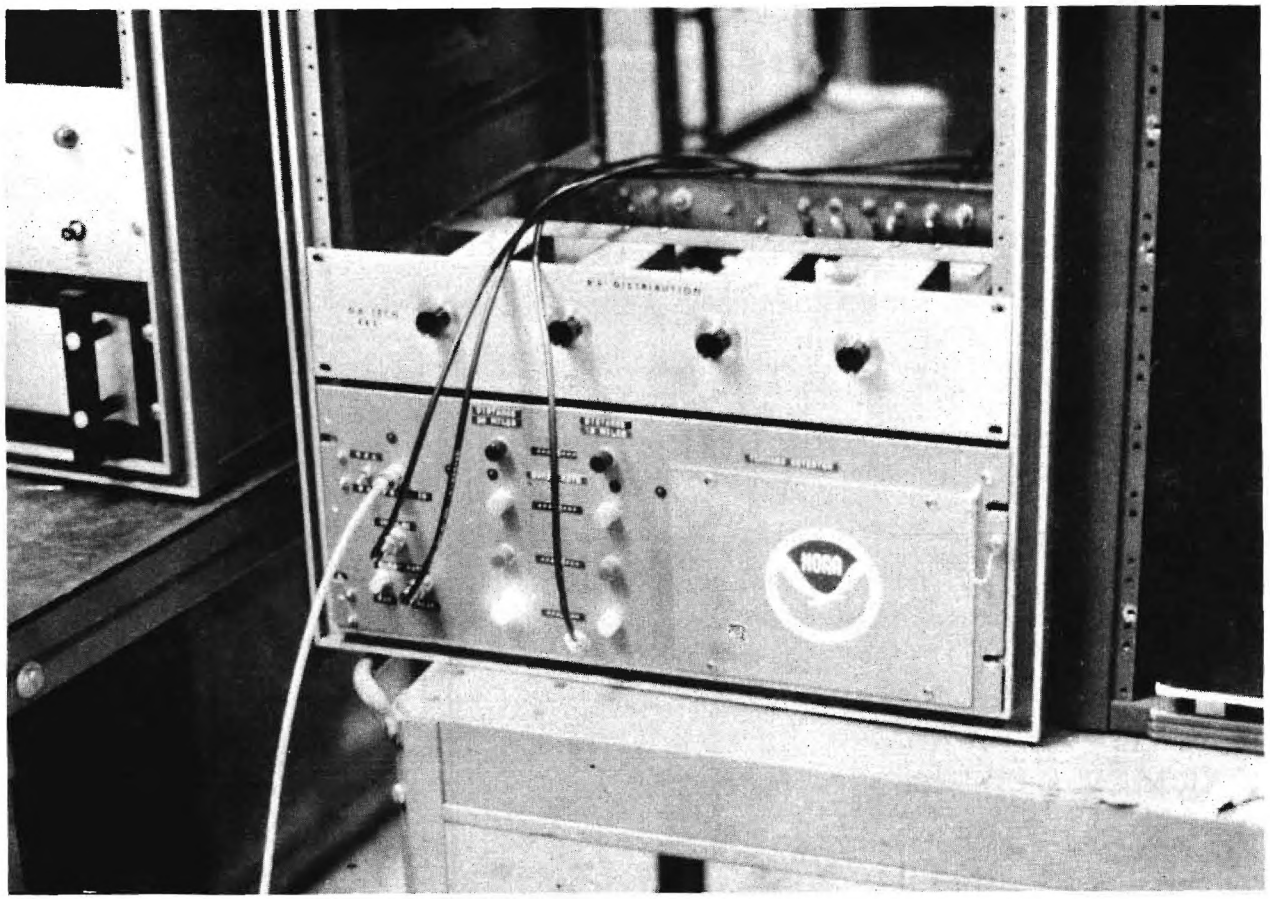

Figure 27. Photograph of NOAA sferics receiver on loan from W.L. Taylor for incorporation into Georgia Tech sferics monitoring package used in NASA test.

basis, and illustrates the rapid fluctuations in burst count that occur between successive 1-minute intervals.

The NOAA receiver began to indicate severe weather activity (white light) about 6:45 a.m., concurrently with the burst rate increase indicated by the Georgia Tech sferics receiver. The burst rate increased to medium (green light) at 6:55 a.m. and continued at this level until 7:08 a.m. Between 6:55 and 7:08 a.m., when the NOAA receiver was indicating a "green" condition, the burst rate indicated by the Georgia Tech receiver decreased significantly for a brief period of time. The reason for this absence of burst rate correlation between the two receivers is unknown, although it is possible that a brief status change of the NOAA receiver may have gone unnoticed by the operator. The sferics data from the Georgia Tech receiver were automatically recorded by a digital printer, whereas data from the NOAA receiver were recorded manually by the operator.

At 7:08 a.m. the high burst rate indicator (red light) became active for approximately 2 minutes. This red indication occurred about 20 minutes prior to confirmed touchdown of the tornado but simultaneously with reported funnel cloud formation. At 7:10 a.m. the NOAA receiver dropped from "red" to "white" status and continued to indicate either low burst rate or no counts (all lights out) until 7:45 a.m. Beginning about 7:40 a.m. the Georgia Tech sferics receiver indicated a marked increase in burst rate and at 7:45 a.m. the NOAA receiver again went to "red"status. This increase in burst rate occurred about the time the tornado completed its ground track. Figure 26 shows that between 7:40 and 8:05 a.m. the burst rate increased and then decreased and that a good correlation existed between the NOAA and Georgia Tech receivers. During the later period of activity from 8:05 to 10:45 a.m.

as indicated by the Georgia Tech receiver, no sferics activity was recorded by the NOAA receiver.

In general, good data agreement existed between the Georgia Tech and NOAA receivers during the morning hours of 24 March 1975. The only major deviation existed about 7:30 a.m. when the Georgia Tech receiver recorded a period of low activity while the NOAA receiver was indicating moderate activity. As was noted, however, this lack of correlation may have been the result of a change unnoticed by the equipment operator.

F. Correlation of Sferics and Radar Data

Figure 28 shows radar measured top heights and sferics burst rate counts for the 6:00 - 8:00 a.m. EDT period. During the 6:10 - 7:05 a.m. time period a significant correlation exists between the amplitudes of the top heights and the sferics burst count. This relationship could have existed for a longer period of time than shown; however, the radar was used to study the "hook" phenomenon at 7:05 a.m. and no "tops" data were taken after this period until 7:45 a.m. One possible explanation for this occurrence is advanced by Larsen [26] as a result of a similar sferics study in Canada. Larsen found that lightning activity as indicated by the sferics rate was roughly proportional to the area of heavy precipitation at the -30 degree C (-22 degree F) altitude. In a multi-cell situation the sferics rate and radar reflectivity increased in phase, while in a single cell situation the lightning activity lagged the development of precipitation by 10 minutes. Larsen also found that the occurrence of lightning was not closely related to regions of precipitation with reflectivity less than about 43 dBZ at the -30 degree C level, or to regions of high reflectivity at lower levels.

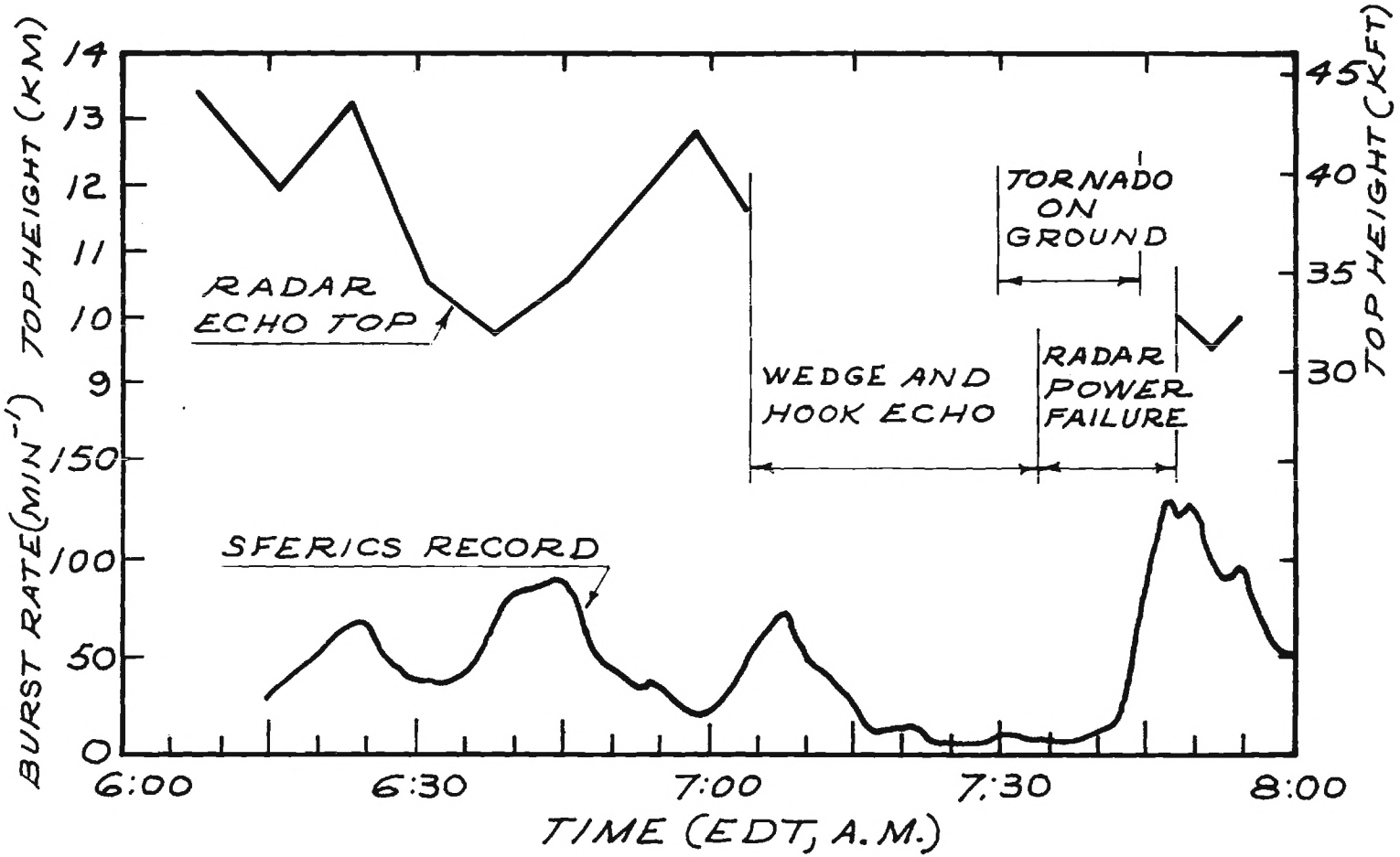

Figure 28. Radar top heights of Atlanta tornado-producing thunderstorm displayed versus time with sferics burst rate shown.

The data are insufficient to support similar detailed conclusions in the case of the Atlanta tornado thunderstorm. However, some particular features in Figure 28 should be noted. The peak of the sferics burst rate and the radar tops appear to occur in phase at 6:25 a.m. The sferics maximum at 6:45 a.m. leads the radar tops by approximately 15 minutes, while the maximum at 7:07 a.m. lags the echo top by about 10 minutes. Despite the temporal difference in their development, the two phenomena correlate closely enough to verify the original assumption that the sferics recorded between 6:00 and 8:00 a.m. all originated within the thunderstorm that generated the Atlanta tornado. The most significant feature of the sferics data is the cessation of sferics activity during the time that the tornado was on the ground. The implications of this phenomenon for understanding of tornado dynamics and for short-term warning are significant, particularly if it can be observed in a wide range of tornado occurrences.

G. Aerial Observations

The entire tornado track was photographed from the air. Flights were also made 20 nmi from each end of the 12.5-mile track to determine if the tornado had caused additional unreported damage. Photographs shown in Figures 29 and 30 are typical of the type damage occurring in residential areas along Atlanta's northwest side. The large number of downed trees shows the localized wind field patterns generated by the vortex. The first damage, on the southwest end of the track occurred one mile south-southwest of the Perry Homes Subdivision (see Figure 23). An eyewitness reported a funnel cloud west of Greenbriar Shopping Center, or approximately 15 miles south-southwest of the point of touchdown, between 7:00 and 7:15 a.m. This location

Figure 29. Damage along Atlanta's northwest section caused by the March 24, 1975, tornado.

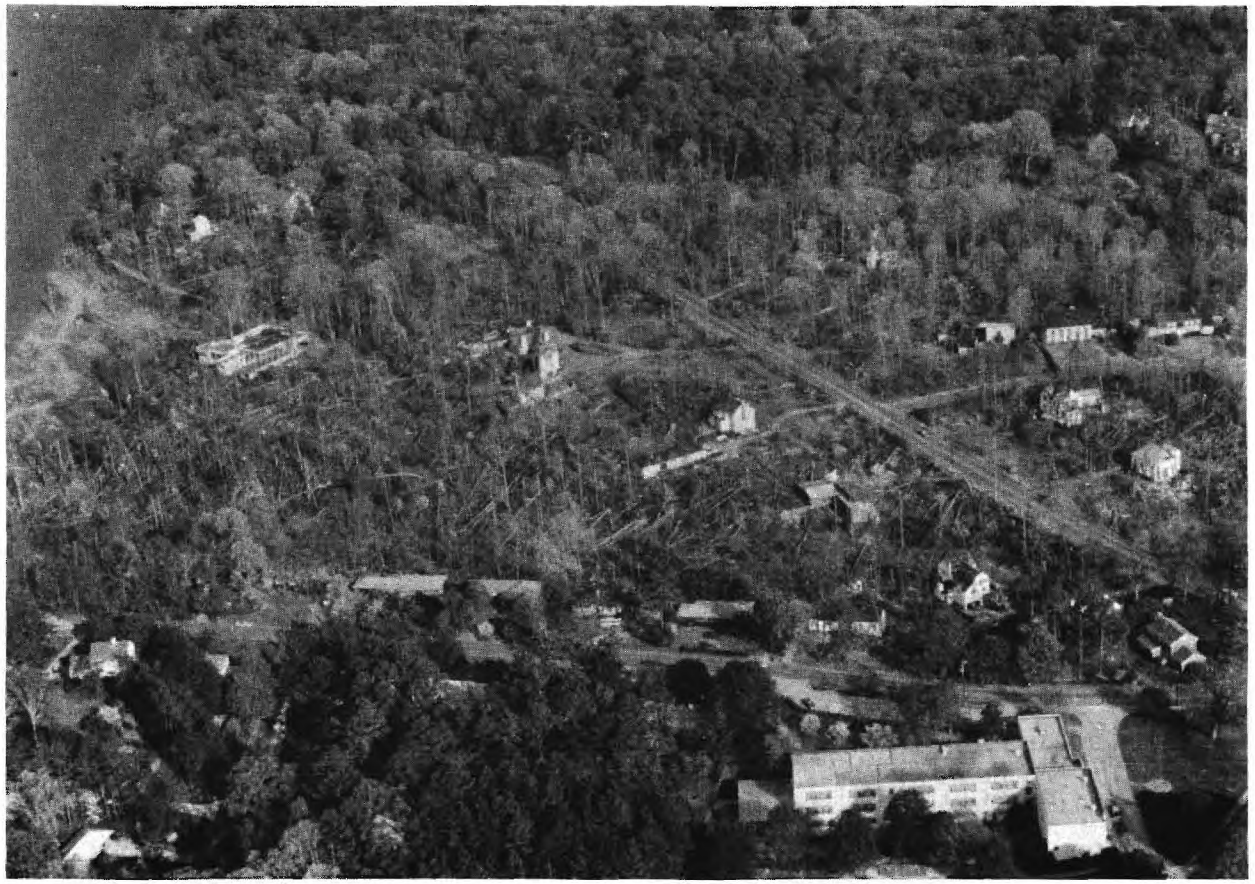

Figure 30. Damage along Atlanta's northwest section caused by the March 24, 1975, tornado.

is in line with the observed ground track of the tornado, but no damage was found southwest of the point of touchdown.

To the northeast there was evidence of sporadic damage beyond the official 12.5-mile ground track. This damage took the form of trees uprooted from the ground in no specific pattern. A number of trees were uprooted in a wooded area south-southwest of Buford where a second "hook" echo was observed at 8:04 a.m. EDT. However, it could not be determined from the air whether these trees were felled by straight-line winds or a tornado at tree-top level.

H. Summary

The Atlanta tornado was one of the best documented occurrences during the January to June 1975 Georgia tornado season. The isolated thunderstorm that generated the Atlanta tornado was observed by NWS and Georgia Tech radars. Georgia Tech sferics receiving equipment monitored the electrical activity of the storm.

Eyewitness reports, aerial photographs, and radar observations place the location of the "hook" echo and funnel cloud within 1 mile of each other. The tornado formed at the interface of two merging cells within the same thunderstorm mass that formed a wedge-shaped pattern of extremely heavy precipitation. The wedge turned into the classic "hook" 15 minutes (14.9 miles) before any reported tornado damage occurred.

The sferics data indicated a marked increase in burst count some 15 minutes prior to touchdown of the tornado. If such a burst rate increase always precedes touchdown then this form of data would be a valuable factor in an early warning system. Further research and system refinement are needed to determine if this phenomenon is always present and further if it can be

detected when distant from the sferics receiver and co-existent with numerous other thunderstorms.

The sferics data further indicated that when the funnel touched the ground the radiated electromagnetic signals from the storm fell to an extremely low level. The unusual cloud-to-ground discharge observed at the moment of tornado touchdown suggests that the tornado acted to "short circuit" the electric field of the thunderstorm.

If the sferics cessation phenomenon is valid for most tornado occurrences in Georgia, detection of the phenomenon could serve as a warning that a funnel is on the ground. While not offering the desired early warning, this limited capability could serve to warn those persons further along the tornado's projected path. Such a capability would serve as an interim warning tool, while further research is devoted to the identification of tornado signatures in the sferics and radar data.

SECTION VIII

PRESENT SYSTEM

The present sferics/radar tracking system consists of three elements: (1) a 3-cm radar, (2) a plotting/tracking center co-located with the radar, and (3) a 3-station sferics receiving network. The equipment actually used in the 1975 observations is described in this section. Preliminary studies under this project, also described, postulated a comprehensive sferics receiver network which was not constructed for reasons discussed below.

A. Radar System

The Radar Technology Division's 3-cm, noncoherent, 250 kW pulsed radar developed for this project is located on the 7th floor of the Georgia Tech Graduate Library. The radar operator display and control console is co-located in the radar/plotting room as shown in Figure 31A. The 250 kW transmitter shown in Figure 31B and accompanying receiving equipment are located on the 8th floor of the Graduate Library.

The 4-foot antenna shown in Figure 32A is simultaneously steerable in azimuth and elevation and is located on the roof of the library. The transmitted signal is vertically polarized, and the antenna utilizes a dual-mode feed allowing both the parallel and cross components of the received signal to be processed simultaneously. This feature was included to facilitate future severe weather investigation using polarization as a discriminant. Table I lists the parameters of this radar system.

B. Plotting Operation

Radar and sferics track data are plotted on a 5 x 4 foot backlighted map covered by acrylic plastic as shown in Figure 32B. The plotting board

Figure 31A. Radar console and plotting board shown in the plotting and tracking center located on the 7th floor of the Georgia Tech Graduate Library.

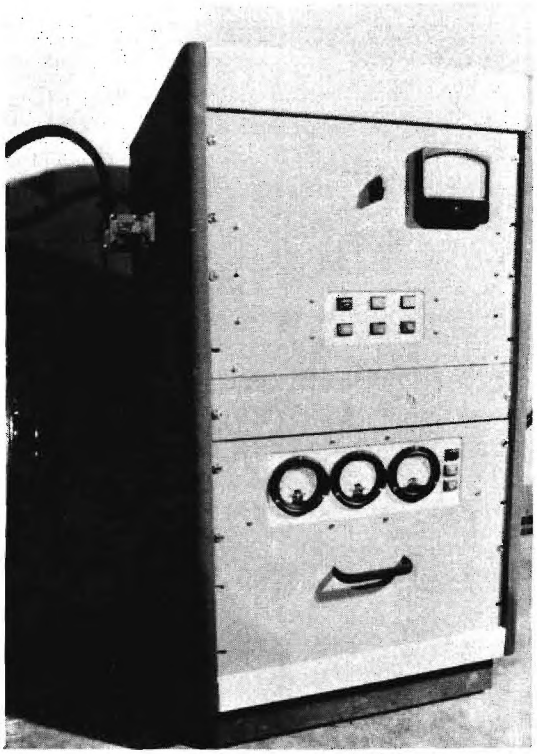

Figure 31B. Noncoherent 250-kW 3-cm transmitter used during the 1975 tornado tracking period.

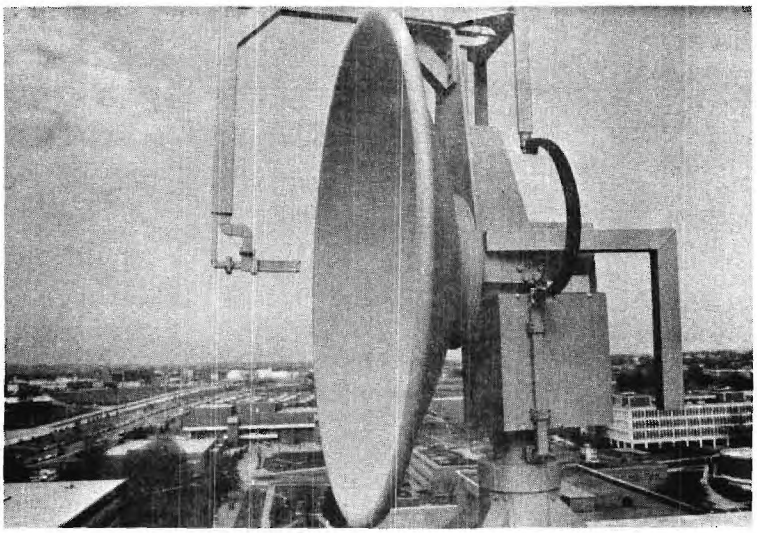

Figure 32A. Four-foot 39-dB gain antenna shown atop the Georgia Tech Graduate Library with polarization dual channel feed attached.

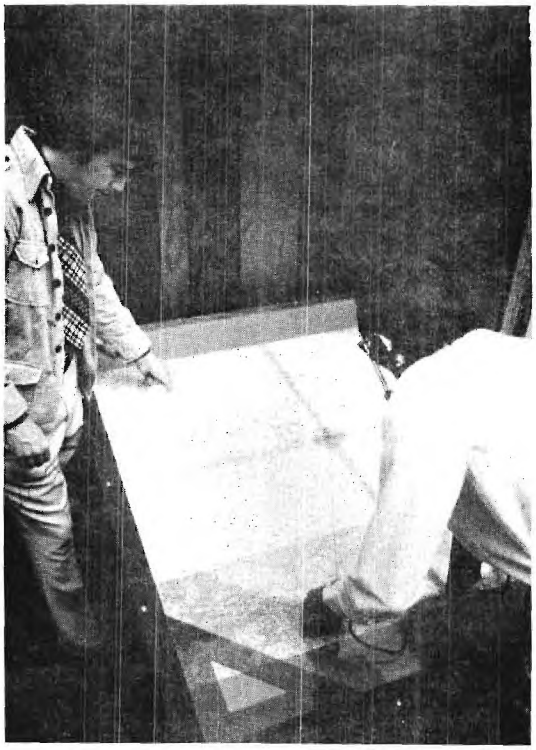

Figure 32B. Plotting board shown from top view.

TABLE I. Weather Radar System Parameters

Indicators	PPI, A-scope, Digital Antenna Elevation Readout, 35 mm and 16 mm scope cameras
Transmitter Power	250 kW
Pulsewidth	2.5 and 0.5 μs selectable
PRF	Selectable between 250 and 2500 PPS depending on duty cycle
Frequency	Tunable 8.7 - 9.35 GHz (3.45 - 3.21 cm)
Antenna Type	4 Ft Diameter Parabolic
Antenna Gain	39 dB
Beamwidth (3 dB)	1.8^{o}
Feed	Dual Mode Coupler
Polarization	Transmit vertical, receive vertical/ horizontal simultaneously

is located in the same room as the radar console on the 7th floor of the Graduate Library. Two telephone lines link the plotting board operator with the remotely located sferics station operators. The radar plot data are received directly from the radar operator.

The plotting board was utilized during 1975 when a number of fast-moving thunderstorms were being tracked simultaneously. Plot data are updated on each target approximately every 5 minutes or less depending on the number of targets being tracked. The advantages of plotting weather in this fashion are: (1) a large number of targets can be handled simultaneously; (2) sferics data can be plotted simultaneously with radar data, thus reducing ambiguities; (3) exact geographic locations of thunderstorms can be immediately determined at any time; (4) thunderstorm speed and direction of travel are presented geographically, thus allowing times of arrival to be predicted for communities downstream; and (5) the time/history nature of the plots enables immediate assessment of thunderstorm development.

C. Sferics System Design

The design of the sferics receiving equipment was postulated on the known characteristics of sferics measurements presented in current literature. Figure 33 shows a simplified functional block diagram of the sferics DF system. The system is basically a crossed loop Watson-Watt DF receiver using tuned-radio-frequency (TRF) receivers and post-detection circuitry to (1) obtain sferics pulse and burst counts, and (2) resolve bearing sense and ambiguities.

The bearing information is obtained in the following manner. Consider a vertically-polarized sferics arriving at an azimuth angle θ relative to

North and elevation angle Φ relative to the horizon. The X and Y signals that are presented to the display oscilloscope are given by:

$$V_x = K \sin\theta \cos\Phi \sin\omega t \quad \text{and}$$

$$V_y = K \cos\theta \cos\Phi \sin\omega t$$

where ω is the tuned frequency of the matched TRF receivers, and K is a function of the loop physical configuration. When V_x and V_y are applied to an XY cathode ray tube, it can be shown that the inclination τ of the major axis of the resultant line display with respect to the X-axis is given by

$$\tau = 1/2 \tan^{-1}\left[\frac{2 \sin\theta \cos\theta}{\sin^2\theta - \cos^2\theta}\right]$$

$$= 1/2 \tan^{-1}\left[-\frac{\sin 2\theta}{\cos 2\theta}\right]$$

$$= 1/2 (-2\theta)$$

$$= -\theta \quad .$$

Thus, the XY signals presented to the display oscilloscope provide a direct indication of the sferics bearing angle, except for a 180-degree ambiguity, which is resolved by the use of the monopole antenna, its associated TRF receiver and the sense selector logic.

The burst counter, shown in the block diagram in Figure 33, accepts the omnidirectional signal from the C channel TRF receiver, derives a video signal from an envelope detector, then processes the video signal to sense the number of sferics pulses occurring above a predetermined amplitude level. These sferics pulses are subsequently integrated to obtain burst data that are finally presented in the form of a digital readout.

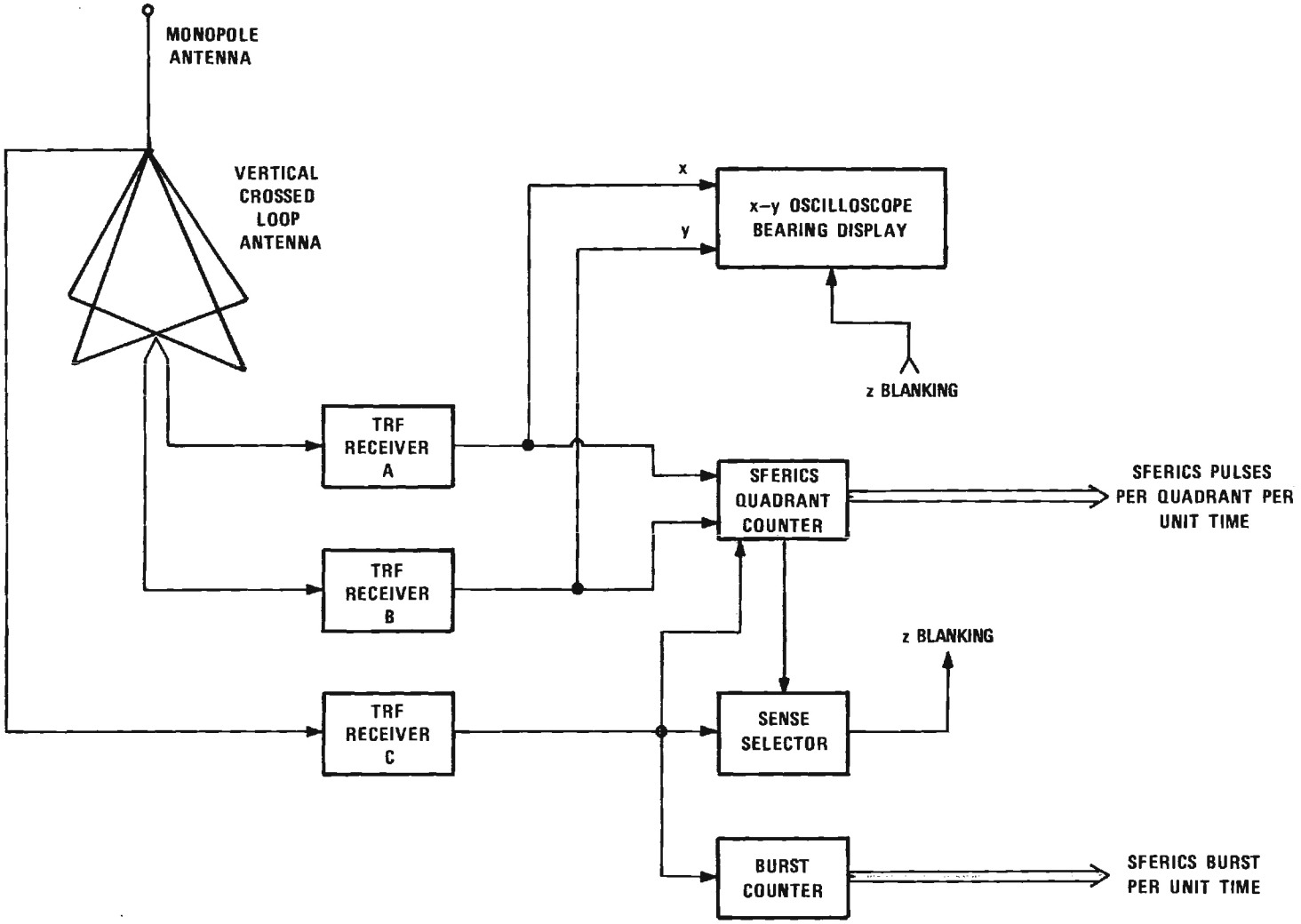

Figure 33. Simplified block diagram of sferics receiver.

A complete description of the sferics receiver design is presented in the Appendix. Several recommended changes to the present design and the reasons for each are discussed in the following section.

D. Choice of Operating Frequencies

The operating frequency of the sferics DF system was selected to be 2.8 MHz with a total bandwidth of 600 kHz. This large percentage bandwidth is necessary to provide faithful reproduction of the fast rise-time sferics pulses. The 2.8 MHz operating frequency was selected as a band sufficiently below the 80-meter amateur radio band to avoid interference, yet high enough in frequency to escape interference from LORAN signals. During the day this lower portion of the HF band is relatively free of ionospherically-propagated signals due to heavy D- and E-layer absorption factors. At night, the lower HF activity increases, but remains at a fairly low level relative to the middle and upper portions of the HF band. Overall, 2.8 MHz is a good choice for the operating frequency.

E. Planned Sferics System

The original concept was to use two different types of receivers. A "smart" DF system located at Georgia Tech was to have the capability of obtaining various types of sferics rate information. A second system concept, used for two "outstation" sites would provide basic bearing data and a coarse indication of sferics pulse rate.

It was planned that the "smart" DF system would:

(1) indicate the direction of arrival of sferics,

(2) determine the number of sferics pulses per unit time per azimuth quadrant,

(3) determine the number of sferics bursts per unit time in each 10-degree azimuth sector,

(4) measure the total number of sferics bursts per minute.

The outstation receivers were designed to indicate the direction of arrival of sferics and determine the number of sferics pulses per unit time per 90-degree azimuth sector.

A 3-station network was postulated for the 1975 tornado season. Two outstation receivers were to be located at Athens and Macon, Georgia. The smart receiver was to be located on the Georgia Tech campus. The typical accuracies that could be obtained with this configuration were computed using circular error probability analysis. The system was not fully deployed as planned during the 1975 tornado season for reasons to be discussed. However, a CEP analysis was performed for the proposed pilot sferics DF net consisting of sites at Atlanta (ATL), Athens (ATH), and Macon (MAC), to determine how well the system could operate. The assumed standard deviation (bearing accuracy) for each site is $\pm$ 10 degrees, and a circular error probability value of 50 percent was used.

Figure 34 depicts CEP contours for 28 selected signal source locations distributed throughout Georgia. The contours are represented by circles having an area equivalent to the calculated elliptical areas. The numbers within the contours refer to the approximate county coverage based on the average area of all the Georgia counties. (Georgia has a land area of 44,329 square nmi and 159 counties leading to an average area per county of 270 square nmi.) This analysis assumes that signals from each of the 28 locations are detectable at the DF sites (ATL, ATH, and MAC). In actual practice this will not be true, but the assumption does serve to illustrate the capabilities of the 3-station sferics network.

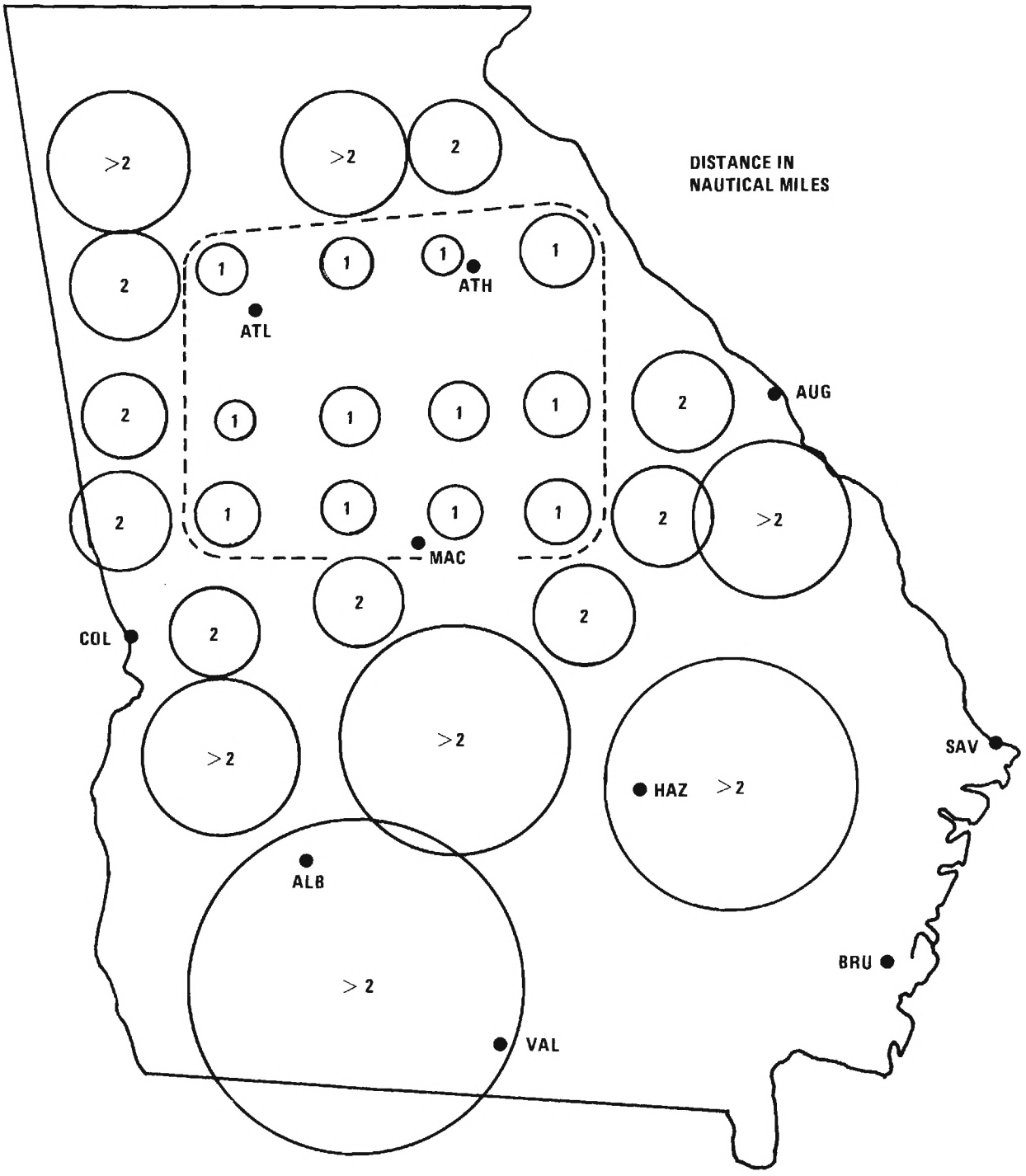

Figure 34. Result of CEP analysis for Atlanta, Macon and Athens sferics receiver locations.

It may be noted that within and around the ATL, ATH, MAC triangle, the CEP contours indicate average areas of uncertainty of approximately 175 square nmi or less. These are indicated by the circles labeled with the Number 1. To state it another way, based on this theoretical analysis, the ATL, ATH, MAC net should be able to ascertain the location of a sferics source to $\pm$ 7 nmi about 50 percent of the time for all activity occurring in the general area shown dotted in Figure 34. For a probability of 75 percent, the accuracy is calculated to be $\pm$ 10 nmi.

Figure 35 depicts a postulated sferics DF net configuration for the entire State of Georgia. Ten coverage regions are provided by ten sites as shown below.

Coverage Region	Stations Providing Coverage
I	Atlanta (ATL), Athens (ATH), Macon (MAC)
II	ATL, MAC, Columbus (COL)
III	COL, MAC, Albany (ALB)
IV	ALB, MAC, Hazelhurst (HAZ)
V	ALB, HAZ, Valdosta (VAL)
VI	VAL, HAZ, Brunswick (BRU)
VII	HAZ, BRU, Savannah (SAV)
VIII	HAZ, SAV, Augusta (AUG)
IX	HAZ, MAC, SAV
X	AUG, ATH, MAC

This configuration is such that any sferics activity occurring within Regions I through X is detectable by three stations.

A separate CEP analysis was performed for each of the ten regions shown in Figure 35. The bearing variance used was $\pm$ 10 degrees; the probability

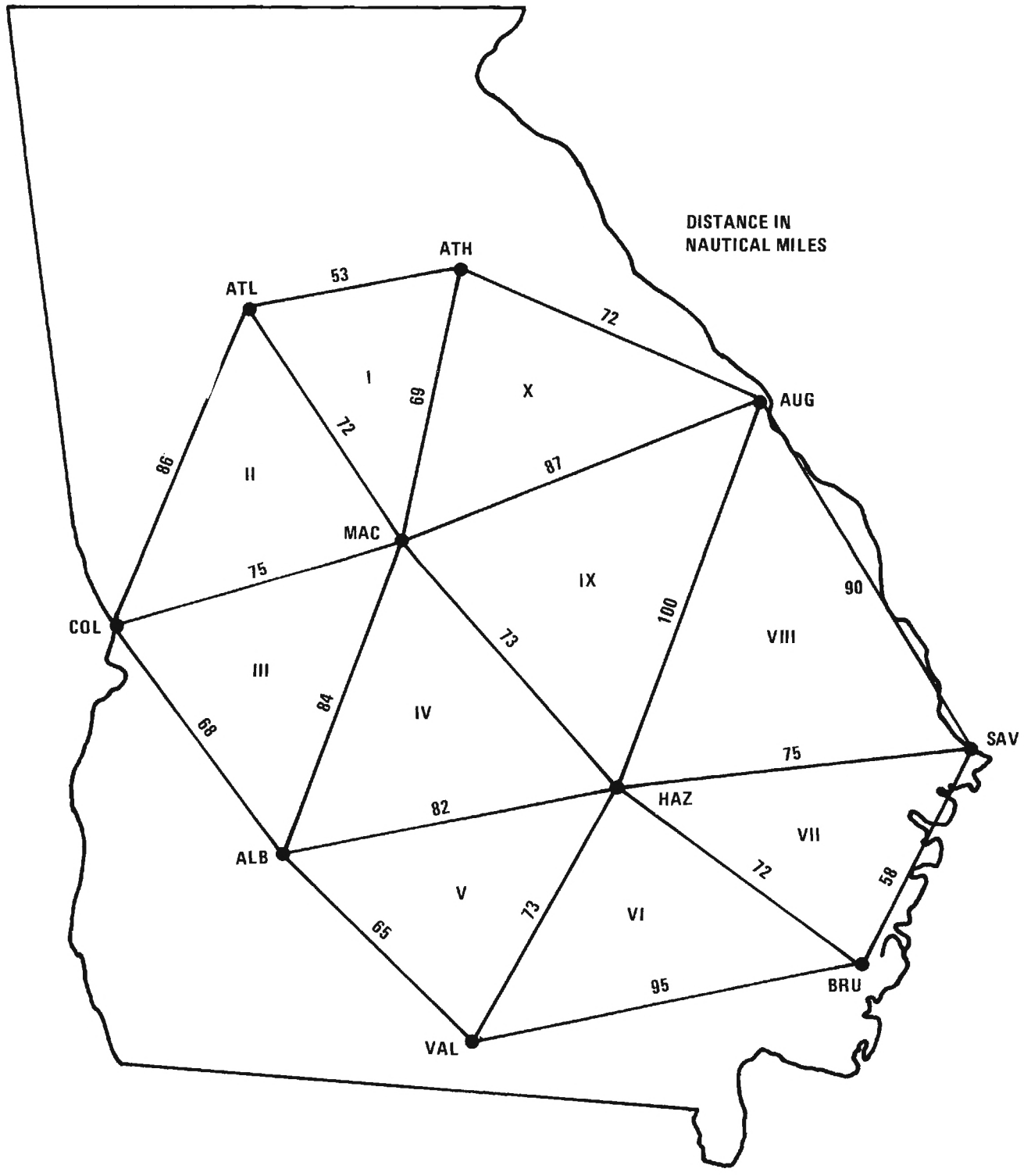

Figure 35. CEP analysis for a postulated sferics network expanded to cover the entire state.

value was 50 percent; and the geographical area of interest included the enclosed areas of the triangle and certain selected areas adjacent to the various regions of interest. The minimum, maximum, and average CEP values for each region are given in Table II.

The regional CEP data provide the following major conclusion. Based on the postulated conditions, a 10-site sferics network, configured as shown in Figure 35, will provide coverage to within a "one-county" area a large portion of the time over most of the region of interest. The maximum CEP areas shown in Table II are all less than 279 square nmi (the average one-county area) except in Region VIII. The average CEPs are all less than 279 square nmi. It should be stressed that the 10-site net represents a minimum acceptable configuration if the entire state were to be covered. Four additional sites in northwest, southwest, northeast, and middle-eastern Georgia would considerably enhance coverage and accuracy of a statewide network. Additional accuracy can be obtained through proper site selection. The $\pm$ 10-degree errors are rather large compared to what might be obtained by locating the sferics receivers at a "good" DF site with few site errors.

F. Actual 1975 System

The smart receiver could not be made to operate in the DF mode on the Georgia Tech campus due to interference from the campus radio station (WREK). The front-end overload by WREK of the RF preamplifiers located with the DF loop antennas severely biased the azimuthal bearings of weak sferics signals emanating from distant storms. The burst counting function, however, was not affected. The Atlanta tornado occurred prior to deployment of the other sferics receivers to their respective outstations and the burst counter was proven a necessary feature. Thus, a decision was made not to

TABLE II. CEP Areas for 50 Percent Probability.

Region	Maximum CEP	Minimum CEP	Average CEP	Equivalent Radius for Avg. CEP*
	nmi^2	nmi^2	nmi^2	nmi
I	196.6	131.2	152.6	7.0
II	206.1	167.7	188.8	7.8
III	179.9	149.7	166.0	7.3
IV	203.1	147.1	177.4	7.5
V	180.8	132.3	161.4	7.2
VI	202.0	126.0	166.9	7.3
VII	165.0	111.0	132.8	6.5
VIII	324.6	233.4	276.2	9.4
IX	264.6	184.4	234.2	8.6
X	234.3	173.3	187.7	7.7

*For 75 percent probability CEP multiply these values by 1.4.

deploy the outstation receivers until burst counters could be added to each. It was also decided that for the remainder of the tornado season a receiver with only burst counter capability would be kept on the Georgia Tech campus. Thus no receiver was installed in Macon during 1975.

The first outstation receiver modified with burst counter provisions was installed at the Georgia Tech DF site west of Marietta in a remote location away from sources of interference. The field site installation shown in Figure 36A proved optimum. The direction finder accuracy proved to be better than $\pm$ 3 degrees based on data collected on thunderstorms tracked at various ranges between 1 and 60 nmi.

The second receiver was modified and installed in the Journalism Building on the campus of the University of Georgia in Athens. This receiver, shown in Figure 36B, is located in a 5th floor equipment room and the antenna is located on the roof. Dr. W. W. McDougald of the University of Georgia School of Journalism graciously consented to operate the system provided that it be located on the Journalism Building. The optimum location for the sferics station in the Athens area is the county airport. However, equipment will not be moved from the University of Georgia campus until direction finder site errors for the Journalism Building can be determined.

A multi-station network proved its worth numerous times during the 1975 operating period. Occasionally a highly charged thunderstorm cell would move over the Marietta site producing corona discharge during passage. The resulting interference made data collection impossible. However, the duplicity of systems at Georgia Tech and Athens allowed continuous data to be taken.

Figure 36A. Installed sferics receiving equipment at the Georgia Tech operated Marietta, Georgia, field site.

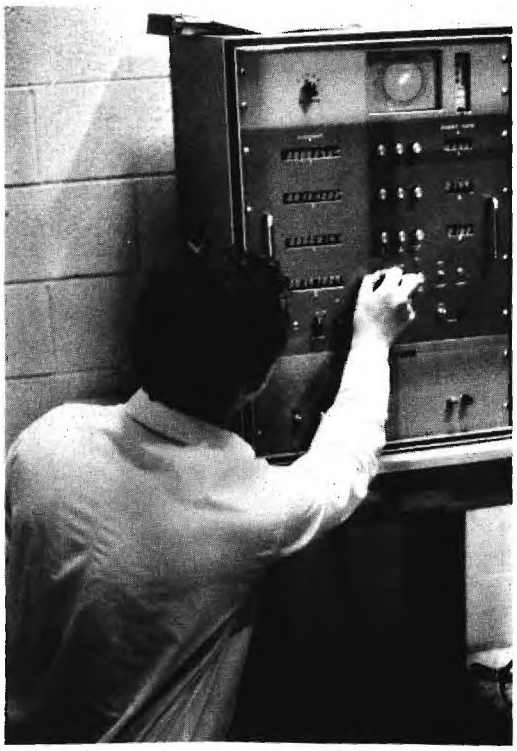

Figure 36B. Installed sferics receiving equipment at the University of Georgia School of Journalism.

SECTION IX

IMPROVEMENTS TO THE STORM DETECTION SYSTEM

A. Present Warning Techniques

The goal of this project has been to find distinctive characteristics of thunderstorms that produce tornadoes, particularly characteristics that can be discerned unambiguously prior to the time of tornado touchdown. Sferics observations have revealed the sharp decrease of electrical activity associated with a tornado, but this occurs only after the tornado has reached the ground. The high level of sferics counts prior to tornado development provides some warning capability, but at present this is essentially a "probability" approach. In other words, if one establishes a criterion for tornado warning based on sferics burst rate alone the number of "false alarms" will be unacceptable. However, sferics observations are valuable when used in conjunction with other weather sensors.

Certain features of radar echoes have come to be taken as indicators of tornadoes and other severe weather. Most distinctive is the "hook" which often forms on the side of the storm echo as a result of the vortex circulation within the storm. Merging and splitting of storm cells are also indicators of severe winds or tornadoes, because such anomalous cell motions imply major variations in the wind flow in or around the storm. In the case of splitting cells, at least one of the resulting cells usually exhibits marked rotation, and the merging of a small cell into a larger one is generally associated with a very strong updraft in the larger one or a concentration of the vorticity, or atmospheric "spin," at low levels. The Fort Valley and Lyons tornadoes discussed in Section VI and the Atlanta tornado discussed in Section VII were preceded by a merging of radar echoes at least 15 minutes before the tornadoes

touched down. The key to understanding and ultimately predicting tornadoes evidently lies in the wind flow within and around storms.

B. Doppler Radar

A particular type of radar, known as "coherent" or "Doppler" radar, can measure the velocities of particles within the beam. This is accomplished by measuring the change in frequency of the returned signal relative to the transmitted signal. The frequency shift associated with the motion of the target is called the Doppler shift, after its discoverer. In the case of meteorological targets, which are composed of many scattering particles, the Doppler radar measures a distribution, or spectrum, of velocities, usually centered at some average frequency and having a spread about the average due to air motions within the radar resolution cell.

Utilization of Doppler radars for research has increased rapidly in recent years with the advent of high-speed, large-capacity data processing equipment. Previously it was possible to examine only a small portion of the data in real time; most of the lengthy analysis had to be done later. Meteorological Doppler radar therefore was limited to use as a research tool for studying storm dynamics. Major efforts focused on the development of more effective devices for data handling and display. One such device, called the Plan Shear Indicator (PSI), was developed at Air Force Cambridge Research Laboratories [27]. The PSI consists of a series of arcs, concentric to the radar, on a circular display; the outline of the area crossed by the arcs is the same storm outline as would be seen on a conventional PPI display. Motion of the target toward or away from the radar is represented by radial displacement of the arcs from their "zero" position. This display provides easy detection of regions of extreme turbulence, which appear as

sharp, irregular fluctuations of the arcs. Persistent storm features such as a major vortex produce a distinct "signature" on the PSI display. Experiments conducted in cooperation with the National Severe Storms Laboratory [28] revealed a distinct vortex circulation at 20,000 ft altitude in a thunderstorm about 15 minutes before a tornado touched down. This observation is illustrated in Figure 37. Successive scans showed the intense vortex extending to progressively lower altitudes. Note in Figure 37 that the outline of the storm echo forms the classic "hook," but that the vortex center revealed by the PSI is displaced from the "hook."

Developments in digital computer hardware in the past few years now permit the actual calculation of the average, or "mean," and the spread, or "variance," of the Doppler velocity spectrum in real time. Further, these quantities together with the reflectivity can be color coded according to magnitude and displayed on television-type monitor screens while the radar is scanning [29,30]. Memory units make it possible to store and recall data for comparison of displays over a period of time. Developments such as these promise easier interpretation of radar data for operational purposes as well as more effective use of radar in research, as data acquisition can be concentrated in regions of a storm which are immediately known to contain hail, severe turbulence, or vortex circulations. There are, unfortunately, disadvantages and limitations in the use of Doppler radar. The most notable disadvantage is cost, which may be twice as much as for a conventional radar. Also, the measurement of a wide span of velocities is achieved only by sacrificing long-range surveillance capability.

With current technology a vortex can be detected within a storm, and its strength and vertical extent can be determined. On the basis of this

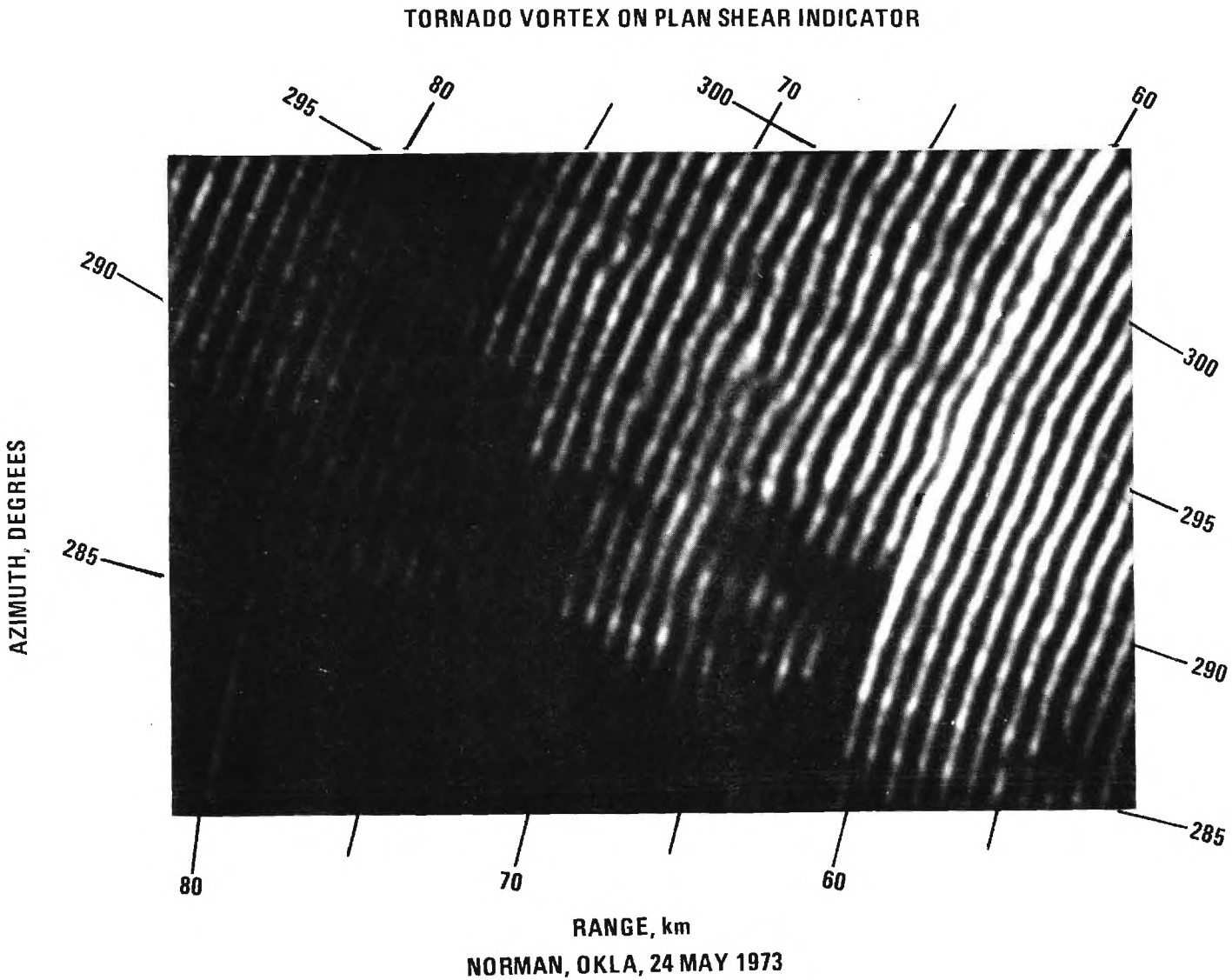

Figure 37. Photograph of plan shear indicator taken during period of tornado passage. Perburbations in concentric circles indicate zones of shear. (Photo courtesy of Donaldson AFCRL).

information a warning can be issued with an approximate indication of the area that is most likely to be hit. Successive observations of the vortex, its downward development, and its horizontal motion may permit even more precise warnings of the endangered area. Such precise warnings would have the effect of reducing "false alarms" in adjacent areas. Precise reliable early warning capability would instill public confidence in the system. Fast reaction by the public is necessary if lives are to be saved.

C. Potential Sferics System Error Sources

The observations made during the nontornadic thunderstorms proved extremely valuable in understanding potential sources of error in using sferics equipment for the purpose of severe storm detection.

The directional errors experienced on the Georgia Tech campus and on the University of Georgia campus are primarily the result of the sferics signal being re-radiated from natural and man-made objects. These features in the immediate vicinity (within several miles) of the DF site cause directional errors by generating multipath signal components. These errors are mostly nondeterministic and are functions of the ground conductivity and signal parameters such as frequency, angle-of-arrival (both azimuth and elevation), and polarization. Site calibration can be used to estimate these errors but is usually beneficial only for indicating error due to objects close (within several wavelengths) to the DF array. In general, site errors are time-variable functions and can only be treated on a statistical basis. Strong signals from nearby radio transmitters can also introduce errors into the system and mask the storm signals.

Observational errors are those introduced by the operator because of factors such as inexperience, lack of time to obtain reliable bearing data,

and improper use of equipment. When observing sferics DF strobes the operator must assess angle-of-arrival on the basis of a 1/4 - 1/2 second look at the signal on the X-Y oscilloscope. Operators found difficulty in manually recording the contents of the four 8-digit sferics quadrant registers because of the 8-digit magnitude of the numbers and the 1 minute or less recording time allowed before reset.

Propagation errors with a loop DF system can result in an incorrect relationship between the direction of propagation and the polarization of the received signal. These propagation errors are manifested by received azimuth angles-of-arrival which are not coincident with the great circle bearing (GCB). Major causes of these errors are multiple propagation paths (multipath), lateral ionospheric deviation and scatter propagation.

Corona discharge from nearby powerlines, lightning rods and the sferics receiving antenna occurred numerous times during the 1975 test period as highly charged clouds moved over the sferics receiver site. The corona discharge phenomenon if undetected will be counted as a high burst rate due to its characteristic pulse waveform. In order to detect data corrupted by corona, communications receivers tuned to 2.8 MHz were employed at each site to allow the operator to aurally monitor sferics burst and detect corona discharge. Corona could be readily distinguished aurally by operators who had previously had the sound of corona discharge identified.

The advantage of the multistation system was proven during tests with non-severe thunderstorms. Numerous times one sferics site would be "covered up" because of corona discharge or heavy electrical activity from a thunderstorm within 5 miles. The duplicity of systems enables uninterrupted data to be collected by the other stations.

One of the most important observations made during the period pertained to the problems of using a nondirectional burst counter for monitoring line thunderstorms. The nondirectional burst counter summed the sferics signals originating from all active cells within the squall line, thus masking individual cell activity. The nondirectional summation was not a problem when isolated thunderstorms were being observed as in the case of the Atlanta tornado.

D. Suggested System Improvements

When future operations are undertaken the following changes should be made in the system:

1. Additional sferics receivers should be deployed to increase area coverage.
2. The data from the sferics quadrant counters should not be used except as a general indicator as to which quadrants are active.
3. Refinements to the sferics DF receivers should include a capability that would allow the operator to record burst rate within a narrow azimuthal sector with the goal of isolating individual, high-activity storm cells.
4. Leaky powerlines and corona discharge points near the sferics antenna should be found and the situation be corrected where possible.
5. Radar data in the future should include Doppler measurements to study the possibility of high level vortex formation 15 to 30 minutes before tornado formation.

6. Automated radar reflectivity contouring and recording equipment should be incorporated to collect data on levels of rainfall as a function of range, height, and azimuth in Georgia tornado situations.

SECTION X

SUMMARY

A. Conclusions

The study of tornadoes in Georgia included the analysis of historical and current National Weather Service data and the observations of tornadic thunderstorms by radar and sferics-receiving equipment at Georgia Tech.

Studies of historical tornado data reveal a subtle change that has occurred during the past five years concerning the periods when tornadoes are most likely to occur, indicating that new warning systems concepts may be in order. During the period 1953 through 1969 a majority of tornadoes occurred during the hours when the public would have access to normal channels of communications (i.e., radio and television stations). The data representing tornado occurrences during the 1970s indicate that the peak in occurrence has shifted to periods of the day when people are either asleep or at work. If this apparent trend continues a majority of tornadoes will occur when the general populace is away from normal warning channels. The Atlanta tornado was one example of such an occurrence. This factor suggests that warning agencies should consider the development of a new type of warning system.

Georgia Tech's radar observations of the Atlanta tornado, examination of NWS radar films during occurrences of confirmed tornadoes elsewhere in Georgia, and findings of other researchers indicate that distinctive characteristics of the wind field of tornadic thunderstorms are identifiable 15 to 20 minutes before tornado touchdown. These wind patterns are evident in radar films when frame-by-frame examination is made of echo movement data. They have also been detected by Doppler radar. Measurement of the wind fields by Doppler radar is the best means of detecting the early stages of tornado formation and

providing a warning to the public some 15 to 20 minutes before tornado touchdown.

The sferics observations made during the Atlanta tornado are not conclusive. However, the cause of sferics cessation while the tornado is on the ground should be investigated further. If the sferics cessation is a repeatable phenomenon associated with the majority of Georgia tornadoes, then a high-resolution sferics system could serve as a remote sensor to indicate funnel touchdown. The validity of the cessation phenomenon could be determined during one and no longer than two more operating tornado seasons. During the same period of time the same research data could be used to better understand the sferics burst rate maxima that are thought to occur minutes before funnel touchdown.

B. Recommendations

We propose a continuing research program in the detection of severe storms by radar and by sferics observations. The American Meteorological Society cited the need for such a research effort in its 1975 policy statement on tornado detection, tracking, and warning [31]. We suggest an on-site survey program during the 1976 season, with minimal radar and sferics detector operations in order to make major equipment improvements. The improved observational equipment would be used in an extensive storm-detection program in the 1977 season.

We recommend that a tornado data-gathering effort be maintained during the spring months of 1976. This program should include on-site visits of all tornadoes with a continuous ground path of 1 mile or greater. Exact path length, orientation, and time of occurrence should be recorded. An aerial survey extending 25 miles beyond either end of the path should be conducted

to determine if unreported damage occurred. The resulting data should be analyzed in conjunction with noncoherent radar films to reconfirm the hypothesis that wind field perturbations occur 15 to 20 minutes before funnel touchdown.

During 1976 the pulsed Doppler radar developed by the Radar Technology Division, Engineering Experiment Station, should be installed at the Graduate Library weather radar site. High-power cross-field amplifiers should be purchased to increase the operating range of the radar. A data acquisition system compatible with the added requirements of Doppler processing should be included as an improvement to the Doppler radar.

Sferics receiving equipment should be recalled from the field sites and modified for high-resolution capability (2 degrees azimuthal resolution), in order that individual thunderstorm cells can be monitored. The third receiver presently located on the Georgia Tech campus should be installed in Macon or at another suitable location to maximize storm detection for the Atlanta area.

Adequate funding should be secured for operation of the Doppler radar and sferics receivers during the 1977 tornado season.

APPENDIX

DETAILED DESCRIPTION OF THE SFERICS RECEIVER DESIGN

A detailed block diagram of the DF sferics system is given in Figure 1A. Each of the three DF receivers has been fabricated as a rack mountable unit with the RF portions of the receiver housed within shielded enclosures and the video and digital logic portions of the system constructed on plug-in circuit cards. Following is a description of the individual subsystems as shown in the block diagram of Figure 1A.

A. Antenna Array

The DF antenna array consists of a non-resonant dipole element and vertical crossed loop (perpendicular) elements shown being mounted on the roof of the University of Georgia Journalism Building, in Figure 2A. The crossed loop antennas are fabricated from one inch square brass tubing for the outer electrostatic shield and a single turn of RG-8 coaxial cable as the inner conductor. The area of each loop is approximately 0.22 square meters. The loop antennas are operated at a frequency (2.8 MHz) significantly below the first resonant mode. The monopole antenna is a non-resonant element with a length-to-wave length ratio of 0.014. The signal derived from the monopole antenna is subsequently used to provide sense for the bearing display.

B. Loop and Monopole Preamplifier

The antenna mounted preamplifiers are used to provide approximately 12.5 dB of signal gain with a 50-ohm output impedance suitable for driving the coaxial cables between the antenna and the DF receiver. This signal gain and low output impedance significantly reduce any signal pickup that might occur on the coaxial cable, thus eliminating this potential source of bearing

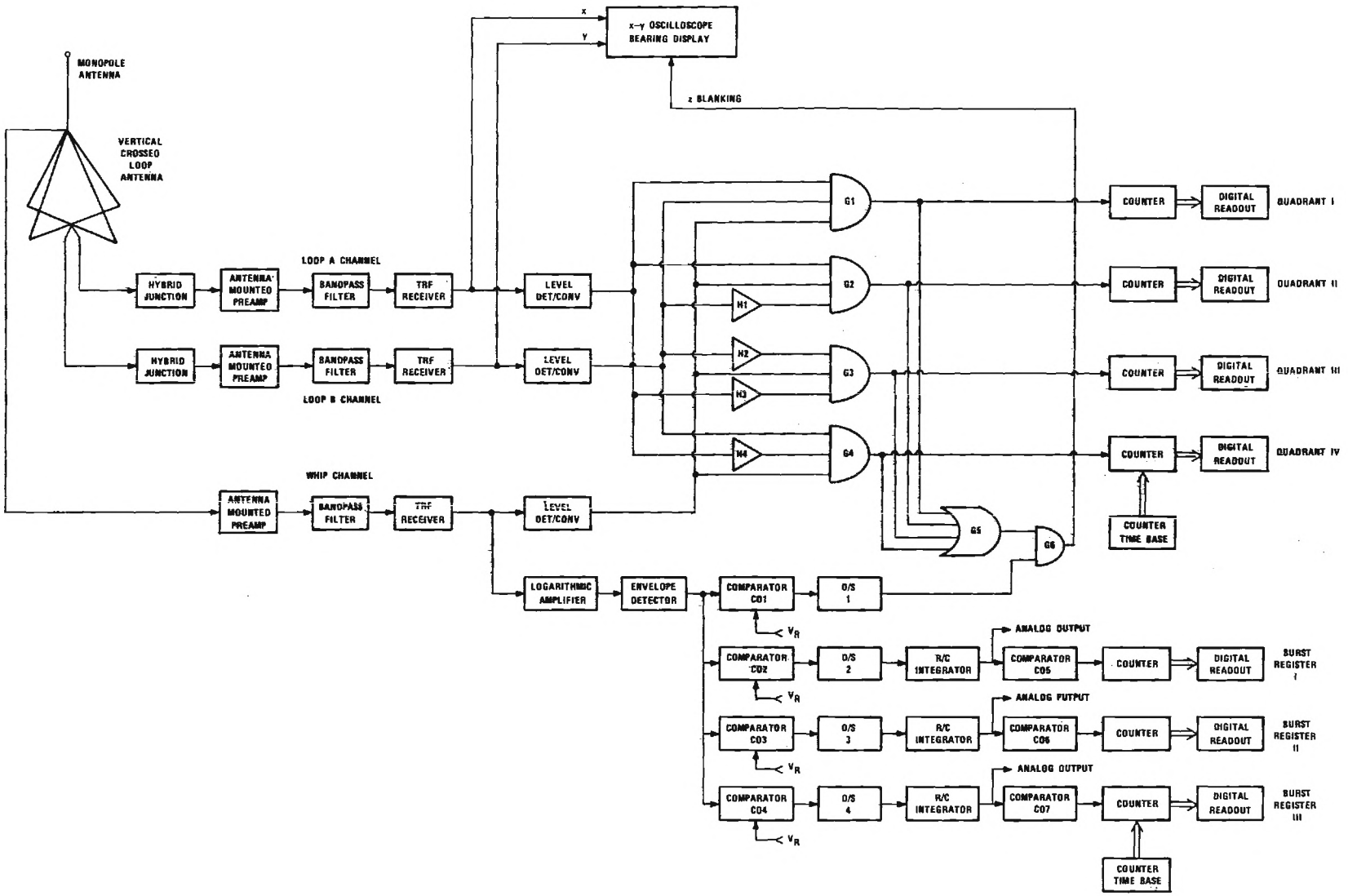

Figure 1A. Detailed block diagram of sferics receiver.

Figure 2A. Sferics antenna being installed on the School of Journalism roof, University of Georgia, Athens, by Engineering Experiment Station personnel.

errors. Hybrid junctions are used at the loop antenna output to provide the balanced-to-unbalanced conversion required for driving the antenna mounted preamplifiers.

C. Tuned Radio Frequency (TRF) Receivers

The three TRF stages were designed to achieve the gain and bandwidth necessary to provide RF output signals to the bearing display oscilloscope and the other signal conditioning subsystems of the DF receiver. The TRF amplifiers were designed to be phase and amplitude matched over the operating frequency bandwidth. It is found imperative that all three stages maintain phase and amplitude match throughout the RF circuitry to the receiver outputs. Any unbalance shows up as a bearing inaccuracy.

In regard to phase and amplitude match, the input bandpass filters are the most critical elements since the TRF amplifiers can be broad band phase and amplitude matched with little difficulty. To achieve a good phase and amplitude match between the three 8-pole bandpass filters all individual components were bridge-matched prior to insertion in their respective printed circuit boards. The pre-insertion adjustment was followed by an on-the-board alignment to achieve a phase match of $\pm$ 2 degrees and an amplitude match of $\pm$ 1 dB.

D. Bearing Display

The outputs of the A and B channel TRF receivers are applied to the X and Y inputs of a commercial (Tektronix Model 604) oscilloscope. The oscilloscope uses a CRT with a P7 phosphor. The oscilloscope has a Z axis input which is subsequently used for sense blanking.

E. Level Converter

The RF signals from each of the TRF receivers are fed to their respective level detector/converters to convert the receiver sinusoidal outputs into fast-rise-time, square waves required for logic operations in the quadrant count, sferics count, and sense selection subsystems. The level detectors are biased to operate only when the received signal is greater than 6 dB above the receiver noise level. After level detection the RF signals are further processed to achieve the voltage and impedance levels required to operate the digital logic that in turn provides for sense and the burst and quadrant counter signals.

F. Bearing Sense Selection

Without the bearing sense selection, a 180-degree ambiguity exists in the bearing displays. This ambiguity is resolved by four triple-input AND gates (G1-G4) fed from the three receiver outputs through appropriate phase inverters (H1-H4). The relative RF phases of the three receiver outputs indicate which quadrant contains the correct azimuth angle-of-arrival. The gates open and unblank the display only on the first half cycle of the receiver outputs. The relative polarities of the signals during the first half cycle then create a display in the proper quadrant without sense ambiguity. Without sense capability should the sferics pulse arrive in the first quadrant, the bearings would be presented in both the first and third quadrants. With sense selection, the only AND gate opened (all inputs must be positive to open the gates) is G1 and it opens only when all inputs are positive. Hence, the improper third quadrant bearing is blanked out.

When the sferics pulse occurs in the second quadrant, the signals from the channel A and channel C TRF receivers are in-phase and the signal

from the B channel is out-of-phase. However, the inverter (H1) on the B input to G2 places A, B, and C in-phase at G2, opening G2 and unblanking the display on the first half cycle. For third quadrant reception, both A and B channel signals are inverted for G3 activation on the first half cycle and quadrant 3 unblanking. The operation is similar for quadrant 4 reception. Each of the four gates (G1-G4) drives its respective counters which in turn provide a digital readout of the number of sferics pulses occurring in each of the four quadrants. In addition, the signals from each of the four gates are OR'ed in G5 and then applied to a 2-input AND gate (G6). The other input to G6 is a processed signal from the monopole channel.

The monopole signal is processed in the following manner. The output from the C channel TRF receiver is applied to a logarithmic amplifier with a dynamic range of approximately 60 dB. It is then rectified and smoothed and applied simultaneously to four comparators (CO1-CO4). When the input signal to the first comparator (CO1) exceeds the threshold, as determined by a reference voltage V_R, the comparator is activated and drives one input of AND gate G5. Where both inputs to G5 are active, an unblanking signal is applied to the Z-input of the CRT. Hence, the monopole channel provides for sense resolution display unblanking and sferics pulse count activation in addition to burst count, which will be described later.

G. Sferics Pulses per Quadrant Counter

The outputs from AND gates G1-G4 drive four counters which feed digital displays. The cumulative outputs of the four AND gates indicate the number of sferics bursts occurring per unit time in the corresponding quadrant.

The integrated circuit quadrant counting units containing all of the circuitry necessary to count, latch, multiplex, and scan to produce display

outputs. The count time base is determined by an IC timer, which applies reset, strobe, and data transfer inputs to the counters. The count interval is selectable for either one, ten or sixty seconds. An accumulative mode is also provided for long-term accumulation of the sferics pulses.

Each counter feeds eight-digit displays. The use of this number of digits is based on the results of previous investigators who have shown that sferics pulse rates can exceed 10^7 per minute, thus requiring the eight-digit display for several minutes' accumulation.

H. Burst per Unit Time Counter

The signal for the burst-per-unit-time counter is derived from the monopole antenna. The manner in which the signal is processed to derive the burst count information is similar to the method described by Taylor [2].

The RF output from the C channel TRF receiver is applied to the 60 dB dynamic range, logarithmic amplifier. The logarithmic amplifier compresses the relatively large dynamic range of the RF output signal. The log amp output is rectified and smoothed to detect the sferics envelope and convert it to baseband. This baseband signal is then applied to the four comparators (CO1-CO4) as noted in the discussion on the bearing sense selection subsystem. The three comparators (CO2-CO4) have independent threshold reference levels with each of the three levels set for a different operating point. The three reference levels correspond to low, medium, and high sferics field strength levels. The three one-shot multivibrators (OS/2-OS/4) serve to normalize the pulse widths of their respective comparator signals.

Since each burst consists of thousands of individual sferics pulses, it is necessary to integrate the one-shot multivibrator outputs which correspond

to individual sferics pulses. Integration is performed by use of adjustable time constant RC filters and operational amplifier buffers. The RC time constants are adjustable over a range of 0.03 to 1 second. It has been determined experimentally that the lower time constant of 0.03 second represents the best value for normal operation.

After integration the three outputs are split to provide (1) buffered analog signal outputs and (2) drive signals for three additional comparators (C05-C07). The buffered analog outputs drive the strip chart, "hard-copy" recorder. Comparators C05-C07 are biased to activate when the integrator signal exceeds a preset threshold thus rejecting normal ambient circuit noise. These three comparator signals are fed to their respective counters to produce a digital readout of the burst count per unit time. The burst rate counters are identical to the type used for the sferics pulse counters, with the exception that a 4-digit display is used as compared with the 8-digit sferics pulse counters. The time base for the burst rate counter is selectable for either a ten second or a one minute time frame.

I. Summary

The burst count circuitry supplies basic burst-per-minute data to the operator. Three displays are available. The variable circuit parameters are (1) comparator threshold levels corresponding to incident signal strength and (2) integrator time constants for variable data smoothing. The circuitry is designed to be flexible with respect to the type of display data. For example, the three displays could display counts for the same field strength input, but three different integrator time constants; or the displays can be for three different field strengths but with the same time constant. Various combinations of field strengths and time constants could be used.

REFERENCES

1. E. F. Greneker, H. H. Jenkins, H. A. Ecker, E. E. Martin, and J. L. Eaves, "A Study of Techniques for the Establishment of a Pilot Electronic Tornado Detection System in Georgia," Engineering Experiment Station, Georgia Institute of Technology, Final Report Planning Study E230-902, December 1973.

2. W. L. Taylor, "Remote Sensing of the Troposphere," Chapter 17, edited by V. E. Derr, Supt. of Documents, U.S. Government Printing Office, August 15, 1972.

3. K. Shanmugam and E. J. Pybus, "A Note on the Electrical Characteristics of Locally Severe Storms," Proceedings of the 7th Conference on Severe Local Storms, Kansas City, Missouri, Pages 86-90, 1971.

4. J. L. Stanford, M. A. Lind and G. S. Takle, "Electromagnetic Noise Studies of Severe Convective Storms," Journal of Atmospheric Sciences, Vol. 28, pages 436-448, 1971.

5. D. A. Kohl and J. E. Miller, "500-kc/sec Sferics Studies in Severe Storms," General Mills, Inc., National Severe Storms Project, Report No. 13, U.S. Department of Commerce, 1963.

6. U.S. Air Weather Service (MATS), "Project Tornado Sferics," Final Report, ASTIA AD 218-741, 1957.

7. U.S. Air Weather Service (MATS), "Project Tornado Sferics 1960 Phase," Final Report, ASTIA AD 254-827, 1961.

8. H. L. Jones and R. D. Kelly, "Research on Tornado Compendium for Period 1 January 1952 to 31 December 1956," Signal Corps Contract DA-36-39-SC-64436, Oklahoma A&M College, 1957.

9. N. B. Ward, C. H. Meeks and E. Kessler, "Sferics Reception at 500-kc/sec, Radar Echoes, and Severe Weather," Papers on Weather Radar, Atmospheric Turbulence, Sferics and Data Processing, National Severe Storms Laboratory Report No. 24, Washington, D.C., August 1965.

10. John D. Rompel, "Lightning Direction Finder," U.S. Forest Service, Northern Forest Fire Laboratory, Missoula, Montana, March 1966.

11. P. L. Smith, K. R. Hardy, and K. M. Glover, "Applications of Radar to Meteorological Research," Proceedings of the IEEE, Vol. 62, No. 6, June 1974.

12. L. J. Battan, Radar Observation of the Atmosphere, University of Chicago Press, 1973.

13. G. E. Stout and H. A. Huff, "Radar Records Illinois Tornadogenesis," Bulletin American Meteorological Society, Vol. 34, No. 6, June 1953, pp. 281-284.

14. J. R. Fulks, "On the Mechanics of the Tornado," National Severe Storms Project Report No. 4, U.S. Weather Bureau, 1962.

15. T. Fujita, "Mesoanalysis of the Illinois Tornadoes of April 9, 1953," Journal of Meteorology, Vol. 15, No. 3, June 1958.

16. J. P. Marwitz, J. H. Auer, Jr., and D. L. Veal, "Locating the Organized Updraft on Severe Thunderstorms," Journal of Applied Meteorology, Vol. 11, No. 1, 1972, pp. 236-238.

17. T. E. Sanford and D. F. Leipper, "Utilization of AN/CPS-9 Radar in Weather Analysis and Forecasting," Final Report Contract No. AF19(604)-6136 A&M Project 237-Reference 60-24T, June 1961.

18. P. A. Barclay, "An Operational System for the Avoidance by Aircraft of Severe Convective Turbulence," Proc. 13th Radar Meteorology Conference, 1968, pp. 438-441.

19. N. B. Ward, C. H. Meeks, and E. Kessler, "Sferics Reception at 500 kc/sec, Radar Echoes, and Severe Weather," Technical Note 3-NSSL-24, August 1965.

20. C. W. Newton and S. Katz, "Movement of Large Convective Rainstorms in Relation to Winds Aloft," Bulletin of the American Meteorological Society, Vol. 39, No. 3, March 1958, pp. 129-136.

21. C. W. Newton and J. C. Fankhauser, "On the Movement of Convective Storms, with Emphasis on Size Discrimination in Relation to Water-Budget Requirements," Journal of Applied Meteorology, Vol. 3, No. 6, December 1964, pp. 651-668.

22. K. A. Browning and T. Fujita, "A Family Outbreak of Severe Local Storms: A Comprehensive Study of the Storms in Oklahoma on May 26, 1963," Part 1, Special Reports, No. 32, Contract No. AFCRL-65-695 (1), U.S. Air Force Cambridge Research Laboratories, Bedford, Mass., Sept. 1965, p. 346.

23. G. E. Stout and H. E. Hiser, "Radarscope Interpretations of Wind, Hail, and Heavy Rainstorms between May 27 and June 8, 1954," Bulletin of the American Meteorological Society, Vol. 36, No. 10, December 1955, pp. 519-527.

24. Horace M. Carter, "Georgia Tornadoes," ESSA Technical Memorandum EDSTM 16, U.S. Dept. of Commerce, Environmental Science Services Administration, Environmental Data Service, Silver Spring, Maryland, 1970, p. 80.

25. "Storm Data," NOAA, Asheville, N.C., Vol. 17 Nos. 1-6 (Jan.-June).

26. Howard R. Larsen, "Studies of Thunderstorms by Sferics and Radar," Scientific Report MW-79, Stormy Weather Group, McGill University, Montreal, November 1973.

27. G. M. Armstron, and R. J. Donaldson, Jr., "Plan Shear Indicator for Real-Time Doppler Radar Identification of Hazardous Storm Winds," Journal of Applied Meteorology, Vol. 8, No. 2, 1969, pp. 376-383.

28. R. J. Donaldson, Jr., "History of a Tornado Vortex Traced by Plan Shear Indicator," Preprints of the 16th Radar Meteorology Conference, American Meteorological Society, 1975, pp. 80-82.

29. A. J. Jagodnik, L. R. Novick, and K. M. Glover, "A Weather Radar Scan Converter/Color Display," Preprints of the 16th Radar Meteorology Conference, American Meteorological Society, 1975, pp. 14-20.

30. G. Gray, R. Serafin, and J. Boyajian, "Real Time Color Display for Meteorological Radar," Preprints of the 16th Radar Meteorology Conference, American Meteorological Society, 1975, pp. 21-25.

31. "Policy Statement of the American Meteorological Society on Tornado Detection, Tracking, and Warning," Bulletin of the American Meteorological Society, Vol. 56, No. 4, April 1975, pp. 464-466.